

This Page Is Inserted by IFW Operations
and is not a part of the Official Record

BEST AVAILABLE IMAGES

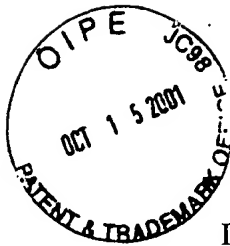
Defective images within this document are accurate representations of the original documents submitted by the applicant.

Defects in the images may include (but are not limited to):

- BLACK BORDERS
- TEXT CUT OFF AT TOP, BOTTOM OR SIDES
- FADED TEXT
- ILLEGIBLE TEXT
- SKEWED/SLANTED IMAGES
- COLORED PHOTOS
- BLACK OR VERY BLACK AND WHITE DARK PHOTOS
- GRAY SCALE DOCUMENTS

IMAGES ARE BEST AVAILABLE COPY.

**As rescanning documents *will not* correct images,
please do not report the images to the
Image Problem Mailbox.**



PATENT
025098-1406 (Formerly 238/298)

#19
BP
10-189
OCT 18 2001
TECH CENTER 1600/2900
RECEIVED

IN THE UNITED STATES PATENT AND TRADEMARK OFFICE

In re the Application of:

Baird, *et al.*

Serial No.: 09/374,704

Title: INHIBITION OF MAJOR GROOVE
DNA BINDING PROTEINS BY
MODIFIED POLYAMIDES

Filing Date: August 12, 1999

Group Art Unit: 1635

Examiner: Janet L. Epps

APPEAL BRIEF

Commissioner for Patents
Washington, D.C. 20231

Sir:

Applicants (herein, "Appellants") hereby appeal the Final Rejection of claims 1-19 and 25-26. This Appeal Brief is accompanied by the requisite fee set forth in 37 C.F.R. § 1.17(f). If this fee is incorrect or if any additional fees are due in this regard, please charge or credit our Deposit Account No. 50-0872 for the appropriate amount.

10/17/2001 CNGUYEN 00000016 09374704

02 FC:220

160.00 OP

023.201285.1

CERTIFICATE OF MAILING

I hereby certify that this paper (along with any referred to as being attached or enclosed) is being deposited with the United States Postal Service as First Class Mail with sufficient postage in an envelope addressed to the Commissioner for Patents, Washington, D.C. 20231, on the date below.

10/18/01
Date of Deposit

Jodie M. Price
Name of Person Mailing Paper

Signature of Person Mailing Paper

Table of Contents

Table of Publications	3
Real Party in Interest.....	4
Related Appeals and Interferences.....	4
Status of Claims	4
Status of Amendments.....	4
Summary of the Invention	4
Issues	7
Grouping of Claims	8
The Examiner's Rationale	8
Argument.....	10
 <u>35 U.S.C. §103</u>	
<i>Applicable Legal Standard</i>	<i>10</i>
<i>Proline, Histidine, and Arginine are not structurally similar to N-methylpyrrole, N-methylimidazole, and N,N dimethylamino-propylamide, as the Examiner alleges</i>	<i>11</i>
<i>Proline, Histidine, and Arginine are also not functionally similar to N-methylpyrrole, N-methylimidazole, and N,N dimethylamino-propylamide, as the Examiner alleges</i>	<i>14</i>
<i>The skilled artisan would lack a reasonable expectation of success in grafting an Arg-Pro-Arg sequence to a polyamide molecule to provide the instantly claimed molecules</i>	<i>16</i>
<i>The skilled artisan would not seek to graft an Arg-Pro-Arg sequence to a polyamide molecule to provide the "positive patch" of the instant claims</i>	<i>18</i>
<i>The Examiner Has Used Impermissible Hindsight in Making Selections and Combinations</i>	<i>20</i>
 Conclusion.....	 18
 Appendix A: Text of the Claims Involved in the Appeal	
Appendix B: Search results from PIR database	

Table of Publications

Swalley <i>et al.</i> , <i>J. Am. Chem. Soc.</i> 118, 8198-8206 (1996)	9, 10, 13, 14, 16, 18
Parks <i>et al.</i> , <i>J. Am. Chem. Soc.</i> 118, 6153-6159 (1996)	9, 10, 13, 14, 16, 18
Trauger <i>et al.</i> , <i>J. Am. Chem. Soc.</i> 118, 6160-6166 (1996)	9, 10, 13, 14, 16, 18
Feng <i>et al.</i> , <i>Science</i> 263, 348-355 (1994)	9, 10, 13, 14, 15, 16, 17, 18, 19
<i>In re Vaeck</i> , 20 USPQ2d 1438 (Fed. Cir. 1991); MPEP § 2143.....	10
MPEP § 2143	10
<i>In re Jones</i> , 21 USPQ2d 1941, 1943 (Fed. Cir. 1992).....	13
MPEP § 2144.08(II)(A)(4)	13
<i>W.L. Gore & Associates, Inc. v. Garlock, Inc.</i> , 220 USPQ 303 (Fed. Cir. 1983), <i>cert. denied</i> 469 U.S. 851 (1984)	15
<i>In re Mahurkar</i> , 28 USPQ2d 1801, 1817 (N.D. Ill. 1993)	19
<i>In re Fine</i> , 5 USPQ2d 1596 1600 (Fed. Cir. 1988)	19

Real Party in Interest

The real party in interest in this appeal is California Institute of Technology, Pasadena, California, which is the assignee of the present application.

Related Appeals and Interferences

Appellants are not aware of any related appeals or interferences that will directly affect or be directly affected by or have a bearing on the Board's decision in the pending appeal.

Status of Claims

The Examiner's Action of March 28, 2001 made final the rejection of claims 1-19 and 25-26. On July 24, 2001, the Applicants appealed. The status of the claims is as follows: Claim 2 was canceled in the amendment filed July 24, 2001; Claims 1, 3-19 and 25-26 stand rejected under 35 U.S.C. §103(a) and are the subject of this appeal. Claims 20-24 are allowed.

Status of Amendments

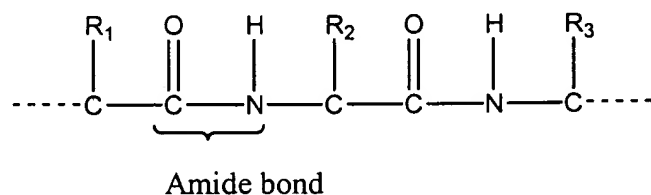
Applicants submitted amendments on July 24, 2001. These amendments were entered and acknowledged by the Examiner in the Advisory Action mailed August 2, 2001. No amendments remain outstanding in the application.

Summary of The Invention

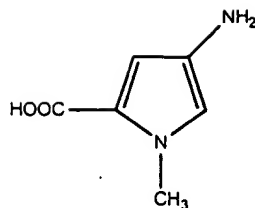
The rejected claims relate to polyamide molecules comprising one or more amino acids containing N-methylpyrrole, 3-hydroxy-N-methylpyrrole, or N-methylimidazole moieties, and a

positive patch consisting of a rigid group adjacent to a positive charged group. The rigid group of the polyamide molecule comprises a first amino acid of arginine, proline, lysine, or hydroxyproline, and a second amino acid of proline, glycine, serine, threonine, leucine, isoleucine, valine, alanine, or hydroxyproline, respectively. Such molecules can provide sequence-specific binding within the minor groove of a DNA molecule, while presenting the positively charged group in an orientation that allows the polyamide molecule to disrupt interactions between proteins and the phosphate backbone or major groove of the DNA molecule.

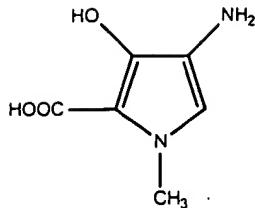
At the time the instant patent application was filed, polyamide molecules were well known in the biological and chemical arts. For example, proteins, which play a critical role in virtually all biological processes, were known to the skilled artisan to be polymers of individual residues – known as amino acids. There are 20 different amino acid residues that commonly make up proteins, which are linked together through amide bonds to form the protein:



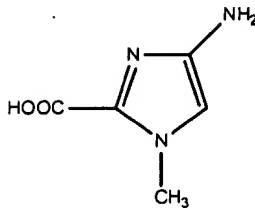
The compositions of present invention also comprise individual molecular building blocks linked by amide bonds, and are thus also referred to by the skilled artisan by the generic term “polyamide.” However, these molecular building blocks, recited in the claim as being N-methylpyrrole, 3-hydroxy-N-methylpyrrole, and N-methylimidazole, are unlike those traditionally used by nature to form proteins:



N-methylpyrrole



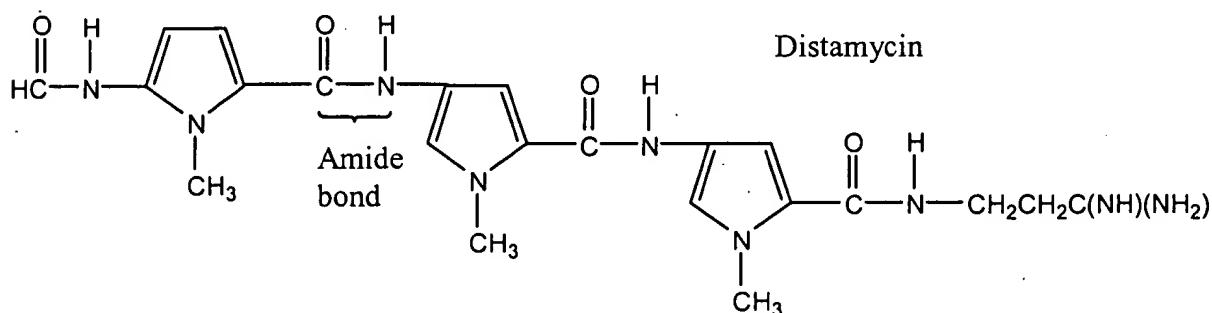
3-OH-N-methylpyrrole



N-methylimidazole

For example, traditional amino acid residues are α -amino acids (*i.e.*, the NH_2 group and the COOH group that participate in the amide bond are both connected to the same carbon atom), while the imidazole- and pyrrole-based residues are not. Also, unlike traditional amino acids, the imidazole- and pyrrole-based residues are aromatic structures. The aromatic nature of these residues (including the SP^3 nature of the α -carbon) results in a substantially planar structure that is unlike that of any of the traditional α -amino acids.

With rare exceptions, imidazole- and pyrrole-based polyamides are not naturally occurring molecules. One example of such naturally occurring imidazole- and pyrrole-based polyamides is Distamycin:



Distamycin, and other similar naturally occurring polyamides, exhibit antibiotic, antiviral, and antitumor activity, mediated by the ability of these polyamides to bind double-stranded DNA. One drawback to these polyamides, however, is that, while they bind double-stranded DNA, they do so with poor sequence specificity. *See, e.g.*, specification, page 2, lines 1-16. This makes targeting such molecules to a specific DNA sequence difficult, if not impossible.

In contrast, through the use of N-methylpyrrole, 3-hydroxy-N-methylpyrrole, and N-methylimidazole residues, the present invention provides improved sequence-specificity of DNA binding. Moreover, the instantly claimed polyamides include a “positive patch” consisting of a rigid group comprising at least 2 amino acids adjacent to a positively charged group. The inclusion of the positively charged group allows for the alteration of the chemical environment surrounding the DNA molecule, allowing the polyamide molecule to disrupt interactions between proteins and the phosphate backbone or major groove of the DNA molecule. *See, e.g.*, specification, page 13, lines 10-17.

Thus, the present invention may provide antibiotic, antiviral, and antitumor compositions that can be specifically targeted to a DNA sequence. These compositions can provide a true pharmaceutical “magic bullet;” that is, a composition designed to specifically attack a DNA sequence that is mediating a disease, while ignoring non-target DNA sequences in the patient.

Issues

1. Whether claims to polyamides that bind in a sequence-specific manner to the minor groove of a DNA molecule, wherein the polyamide comprises one or more amino acids comprising moieties of N-methylpyrrole, 3-hydroxy-N-methylpyrrole, or N-methylimidazole, and

a positive patch consisting of a rigid group comprising at least 2 specified amino acids adjacent to a positively charged group, are unpatentable under 35 U.S.C §103 over various cited publications, when the skilled artisan would lack both a motivation to combine the references as suggested by the Examiner, and a reasonable expectation of success in combining the references to arrive at the instantly claimed invention.

Grouping of Claims

Claims 1, and 3-11 stand or fall together, and claims 12-19 stand or fall together, and claims 25-26 stand or fall together. Specifically, Claims 1, 3-11, and 25-26 relate to polyamides that specifically bind to base pairs in the minor groove, comprising one or more amino acids comprising moieties of N-methylpyrrole, 3-hydroxy-N-methylpyrrole, or N-methylimidazole, and a positive patch consisting of a rigid group comprising a first and a second amino acid adjacent to a positively charged group, the first amino acid being selected from the group consisting of arginine, proline, lysine, and hydroxyproline; and the second amino acid being selected from the group consisting of proline, glycine, serine, threonine, leucine, isoleucine, valine, alanine, and hydroxyproline; claims 12-19 relate to such polyamides, further comprising a symmetrical number of carboxamide groups on each side of a hairpin linkage; and claims 25-26 relate to methods of inhibiting gene expression using such polyamides.

The Examiner's Rationale

The Examiner's rationale for rejecting claims 1, 3-19, and 25-26 is stated in the final Office Action mailed on March 28, 2001 ("Paper No. 10"), and the Advisory Action mailed on

August 2, 2001 ("Paper No. 15"). The Examiner contends that the claims are unpatentable under 35 U.S.C. 103(a) over Swalley *et al.*, *J. Am. Chem. Soc.* 118: 8198-206 (1996), Parks *et al.*, *J. Am. Chem. Soc.* 118: 6153-9 (1996), and Trauger *et al.*, *J. Am. Chem. Soc.* 118: 6160-6 (1996), in view of Feng *et al.*, *Science* 263: 348-55 (1994).

Specifically, the Examiner asserts that the Swalley, Parks, and Trauger publications disclose polyamide compounds comprising amino acid moieties bearing N-methylimidazole and N-methylpyrrole, and N,N-dimethylaminopropyl-amide moieties (Paper No. 10, p. 4). The Examiner alleges that proline, arginine, and histidine are chemically and functionally similar to N-methylpyrrole, N,N-dimethylamino-propylamide, and N-methylimidazole (Paper No. 10, pp. 4-5). The Examiner further asserts that the Feng publication discloses a polyamide compound that specifically interacts with the minor groove of DNA utilizing the sequence Gly-Arg-Pro-Arg at the carboxyl terminal domain, and binds to the major groove involving a helix-turn-helix α -helix motif.

The Examiner contends that it would have allegedly been obvious to modify the polyamides of the Swalley, Parks, and Trauger publications with a sequence of amino acids comprising Arg-Pro-Arg because "polyamide compounds comprising these sequences are known to bind DNA with high affinity in a sequence specific manner." (Paper No. 10, page 5). The Examiner does not specifically address the rationale with regard to claims 25-26, which relate to inhibiting gene expression using the claimed polyamides.

Argument

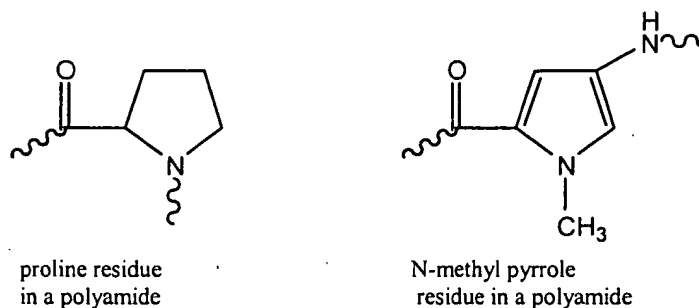
Appellants respectfully request that the rejection of claims 1, 3-19, and 25-26 be withdrawn or reversed, and that the instant claims be permitted to proceed to allowance, because the Examiner has failed to establish a *prima facie* case of obviousness. The skilled artisan would lack a motivation to select the three amino acid “arg-pro-arg” sequence from the larger Hin recombinase molecule and combine this sequence with the polyamides of the Swalley, Parks, and Trauger publications, because arg and pro are neither chemically nor functionally similar to the pyrrole- and imidazole-based residues disclosed in the Swalley, Parks, and Trauger publications. Moreover, the skilled artisan would not have a reasonable expectation of success in combining the three amino acid “arg-pro-arg” sequence with the polyamides of the Swalley, Parks, and Trauger publications to provide the instantly claimed polyamides, because these residues in isolation do not possess DNA binding characteristics. Instead, the Examiner has fallen victim to reconstructing the claimed invention by hindsight.

Applicable Legal Standard

To establish a *prima facie* case of obviousness, three criteria must be met; there must be 1) some motivation or suggestion, either in the cited publications or in knowledge available to one skilled in the art, to modify or combine the cited publications; 2) there must be a reasonable expectation of success in combining the publications to achieve the claimed invention; and 3) the publications must teach or suggest all of the claim limitations. *In re Vaeck*, 20 USPQ2d 1438 (Fed. Cir. 1991); MPEP § 2143.

Proline, Histidine, and Arginine are not structurally similar to N-methylpyrrole, N-methylimidazole, and N,N dimethylamino-propylamide, as the Examiner alleges

The Examiner's asserted *prima facie* case first relies on the incorrect contention that the person of ordinary skill would understand that proline and arginine are "chemically and functionally similar" to the N-methylpyrrole N-methylimidazole, and N,N-dimethylaminopropylamide recited in the claims. See, e.g., Paper No. 10, page 4. Referring to the structures below, those skilled in the art would readily recognize that the amino acids proline and arginine are not chemically or structurally similar to N-methylpyrrole and N,N-dimethylaminopropylamide. For example, proline comprises a saturated heterocyclic moiety, whereas an amino acid derived from N-methyl pyrrole is an aromatic molecule, the chemical and structural nature of which is entirely different from proline:

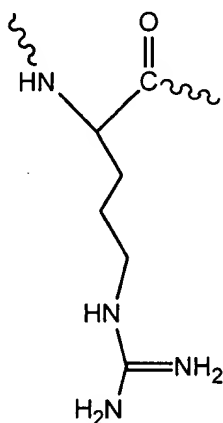


It is well-known, for example that the lone electron pair on the ring nitrogen atom of N-methylpyrrole interacts with the double bonds to impart a significant degree of aromatic character to N-methylpyrrole. In contrast, aromaticity is clearly not possible with the saturated heterocyclic moiety of proline. Such aromatic rings differ significantly from their non-aromatic counterparts in many ways (e.g., structurally, physical properties, reactivity). For example, in contrast to proline, the N-methylpyrrole structure is a substantially planar molecule. The skilled artisan

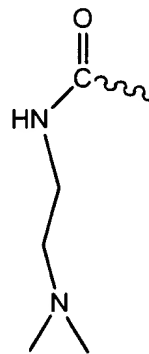
would understand that this difference in structure would in significantly different binding interactions with a target DNA molecule.

Additionally, while proline in a polyamide is an α -amino acid linked through the ring nitrogen, N-methylpyrrole is not an α -amino acid and contains a methyl group at the ring nitrogen. The skilled artisan would understand that any contacts made by proline with a DNA molecule would be completely different than those made by N-methylpyrrole. It is precisely these very different molecular interactions with DNA, provided by the pyrrole- and imidazole-based residues of the present invention when compared to naturally occurring proteins, that provide the advantageous DNA binding characteristics of the instantly claimed polyamides.

Similarly, referring to the structures below, it is clear that arginine is not similar to N,N-dimethylaminopropylamide.



arginine residue in a polyamide

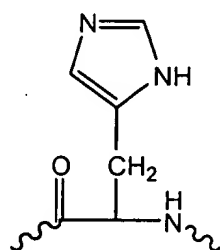


N,N-dimethylaminopropylamide moiety

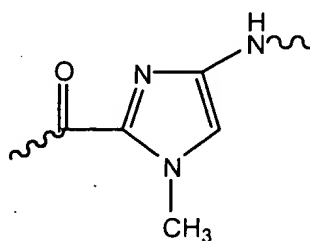
First, the guanidine moiety which is present in arginine is conspicuously absent in N,N-dimethylaminopropylamide. Second, in contrast to N,N-dimethylaminopropylamide, arginine contains several basic nitrogen atoms. Clearly, when these molecules are incorporated into a polyamide, significantly different three dimensional structures, exhibiting significantly different

interactions with a target DNA molecule, will result. Accordingly, the Examiner's assertion that arginine and N,N-dimethylaminopropylamide are chemically similar is respectfully submitted to be in error.

Finally, the referring to the structures below, it is equally clear that the skilled artisan would also understand that histidine is neither functionally nor structurally similar to N-methylimidazole, as the Examiner asserts:



histidine residue
in a polyamide



N-methylimidazole
residue in a polyamide

Thus, given the number of variables that must be selected and modified, the nature and significance of the differences between the various molecules, and the absence of any scientific reason to believe the individual moieties would function in an similar manner to one another, there is no motivation for the skilled artisan to incorporate Arg-Pro-Arg from the Feng *et al.* publication into the polyamide compounds of Swalley, Parks, and Trauger. *See, e.g., In re Jones*, 21 USPQ2d 1941, 1943 (Fed. Cir. 1992) (in an obviousness determination, the number of variables that must be selected or modified and the nature and significance of the differences should be considered); *See also*, MPEP § 2144.08(II)(A)(4) ("The prior art, and not the applicant's disclosure, must provide one of ordinary skill in the art the motivation to make the

proposed molecular modifications needed to arrive at the claimed compound”). Therefore, the Examiner’s rejection cannot be maintained on the basis of “structural similarity.”

Proline, Histidine, and Arginine are also not functionally similar to N-methylpyrrole, N-methylimidazole, and N,N dimethylamino-propylamide, as the Examiner alleges

In arguing that proline and arginine are functionally similar to the N-methylpyrrole N-methylimidazole, and N,N-dimethylaminopropylamide recited in the claims, the Examiner contends that the Feng *et al.* publication “describe[s] polyamides comprising the residues: Gly, Arg, Pro, Arg, wherein said polyamides can be used to bind the minor groove of DNA in a sequence specific manner.” Paper No. 15, page 2. The Examiner alleges that, because the small polyamides disclosed in the Swalley, Parks, and Trauger publications also bind to DNA in a sequence specific manner, the skilled artisan would combine the Arg-Pro-Arg sequence with the small polyamides. Appellants respectfully submit that this is incorrect.

Unlike the small polyamides disclosed in the Swalley, Parks, and Trauger publications, nothing of record indicates that the sequence Arg-Pro-Arg in isolation can bind DNA at all. The Examiner has arrived at this proposed substitution only by selectively choosing the sequence Arg-Pro-Arg from the much larger Hin recombinase molecule disclosed in the Feng *et al.* publication, while ignoring passages in the Feng *et al.* publication that indicate the fallacy of this choice.

For example, the Feng *et al.* publication discloses that the amino acid sequence Gly₁₃₉-Arg₁₄₀-Pro₁₄₁-Arg₁₄₂ is located at the amino-terminal arm of the Hin DNA-binding domain. Feng provides no information about the Arg-Pro-Arg sequence selected in isolation by the Examiner, but does state that the Gly residue in the sequence Gly₁₃₉-Arg₁₄₀ is essential for sequence specific

DNA binding by Hin recombinase. *See*, Feng *et al.*, page 348, column 3. Thus, the Feng *et al.* publication teaches away from removal of the Gly₁₃₉ residue and selecting Arg-Pro-Arg, as the Examiner is proposing.

Moreover, the Feng *et al.* publication also states that α -helix 3, which is located at the carboxyl-terminal end of the DNA binding domain, is the DNA recognition helix for the Hin protein (Feng, p. 350, left column; Fig. 1, p. 348), that the Gly₁₃₉-Arg₁₄₀-Pro₁₄₁-Arg₁₄₂ sequence adopts an extended conformation to present the 4 amino acid sequence in a proper manner to bind DNA. (*See*, Feng *et al.*, page 351, columns 2-3), and that Ile₁₄₄ is critical in maintaining this orientation. *Id.* at column 3. In short, the authors conclude that DNA binding by Hin recombinase is a function of the entire 3-dimensional structure of the protein, stating that “[s]pecific binding requires both major groove interactions involving a helix-turn-helix (HTH) α -helix motif and minor groove interactions involving the sequence Gly₁₃₉-Arg₁₄₀-Pro₁₄₁-Arg₁₄₂.” *Id.* at 348, right column. *See*, *W.L. Gore & Associates, Inc. v. Garlock, Inc.*, 220 USPQ 303 (Fed. Cir. 1983), *cert. denied* 469 U.S. 851 (1984) (a prior art reference must be considered in its entirety, including teachings that would lead away from the claimed invention).

Thus, the Feng *et al.* publication makes it clear that it is only in the overall three-dimensional structure of Hin recombinase that the Gly-Arg sequence has any role in binding DNA. There is no indication in the cited references that the three amino acid sequence selected by the Examiner is in any way functionally similar to the N-methylpyrrole N-methylimidazole, and N,N-dimethylaminopropylamide recited in the claims, as the Examiner contends. Moreover, since the Feng *et al.* publication makes no statements about the Arg-Pro-Arg sequence in isolation, there is no motivation provided by the references or art to make the selections and

perform the steps the Examiner has suggested for grafting these sequences onto the polyamides disclosed in Swalley *et al.*; Parks *et al.* and Trauger *et al.*

The skilled artisan would lack a reasonable expectation of success in grafting an Arg-Pro-Arg sequence to a polyamide molecule to provide the instantly claimed molecules

Because it is only in the context of the 3-dimensional structure of Hin recombinase that the Arg-Pro-Arg sequence selected by the Examiner participates in DNA binding, the skilled artisan would lack a reasonable expectation that simply grafting these amino acids onto the polaymides disclosed in the Swalley, Parks, and Trauger publications to provide the instantly claimed molecules.

In maintaining the rejection, the Examiner contends that “Feng *et al.* teach that sequence Gly-Arg-Pro-Arg is necessary for minor groove binding to DNA.” Paper No. 15, page 3, emphasis added. This is a very different thing, however, from a teaching that the sequence is sufficient for such DNA binding, particularly since the Feng *et al.* publication makes it clear that it is only in the overall three-dimensional structure of Hin recombinase that the Gly-Arg sequence has any role in binding DNA. Thus, unless the skilled artisan understood that the Arg-Pro-Arg sequence was sufficient to provide DNA binding, there would be no reasonable expectation that selecting these three amino acids in isolation from a much larger protein having numerous other amino acids that are also necessary for sequence specific binding would be of any use at all to the small polyamides disclosed in the Swalley, Parks, and Trauger publications. And the Feng *et al.* publication makes it very clear that the Arg-Pro-Arg sequence is not sufficient to provide DNA binding.

Similarly, the Examiner argues that “Feng *et al.* teach the presence of the Arg-Pro-Arg sequence in *Drosophila* Engrailed is also responsible for minor groove binding.” Paper No. 15, page 3. Here, the Examiner mischaracterizes the teachings of the Feng *et al.* publication, which demonstrates that, just as for Hin recombinase, the Arg-Pro-Arg sequence in *Drosophila* engrailed would not bind to DNA in the absence of numerous other engrailed structures. For example, in the very same sentence referred to by the Examiner, the Feng *et al.* publication indicates that an adjacent threonine residue in engrailed also interacts with the DNA by contacting the phosphate backbone. *See*, Feng *et al.*, page 355, left column. Additionally, DNA binding by engrailed requires contacts with the major groove that are very similar to those of Hin recombinase. *See, e.g.*, Feng *et al.*, Figure 10. Thus, just as in the case of Hin recombinase, the Feng *et al.* publication makes it clear that it is only in the overall three-dimensional structure of engrailed that the Arg-Pro-Arg sequence has any role in binding DNA.

Moreover, an enormous number of other proteins also include the Arg-Pro-Arg sequence selected by the Examiner. An internet search of the well known Protein Information Resource (PIR) database reveals that the sequence Arg-Pro-Arg is present in 11,003 proteins in the database, and nothing indicates that each of these “polyamides with a sequence comprising Arg-Pro-Arg... are known to bind DNA with a high affinity in a sequence specific manner.” (Paper No. 10, page 5). The search results and printouts of the relevant web pages with the first 100 proteins obtained are attached as Appendix B.

Viewed in the context of the enormous number of proteins containing the sequence Arg-Pro-Arg, the person of ordinary skill in the art would understand that it is only in the context of the entire Hin recombinase 3-dimensional structure that the sequence would have any role in

“[binding] DNA with a high affinity in a sequence specific manner.” This is also confirmed by the Feng *et al.* publication, which, as discussed above, states that other parts of the Hin recombinase protein are required for sequence specific DNA binding. Furthermore, the Feng *et al.* publication states that “[a] large body of footprinting, mutation, and chemical derivatization data has indicated [the specific binding] features of Hin-DNA interaction... *are distinctive to prokaryotic DNA binding proteins* (emphasis added) (Feng, p. 348, right column), and not generic to the short Arg-Pro-Arg sequence. Therefore, the person of ordinary skill in the art, upon reviewing Feng *et al.*, would understand that the sequence Arg-Pro-Arg would not be suitable for use in isolation as some sort of DNA-binding motif.

Thus, because the Feng *et al.* completely fails to teach or suggest that this sequence has any general applicability to DNA binding, or any applicability outside of the specific Hin recombinase, there is no reasonable expectation of success in making the combination proposed by the Examiner.

The skilled artisan would not seek to graft an Arg-Pro-Arg sequence to a polyamide molecule to provide the “positive patch” of the instant claims

Furthermore, the Examiner’s arguments in support of the asserted *prima facie* case relies on the contention that the skilled artisan would be allegedly motivated to graft an Arg-Pro-Arg sequence obtained from the Feng *et al.* publication onto the polyamides disclosed in Swalley *et al.*; Parks *et al.* and Trauger *et al.*, to provide the “positive patch” of the instant claims, because of an asserted “similarity” between arg and pro, and the pyrrole- and imidazole-based residues disclosed in the Swalley, Parks, and Trauger publications. But the Examiner ignores the fact that

the “positive patch” of the instant claims does not serve a minor groove binding function, as the Examiner apparently believes.

For example, the inclusion of the positively charged group is intended to disrupt interactions between proteins and the phosphate backbone or major groove of the DNA molecule, and not to bind to the minor groove. *See, e.g.*, specification, page 14, lines 20-29. There is nothing of record in the asserted *prima facie* case to indicate that the skilled artisan would be motivated to select an Arg-Pro-Arg sequence, as disclosed in the Feng *et al.* publication, in order to disrupt interactions between proteins and the phosphate backbone or major groove of the DNA molecule. Furthermore, because nothing of record indicates that an Arg-Pro-Arg sequence would serve such a function, the skilled artisan would lack a reasonable expectation of success in combining the references as suggested by the Examiner to provide the instantly claimed polyamide molecules.

The Examiner Has Used Impermissible Hindsight in Making Selections and Combinations

When the claims are properly interpreted, it is apparent that neither the references cited by the Examiner nor the knowledge available to one of ordinary skill in the art provide a motivation for making the proposed combination, or a reasonable expectation of success in doing so. Applicants respectfully submit that, instead of carrying the burden of establishing a *prima facie* case of obviousness, the Examiner has fallen victim to “...decomposing an invention into its constituent elements, finding each element in the prior art, and then claiming that it is easy to reassemble these elements into the invention...”. *In re Mahurkar*, 28 USPQ2d 1801, 1817 (N.D. Ill. 1993). An obviousness determination cannot be premised on such an impermissible use of hindsight. *See, In re Fine*, 5 USPQ2d 1596, 1600 (Fed. Cir. 1988) (“To imbue one of ordinary

skill in the art with knowledge of the invention in suit, when no prior art reference or references of record convey or suggest that knowledge, is to fall victim to the insidious effect of a hindsight syndrome wherein that which only the inventor taught is used against the teacher.”)

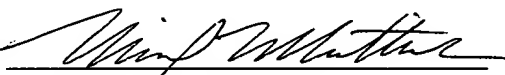
Conclusion

For the reasons discussed above, the Examiner has failed to carry the burden of establishing a *prima facie* case of obviousness. Appellants respectfully submit the instant claims are in condition for allowance, and respectfully request that the rejections be withdrawn or reversed, and that the rejected claims, together with the claims previously indicated as allowable, be allowed to issue.

Respectfully submitted,

FOLEY & LARDNER

Dated: October 8, 2001

By: 
Michael A. Whittaker
Registration No. 46,230

P.O. Box 80278
San Diego, CA 92138-0278
Telephone: (858) 847-6700

Recognition of a 5'-(A,T)GGG(A,T)₂-3' Sequence in the Minor Groove of DNA by an Eight-Ring Hairpin Polyamide

Susanne E. Swalley, Eldon E. Baird, and Peter B. Dervan*

Contribution from the Division of Chemistry and Chemical Engineering,
California Institute of Technology, Pasadena, California 91125

Received April 8, 1996

Abstract: The use of pyrrole-imidazole polyamides for the recognition of core 5'-GGG-3' sequences in the minor groove of double stranded DNA is described. Two hairpin pyrrole-imidazole polyamides, ImImIm- γ -PyPyPy- β -Dp and ImImImPy- γ -PyPyPy- β -Dp (Im = *N*-methylimidazole-2-carboxamide, Py = *N*-methylpyrrole-2-carboxamide, β = β -alanine, γ = γ -aminobutyric acid, and Dp = ((dimethylamino)propyl)amide), as well as the corresponding EDTA affinity cleaving derivatives, were synthesized and their DNA binding properties analyzed. Quantitative DNase I footprint titrations demonstrate that ImImIm- γ -PyPyPy- β -Dp binds the formal match sequence 5'-AGGGA-3' with an equilibrium association constant of $K_a = 5 \times 10^6 \text{ M}^{-1}$ (10 mM Tris-HCl, 10 mM KCl, 10 mM MgCl₂, and 5 mM CaCl₂, pH 7.0 and 22 °C). ImImImPy- γ -PyPyPy- β -Dp binds the same site, 5'-AGGGAA-3', approximately two orders of magnitude more tightly than the six ring polyamide, with an equilibrium association constant of $K_a = 4 \times 10^8 \text{ M}^{-1}$. The eight-ring hairpin polyamide demonstrates greater specificity for single base pair mismatches than does the six ring hairpin. Polyamides with an EDTA-Fe(II) moiety at the carboxy terminus confirm that each hairpin binds in a single orientation. The high affinity recognition of a 5'-GGG-3' core sequence by an eight ring polyamide containing three contiguous imidazole amino acids demonstrates the versatility of pyrrole-imidazole polyamides and broadens the sequence repertoire for DNA recognition.

Introduction

Pyrrole-imidazole polyamide-DNA complexes afford a general method for the design of non-natural molecules for sequence-specific recognition in the minor groove of DNA.¹⁻⁵ Polyamides containing *N*-methylpyrrole (Py) and *N*-methylimidazole (Im) carboxamides bind to the minor groove as side-by-side antiparallel dimers and are capable of specific recognition of sequences containing G-C base pairs, where the N3 of each imidazole forms a hydrogen bond with a single guanine exocyclic amino group.¹ The side-by-side pairing of an imidazole ring from one polyamide with a pyrrole ring from the second polyamide recognizes a G-C base pair, while a pyrrole-imidazole combination recognizes a C-G base pair.¹ Finally, a pyrrole-pyrrole pair recognizes either an A-T or T-A base pair.^{1,2} By employing the 2:1 model, specific recognition of the sequences 5'-(A,T)G(A,T)C(A,T)-3', 5'-(A,T)G(A,T)₂-3', 5'-(A,T)₂G(A,T)-3', and 5'-(A,T)GCGC(A,T)-3' has been achieved.¹⁻⁵

Covalent head-to-tail linkage of two polyamides by γ -aminobutyric acid (γ) to form a "hairpin" polyamide results in both increased affinity and specificity, as compared to the unlinked

polyamides.⁶ For instance, the 1:1 hairpin motif has been used to recognize 5'-(A,T)G(A,T)₂-3' by ImPyPy- γ -PyPyPy-Dp with approximately 300-fold greater affinity than the unlinked polyamides, ImPyPy and PyPyPy.⁶ A C-terminal β -alanine residue increases both affinity and specificity and facilitates solid phase synthesis, as recently demonstrated with ImPyPy- γ -PyPyPy- β -Dp.^{7,8} Furthermore, a sequence containing two contiguous G-C base pairs, 5'-(A,T)GG(A,T)₂-3', has been recognized by ImImPy- γ -PyPyPy- β -Dp.⁹

To further expand the sequence repertoire available with the hairpin motif, two polyamides containing three contiguous imidazole rings, ImImIm- γ -PyPyPy- β -Dp (1) and ImImImPy- γ -PyPyPy- β -Dp (2), and the corresponding affinity cleaving analogs, ImImIm- γ -PyPyPy- β -Dp-EDTA (1-E) and ImImImPy- γ -PyPyPy- β -Dp-EDTA (2-E), were synthesized using solid phase synthetic protocols (Figures 1 and 2).⁷ Specific hydrogen bonds are expected to form between each imidazole N3 and one of the three individual guanine 2-amino groups on the floor of the minor groove (Figure 1). The eight-ring hairpin polyamide, with a pyrrole between the C-terminal imidazole and the γ -linker, was synthesized to examine whether the positioning of the final imidazole immediately adjacent to the turn would adversely affect binding affinity or specificity. We report here the affinities and relative specificities of these tris-imidazole polyamides as determined by three separate techniques: MPE-Fe(II) footprinting,¹⁰ DNase I footprinting,¹¹ and affinity cleaving.¹² Information about binding site size is gained from MPE-Fe(II) footprinting, while quantitative DNase I footprint titrations

* Abstract published in *Advance ACS Abstracts*, August 15, 1996.

(1) (a) Wade, W. S.; Mrksich, M.; Dervan, P. B. *J. Am. Chem. Soc.* 1992, 114, 8783. (b) Mrksich, M.; Wade, W. S.; Dwyer, T. J.; Geierstanger, B. H.; Wenner, D. E.; Dervan, P. B. *Proc. Natl. Acad. Sci. U.S.A.* 1992, 89, 7586. (c) Wade, W. S.; Mrksich, M.; Dervan, P. B. *Biochemistry* 1993, 32, 11385.

(2) (a) Pelton, J. G.; Wenner, D. E. *Proc. Natl. Acad. Sci. U.S.A.* 1989, 86, 5723. (b) Pelton, J. G.; Wenner, D. E. *J. Am. Chem. Soc.* 1990, 112, 1393. (c) Chen, X.; Ramakrishnan, B.; Rao, S. T.; Sundaralingham, M. *Struct. Biol. Nature* 1994, 1, 169.

(3) (a) Mrksich, M.; Dervan, P. B. *J. Am. Chem. Soc.* 1993, 115, 2572. (b) Geierstanger, B. H.; Jacobsen, J.-P.; Mrksich, M.; Dervan, P. B.; Wenner, D. E. *Biochemistry* 1994, 33, 3055.

(4) Geierstanger, B. H.; Dwyer, T. J.; Bathini, Y.; Lown, J. W.; Wenner, D. E. *J. Am. Chem. Soc.* 1993, 115, 4474.

(5) (a) Geierstanger, B. H.; Mrksich, M.; Dervan, P. B.; Wenner, D. E. *Science* 1994, 266, 646. (b) Mrksich, M.; Dervan, P. B. *J. Am. Chem. Soc.* 1995, 117, 3325.

(6) Mrksich, M.; Parks, M. E.; Dervan, P. B. *J. Am. Chem. Soc.* 1994, 116, 7983.

(7) Baird, E. E.; Dervan, P. B. *J. Am. Chem. Soc.* 1996, 118, 6141.

(8) Parks, M. E.; Baird, E. E.; Dervan, P. B. *J. Am. Chem. Soc.* 1996, 118, 6147.

(9) Parks, M. E.; Baird, E. E.; Dervan, P. B. *J. Am. Chem. Soc.* 1996, 118, 6153.

(10) (a) Van Dyke, M. W.; Dervan, P. B. *Biochemistry* 1983, 22, 2373.

(b) Van Dyke, M. W.; Dervan, P. B. *Nucleic Acids Res.* 1983, 11, 5555.

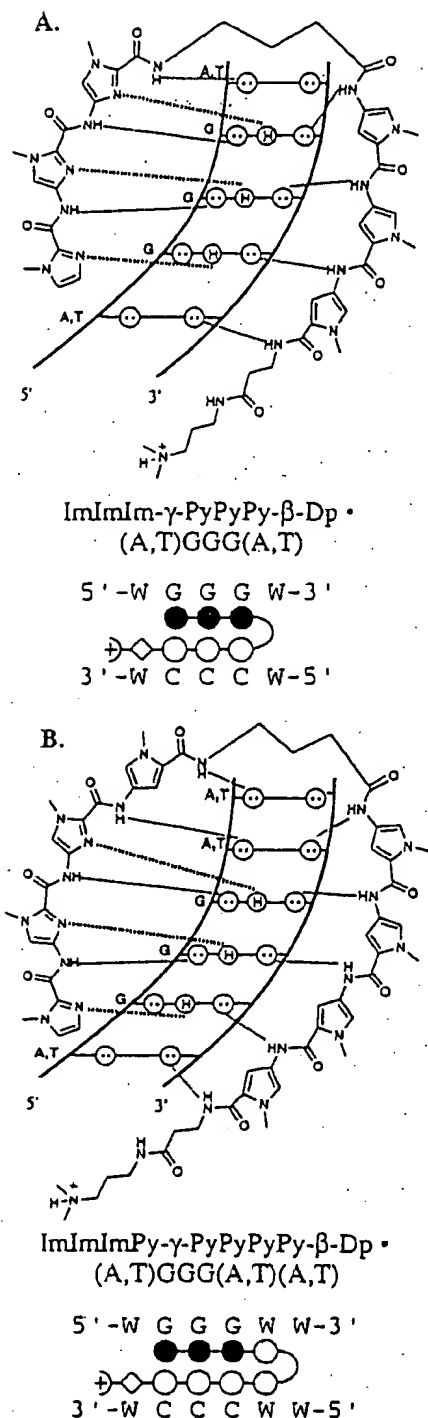


Figure 1. Binding model for the complexes formed between the DNA and either the six-ring hairpin polyamide ImImImPy-γ-PyPyPy-β-Dp (A) or the eight-ring hairpin polyamide ImImImPy-γ-PyPyPyPy-β-Dp (B). Circles with dots represent lone pairs of N3 of purines and O2 of pyrimidines. Circles containing an H represent the N2 hydrogen of guanine. Putative hydrogen bonds are illustrated by dotted lines. Ball and stick models are also shown. Shaded and nonshaded circles denote imidazole and pyrrole carboxanides, respectively. Nonshaded diamonds represent the β-alanine residue. W represents either an A or T base.

allow the determination of equilibrium association constants (K_a) for the polyamides to a variety of match and single base pair mismatch sequences. Affinity cleavage studies confirm the binding orientation and stoichiometry of the 1:1 hairpin:DNA complex.

Results

Synthesis of Polyamides. The polyamides ImImImPy-γ-PyPyPy-β-Dp (1) and ImImImPy-γ-PyPyPyPy-β-Dp (2) were synthesized in a stepwise manner from Boc-β-alanine-Pam resin using recently described Boc-chemistry protocols in 14 and 18 steps, respectively.⁷ The polyamides were then cleaved by a single step aminolysis reaction with ((dimethylamino)propyl)-amine and subsequently purified by HPLC chromatography. The syntheses of the polyamides, ImImImPy-γ-PyPyPyPy-β-Dp (2), ImImImPy-γ-PyPyPyPy-β-Dp-NH₂ (2-NH₂), and ImImImPy-γ-PyPyPyPy-β-Dp-EDTA (2-E), are outlined (Figure 3). For the synthesis of the EDTA analog, a sample of resin is treated with 3,3'-diamino-N-methyldipropylamine (55 °C) and then purified by preparatory HPLC to provide 2-NH₂. The polyamide ImImImPy-γ-PyPyPyPy-β-Dp-NH₂ (2-NH₂) provides a free aliphatic primary amine group suitable for modification. This polyamide-amine is then treated with an excess of the dianhydride of EDTA (DMSO/NMP, DIEA, 55 °C) and the remaining anhydride hydrolyzed (0.1 M NaOH, 55 °C). The EDTA modified polyamide is then isolated by preparatory HPLC.

Identification of Binding Site Size and Orientation by MPE·Fe(II) Footprinting and Affinity Cleaving. MPE·Fe(II) footprinting on the 3'- and 5'-³²P end-labeled 274 base pair *EcoRI/PvuII* restriction fragment from plasmid pSES1 (25 mM Tris-acetate, 10 mM NaCl, 100 μM calf thymus DNA, pH 7.0 and 22 °C) reveals that the polyamides, each at 10 μM concentration, are binding to the four designed sites, 5'-AGGGA(A)-3', 5'-AGGCA(A)-3', 5'-TGGGT(C)-3', and 5'-TGGGC(T)-3' (Figures 4 and 5). No footprinting is seen with either compound at the single base pair mismatch site, 5'-AGGAA(A)-3' (Figure 4, quantitated data not shown). The footprinting patterns for the six-ring polyamide are consistent with five base pair binding sites, while the patterns for the eight-ring polyamide are indicative of six base pair binding sites. Affinity cleavage experiments on the same restriction fragment (25 mM Tris-acetate, 200 mM NaCl, 50 μg/mL glycogen, pH 7.0 and 22 °C) by the six-ring and eight-ring EDTA·Fe(II) analogs reveal cleavage patterns that are 3'-shifted and appear on only one side of each binding site (Figures 4 and 5). ImImImPy-γ-PyPyPy-β-Dp-EDTA·Fe(II), at 1 μM, and ImImImPy-γ-PyPyPyPy-β-Dp-EDTA·Fe(II), at 100 nM, show cleavage patterns that demonstrate recognition of the same binding sites identified by MPE·Fe(II) footprinting. No carrier DNA was used in these experiments, and thus the relative cleavage intensities indicate that the six-ring polyamide binds most strongly to the two match sites 5'-AGGGA-3' and 5'-TGGGT-3'; followed by the end mismatch 5'-TGGGC-3'. The core mismatch 5'-AGGCA-3', with little appreciable cleavage at 1 μM concentration, is bound more weakly. Similarly, the eight-ring polyamide binds most strongly at 100 nM to 5'-AGGGAA-3', much less strongly to 5'-TGGGTC-3', and not significantly to 5'-TGGGCT-3' and 5'-AGGCAA-3'.

Determination of Binding Affinities by Quantitative DNase I Footprinting. Quantitative DNase I footprint titration experiments (10 mM Tris-HCl, 10 mM KCl, 10 mM MgCl₂, and 5 mM CaCl₂, pH 7.0 and 22 °C) were performed to determine

(11) (a) Brenowitz, M.; Seneor, D. F.; Shea, M. A.; Ackers, G. K. *Methods Enzymol.* 1986, 130, 132. (b) Brenowitz, M.; Seneor, D. F.; Shea, M. A.; Ackers, G. K. *Proc. Natl. Acad. Sci. U.S.A.* 1986, 83, 8462. (c) Seneor, D. F.; Brenowitz, M.; Shea, M. A.; Ackers, G. K. *Biochemistry* 1986, 25, 7344.

(12) (a) Schultz, P. G.; Taylor, J. S.; Dervan, P. B. *J. Am. Chem. Soc.* 1982, 104, 6861. (b) Schultz, P. G.; Dervan, P. B. *J. Biol. Struct. Dyn.* 1984, 1, 1133. (c) Taylor, J. S.; Schultz, P. B.; Dervan, P. B. *Tetrahedron* 1984, 40, 457.

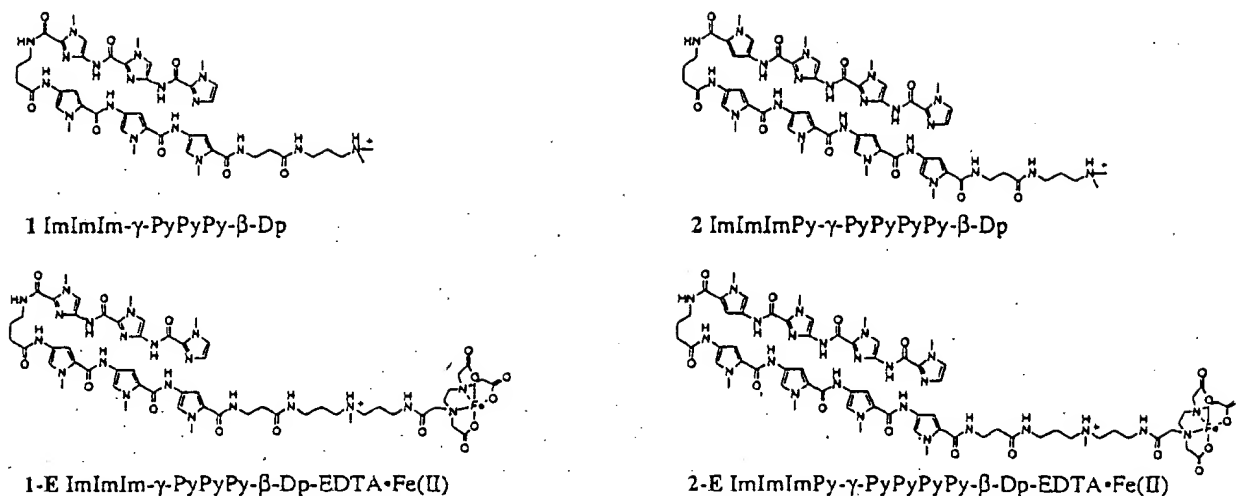


Figure 2. Structures of the tris-imidazole polyamides and their EDTA derivatives synthesized using solid-phase methodology.⁷

the equilibrium association constants of the polyamides for the four bound sites (Table 1).¹¹ ImImIm- γ -PyPyPy- β -Dp binds the two match sites 5'-AGGGA-3' and 5'-TGGGT-3' with equilibrium association constants of $K_a = 4.6 \times 10^6$ and 7.6×10^6 M⁻¹, respectively (Figures 6–8). The sequence 5'-TGGGC-3', which has a mismatch in the non-core final position (an "end" mismatch), is bound with 6-fold lower affinity than the best match, while the core mismatch sequence 5'-AGGCA-3' is bound with 9-fold lower affinity. ImImImPy- γ -PyPyPy- β -Dp binds the match site 5'-AGGGAA-3' with an equilibrium association constant of $K_a = 3.7 \times 10^8$ M⁻¹. The end mismatch 5'-TGGGTC-3' is bound with 26-fold lower affinity, and the two core-mismatches, 5'-AGGCAA-3' and 5'-TGGGCT-3', are bound with 130-fold and 220-fold lower affinity, respectively. Neither polyamide shows any appreciable binding to the core mismatch 5'-AGGAA(A)-3' (data not shown).

Discussion

The two hairpin polyamides recognize the targeted 5'-AGGGA(A)-3' sequence, as determined by MPE·Fe(II) footprinting and affinity cleaving, demonstrating specific recognition by polyamides of sequences containing *three contiguous* G·C base pairs, 5'-GGG-3'. Affinity cleavage data indicate that each polyamide is binding in the minor groove in a single orientation, consistent with the hairpin binding model (Figures 1 and 5). The relative intensities of the cleavage patterns are consistent with quantitative DNase I footprint titration results.

Quantitative DNase I footprint titrations reveal that ImImIm- γ -PyPyPy- β -Dp binds the designed match sites 5'-AGGGA-3' and 5'-TGGGT-3' with equilibrium association constants of $K_a = 5 \times 10^6$ and 8×10^6 M⁻¹, respectively. For comparison, the analogous six-ring hairpins containing only one and two contiguous imidazoles, ImPyPy- γ -PyPyPy- β -Dp and ImImPy- γ -PyPyPy- β -Dp, bind their respective match sites with affinities of $K_a \approx 10^8$ M⁻¹.^{8,9} The addition of the third imidazole reduces binding affinity significantly, perhaps due to the inability of the polyamide to sit deeply in the sterically crowded minor groove, decreasing energetically favorable van der Waals contacts. Examination of the eight-ring hairpin, ImImImPy- γ -PyPyPy- β -Dp, reveals a dramatically increased affinity, the match site 5'-AGGGAA-3' being bound with an equilibrium association constant of $K_a = 4 \times 10^8$ M⁻¹. The 80-fold increase in affinity in expanding from a three-ring to a four-ring hairpin polyamide mirrors the 66-fold enhancement of ImPyPy- β -Dp

over ImPyPy- β -Dp that was observed in the 2:1 homodimeric polyamide:DNA motif.¹³

In addition to the observation that the eight-ring ImImImPy- γ -PyPyPy- β -Dp binds with higher affinity than the six ring ImImIm- γ -PyPyPy- β -Dp, the enhanced specificity is perhaps more significant. The six-ring hairpin polyamide binds 5'-TGGGC-3', an end mismatch site, with 6-fold lower affinity compared to 5'-TGGGT-3' (the highest affinity match), while the eight-ring hairpin polyamide binds its end mismatch site 5'-TGGGTC-3' with 26-fold lower affinity compared to its match site 5'-AGGGAA-3'. Similarly, 5'-AGGCA-3', a site containing a single base pair core mismatch, is bound by the six-ring system with 9-fold lower affinity, while the two core mismatch sites for the eight-ring system, 5'-AGGCAA-3' and 5'-TGGGCT-3', are recognized with 130-fold and 220-fold lower affinity, respectively. For both polyamides, binding of a site with a core single base pair mismatch results in a greater energetic penalty than binding of a site with single base pair mismatch in the end position. The increased specificity of ImImImPy- γ -PyPyPy- β -Dp over ImImIm- γ -PyPyPy- β -Dp may indicate that an imidazole placed immediately to the N-terminal side of the γ turn does not form as strong a hydrogen bond as in other positions.

Implications for the Design of Minor Groove Binding Molecules. Pyrrole-imidazole polyamides have been used to recognize a variety of target sequences containing A·T and G·C base pairs.^{1,2,4,5,9} By recognizing sequences containing *three* contiguous G·C base pairs, 5'-(A,T)GGG(A,T)-3' and 5'-(A,T)GGG(A,T)₂-3', this work expands the sequence-composition repertoire targetable by the hairpin polyamide motif. Both affinity and specificity for a G·C rich sequence are increased by the use of an eight-ring hairpin polyamide. This ability to enlarge the sequence repertoire, combined with rapid solid-phase synthesis, brings us one step closer to a universal approach for the recognition of any desired DNA sequence by strictly chemical methods.

Experimental Section

Dicyclohexylcarbodiimide (DCC), hydroxybenzotriazole (HOBt), 2-(1*H*-benzotriazole-1-yl)-1,1,3,3-tetramethyluronium hexafluorophosphate (HBTU), and 0.2 mmol/g of Boc- β -alanine-(4-carboxamidomethyl) benzyl ester-copoly(styrene-divinylbenzene) resin (Boc- β -Pam-Resin) were purchased from Peptides International. *N,N*-Diiso-

(13) Kelly, J. J.; Baird, E. E.; Dervan, P. B. *Proc. Natl. Acad. Sci. U.S.A.* 1996, 93, 6981.

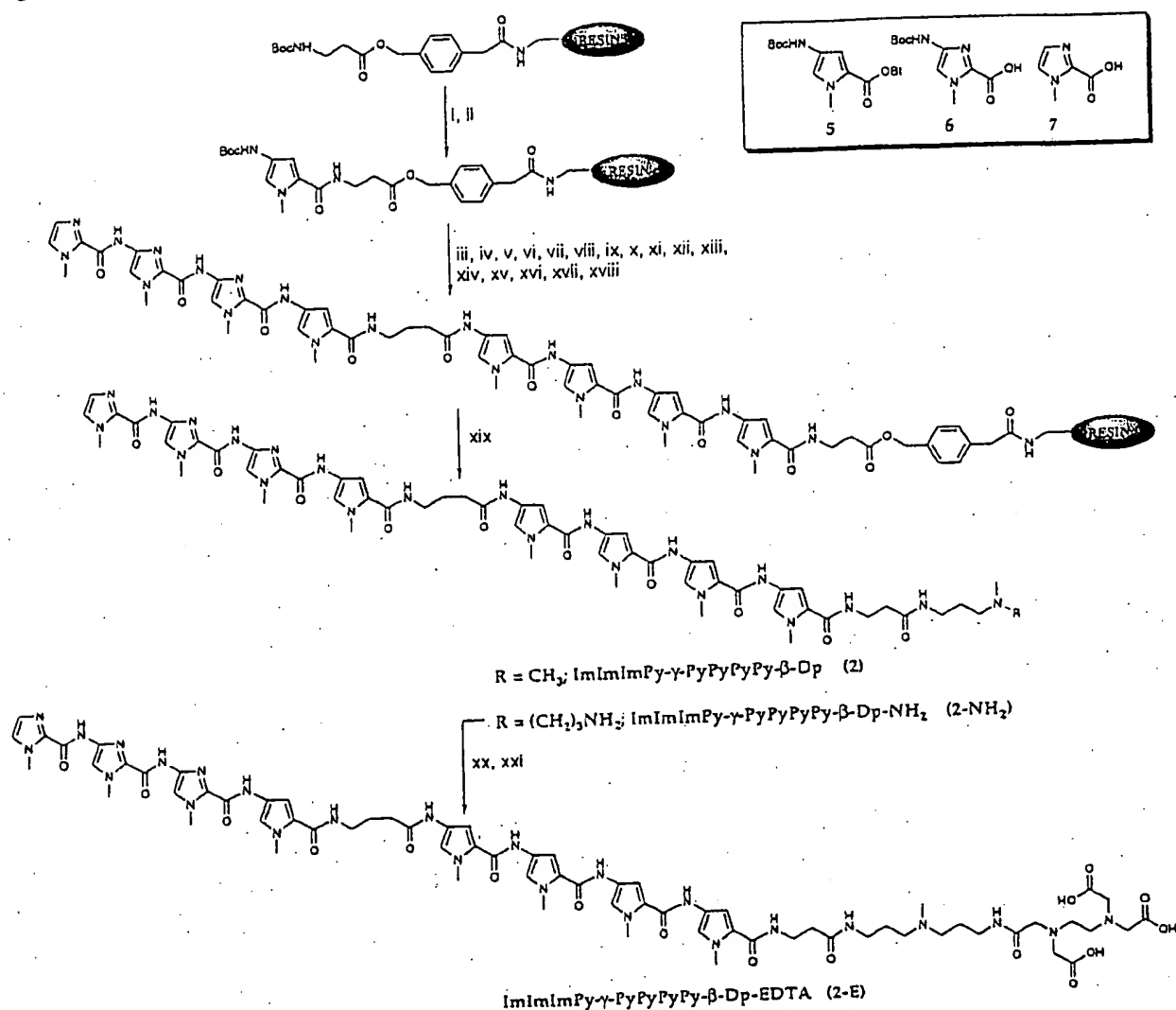


Figure 3. (Box) Pyrrole and imidazole monomers for synthesis of all compounds described here: Boc-pyrrole-OBt ester 5,⁷ Boc-imidazole-acid 6,⁷ and imidazole-2-carboxylic acid 7.¹⁸ Solid-phase synthetic scheme for ImImImPy-γ-PyPyPyPy-β-Dp, ImImImPy-γ-PyPyPyPy-β-Dp-NH₂, and ImImImPy-γ-PyPyPyPy-β-Dp-EDTA prepared from commercially available Boc-β-alanine-Pam-resin (0.2 mmol/g): (i) 80% TFA/DCM, 0.4 M PhSH; (ii) 80% TFA/DCM, 0.4 M PhSH; (iii) BocPy-OBt, DIEA, DMF; (iv) 80% TFA/DCM, 0.4 M PhSH; (v) BocPy-OBt, DIEA, DMF; (vi) 80% TFA/DCM, 0.4 M PhSH; (vii) BocPy-OBt, DIEA, DMF; (viii) BocPy-OBt, DIEA, DMF; (ix) 80% TFA/DCM, 0.4 M PhSH; (x) Boc-γ-aminobutyric acid (HBTU, DIEA), DMF; (xi) 80% TFA/DCM, 0.4 M PhSH; (xii) BocPy-OBt, DIEA, DMF; (xiii) 80% TFA/DCM, 0.4 M PhSH; (xiv) BocIm-OBt (DCC/HOBt), DIEA, DMF; (xv) 80% TFA/DCM, 0.4 M PhSH; (xvi) BocIm-OBt (DCC/HOBt), DIEA, DMF; (xvii) 80% TFA/DCM, 0.4 M PhSH; (xviii) imidazole-2-carboxylic acid (HBTU/DIEA); (xix) ((N,N-dimethylamino)propyl)amine or 3,3'-diamino-N-methyldipropylamine, 55 °C; (xx) 0.1 M NaOH.

propylethylamine (DIEA), *N,N*-dimethylformamide (DMF), *N*-methylpyrrolidone (NMP), DMSO/NMP, acetic anhydride (Ac₂O), and 0.0002 M potassium cyanide/pyridine were purchased from Applied Biosystems. Boc-γ-aminobutyric acid was from NOVA Biochem, dichloromethane (DCM) and triethylamine (TEA) were reagent grade from EM, thiophenol (PhSH), ((dimethylamino)propyl)amine was from Aldrich, trifluoroacetic acid (TFA) was from Halocarbon, phenol was from Fisher, and ninhydrin was from Pierce. All reagents were used without further purification.

Quik-Sep polypropylene disposable filters were purchased from Isolab Inc. and were used for filtration of DCU. Disposable polypropylene filters were also used for washing resin for ninhydrin and picric acid tests and for filtering predissolved amino acids into reaction vessels. A shaker for manual solid-phase synthesis was obtained from St. John Associates, Inc. Screw-cap glass peptide synthesis reaction vessels (5 and 20 mL) with a #2 sintered glass frit were made as described by Kent.¹⁴ ¹H NMR spectra were recorded on a General Electric-QE NMR

spectrometer at 300 MHz in DMSO-*d*₆, with chemical shifts reported in parts per million relative to residual solvent. UV spectra were measured in water on a Hewlett-Packard Model 8452A diode array spectrophotometer. Matrix-assisted, laser desorption/ionization time-of-flight mass spectrometry (MALDI-TOF) was performed at the Protein and Peptide Microanalytical Facility at the California Institute of Technology. HPLC analysis was performed on either a HP 1090M analytical HPLC or a Beckman Gold system using a RAINEN C₁₈ Microsorb MV, 5 μm, 300 × 4.6 mm reversed phase column in 0.1% (wt/v) TFA with acetonitrile as eluent and a flow rate of 1.0 mL/min, gradient elution 1.25% acetonitrile/min. Preparatory reverse-phase HPLC was performed on a Beckman HPLC with a Waters DeltaPak 25 × 100 mm, 100 μm C₁₈ column equipped with a guard, 0.1% (wt/v) TFA, 0.25% acetonitrile/min. The 18MΩ water was obtained from a Millipore MilliQ water purification system, and all buffers were 0.2 μm filtered.

ImImImPy-γ-PyPyPyPy-β-Dp (1). The product was synthesized by manual solid-phase protocols⁷ and recovered as a white powder (2.4 mg, 4% recovery). UV λ_{max} 312 (48 500); ¹H NMR (DMSO-*d*₆) δ

(14) Kent, S. B. H. *Annu. Rev. Biochem.* 1988, 57, 957.

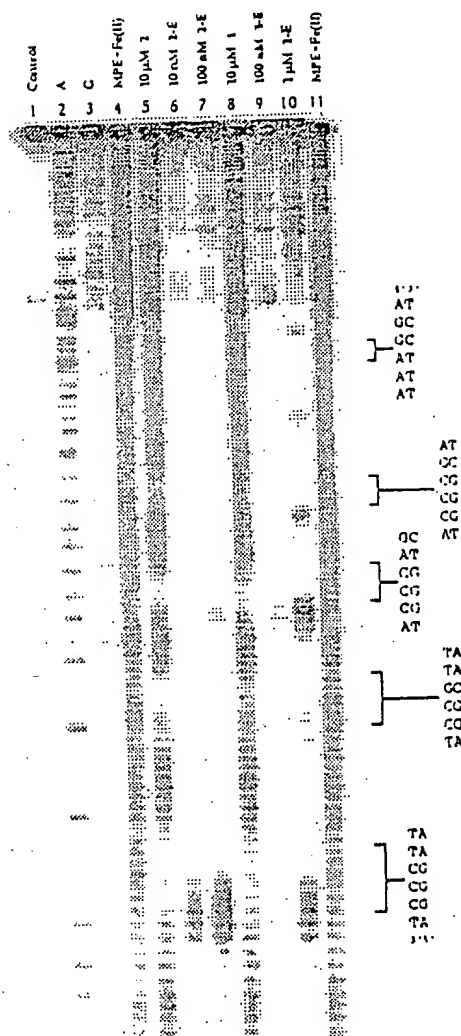


Figure 4. MPE-Fe(II) footprinting and affinity cleavage experiments on a 3'-³²P-labeled 274 bp *EcoRI/PvuII* restriction fragment from plasmid pSES1. The 5'-AGGGA(A)-3', 5'-AGGCA(A)-3', 5'-TGGGT-(C)-3', 5'-TGGGC(T)-3', and 5'-AGGAA(A)-3' sites are shown on the right side of the autoradiogram. Lane 1, intact DNA; lane 2, A reaction; lane 3, G reaction; lanes 4 and 11, MPE-Fe(II) standard; lane 5, 10 μ M ImImImPy- γ -PyPyPy- β -Dp; lanes 6 and 7, 10 nM and 100 nM ImImImPy- γ -PyPyPy- β -Dp-EDTA-Fe(II); lane 8, 10 μ M ImImImPy- γ -PyPyPy- β -Dp; lanes 9 and 10, 100 nM and 1 μ M ImImImPy- γ -PyPyPy- β -Dp-EDTA-Fe(II). All lanes contain 15 kcpm 3'-radiolabeled DNA. The control and MPE-Fe(II) lanes (1, 4, 5, 8, and 11) contain 25 mM Tris-acetate buffer (pH 7.0), 10 mM NaCl, and 100 μ M/base pair calf thymus DNA. The affinity cleavage lanes (6, 7, 9, and 10) contain 25 mM Tris-acetate buffer (pH 7.0), 200 mM NaCl, and 50 μ g/mL glycogen.

10.09 (s, 1 H), 9.89 (s, 1 H), 9.88 (s, 1 H), 9.83 (s, 1 H), 9.57 (s, 1 H), 9.19 (br s, 1 H), 8.36 (t, 1 H, J = 5.6 Hz), 8.03 (m, 2 H), 7.64 (s, 1 H), 7.51 (s, 1 H), 7.45 (s, 1 H), 7.20 (d, 1 H, J = 1.0 Hz), 7.15 (d, 1 H, J = 2.0 Hz), 7.14 (s, 1 H), 7.08 (s, 1 H), 7.04 (s, 1 H), 6.87 (d, 2 H, J = 2.2 Hz), 4.01 (s, 3 H), 3.99 (s, 3 H), 3.95 (s, 3 H), 3.82 (s, 3 H), 3.82 (s, 3 H), 3.79 (s, 3 H), 3.37 (q, 2 H, J = 5.8 Hz), 3.26 (q, 2 H, J = 6.1 Hz), 3.10 (q, 2 H, J = 6.1 Hz), 2.99 (m, 2 H), 2.73 (d, 6 H, J = 4.8 Hz), 2.34 (t, 2 H, J = 7.2 Hz), 2.27 (t, 2 H, J = 7.3 Hz), 1.79 (m, 4 H); MALDI-TOF-MS, 980.1 (980.1 calcd for M + H).

ImImImPy- γ -PyPyPy- β -Dp (2). The product was synthesized by manual solid-phase protocols⁷ and recovered as a white powder (7.6 mg, 11% recovery). UV λ_{max} 248 (42 000), 312 (48 500); ¹H NMR (DMSO-*d*₆) δ 10.32 (s, 1 H), 10.13 (s, 1 H), 9.93 (s, 1 H), 9.90 (s, 1 H), 9.89 (s, 1 H), 9.84 (s, 1 H), 9.59 (s, 1 H), 9.23 (br s, 1 H), 8.09 (t,

1 H, J = 5.3 Hz), 8.04 (m, 2 H), 7.65 (s, 1 H), 7.57 (s, 1 H), 7.46 (d, 1 H, J = 0.6 Hz), 7.22 (m, 3 H), 7.16 (s, 2 H), 7.09 (d, 1 H, J = 0.8 Hz), 7.06 (d, 2 H, J = 1.1 Hz), 7.00 (d, 1 H, J = 1.7), 6.88 (d, 1 H, J = 1.8), 6.87 (d, 1 H, J = 1.8 Hz), 4.02 (s, 3 H), 4.00 (s, 3 H), 3.99 (s, 3 H), 3.84 (s, 3 H), 3.83 (s, 3 H), 3.83 (s, 3 H), 3.83 (s, 3 H), 3.80 (s, 3 H), 3.79 (s, 3 H), 3.37 (q, 2 H, J = 6.2 Hz), 3.21 (q, 2 H, J = 6.4 Hz), 3.10 (q, 2 H, J = 6.2 Hz), 3.00 (m, 2 H), 2.73 (d, 6 H, J = 4.9 Hz), 2.34 (t, 2 H, J = 7.2 Hz), 2.28 (t, 2 H, J = 7.0 Hz), 1.76 (m, 4 H); MALDI-TOF-MS, 1225.9 (1224.3 calcd for M + H).

ImImImPy- γ -PyPyPy- β -Dp-NH₂ (1-NH₂). A sample of machine-synthesized resin (350 mg, 0.17 mmol/g¹⁵) was placed in a 20 mL glass scintillation vial and treated with 2 mL of 3,3'-diamino-*N*-methylpropylamine at 55 °C for 18 h. The resin was removed by filtration through a disposable propylene filter, and the resulting solution was dissolved in water to a total volume of 8 mL and purified directly by preparatory reversed-phase HPLC to provide ImImImPy- γ -PyPyPy- β -Dp-NH₂ (28 mg, 41% recovery) as a white powder. ¹H NMR (DMSO-*d*₆) δ 10.14 (s, 1 H), 9.89 (s, 1 H), 9.88 (s, 1 H), 9.83 (s, 1 H), 9.6 (br s, 1 H), 9.59 (s, 1 H), 8.36 (t, 1 H, J = 5.5 Hz), 8.09 (t, 1 H, J = 5.0 Hz), 8.03 (t, 1 H, J = 5.0 Hz), 7.9 (br s, 3 H), 7.63 (s, 1 H), 7.50 (s, 1 H), 7.44 (s, 1 H), 7.19 (d, 1 H, J = 1.2 Hz), 7.13 (m, 2 H), 7.08 (d, 1 H, J = 1.3 Hz), 7.02 (d, 1 H, J = 1.2 Hz), 6.85 (m, 2 H), 4.01 (s, 3 H), 3.99 (s, 3 H), 3.97 (m, 6 H), 3.80 (s, 3 H), 3.77 (s, 3 H), 3.34 (q, 2 H, J = 5.3 Hz), 3.23 (q, 2 H, J = 6.0 Hz), 3.05 (m, 6 H), 2.83 (q, 2 H, J = 5.0 Hz), 2.70 (d, 3 H, J = 4.0 Hz), 2.32 (t, 2 H, J = 6.9 Hz), 2.25 (t, 2 H, J = 6.9 Hz), 1.90 (m, 2 H), 1.77 (m, 4 H); MALDI-TOF-MS, 1022.8 (1023.1 calcd for M + H).

ImImImPy- γ -PyPyPy- β -Dp-NH₂ (2-NH₂). A sample of machine-synthesized resin (350 mg, 0.16 mmol/g¹⁵) was placed in a 20 mL glass scintillation vial and treated with 2 mL of 3,3'-diamino-*N*-methylpropylamine at 55 °C for 18 h. The resin was removed by filtration through a disposable propylene filter, and the resulting solution was dissolved in water to a total volume of 8 mL and purified directly by preparatory reversed-phase HPLC to provide ImImImPy- γ -PyPyPy- β -Dp-NH₂ (31 mg, 40% recovery) as a white powder. ¹H NMR (DMSO-*d*₆) δ 10.37 (s, 1 H), 10.16 (s, 1 H), 9.95 (s, 1 H), 9.93 (s, 1 H), 9.91 (s, 1 H), 9.86 (s, 1 H), 9.49 (br s, 1 H), 9.47 (s, 1 H), 8.12 (m, 3 H), 8.0 (br s, 3 H), 7.65 (s, 1 H), 7.57 (s, 1 H), 7.46 (s, 1 H), 7.20 (m, 3 H), 7.16 (m, 2 H), 7.09 (d, 1 H, J = 1.5 Hz), 7.05 (m, 2 H), 7.00 (d, 1 H, J = 1.6 Hz), 6.88 (m, 2 H), 4.01 (s, 3 H), 3.99 (s, 3 H), 3.98 (s, 3 H), 3.83 (s, 3 H), 3.82 (s, 3 H), 3.81 (s, 3 H), 3.79 (s, 3 H), 3.78 (s, 3 H), 3.36 (q, 2 H, J = 5.3 Hz), 3.21–3.05 (m, 8 H), 2.85 (q, 2 H, J = 4.9 Hz), 2.71 (d, 3 H, J = 4.4 Hz), 2.34 (t, 2 H, J = 5.9 Hz), 2.26 (t, 2 H, J = 5.9 Hz), 1.85 (quintet, J = 5.7 Hz), 1.72 (m, 4 H); MALDI-TOF-MS, 1267.1 (1267.4 calcd for M + H).

ImImImPy- γ -PyPyPy- β -Dp-EDTA (1-E). EDTA dianhydride (50 mg) was dissolved in 1 mL of DMSO/NMP solution and 1 mL of DIEA by heating at 55 °C for 5 min. The dianhydride solution was added to ImImImPy- γ -PyPyPy- β -Dp-NH₂ (1-NH₂) (8.0 mg, 7 μ mol) and dissolved in 750 μ L of DMSO. The mixture was heated at 55 °C for 25 min, treated with 3 mL of 0.1 M NaOH, and heated at 55 °C for 10 min. TFA (0.1%) was added to adjust the total volume to 8 mL and the solution was purified directly by preparatory HPLC chromatography to provide 1-E as a white powder (3.3 mg, 30% recovery). ¹H NMR (DMSO-*d*₆) δ 10.14 (s, 1 H), 9.90 (s, 1 H), 9.89 (s, 1 H), 9.85 (s, 1 H), 9.58 (s, 1 H), 9.3 (br s, 1 H), 8.40 (m, 2 H), 8.02 (m, 2 H), 7.65 (s, 1 H), 7.51 (s, 1 H), 7.45 (s, 1 H), 7.20 (d, 1 H, J = 1.5 Hz), 7.15 (m, 2 H), 7.08 (d, 1 H, J = 1.1 Hz), 7.04 (d, 1 H, J = 1.5 Hz), 6.86 (m, 2 H), 4.00 (s, 3 H), 3.98 (s, 3 H), 3.94 (s, 3 H), 3.87 (m, 4 H), 3.82 (s, 3 H), 3.81 (s, 3 H), 3.78 (s, 3 H), 3.72 (m, 4 H), 3.4–3.0 (m, 16 H), 2.71 (d, 3 H, J = 4.2 Hz), 2.33 (t, 2 H, J = 5.1 Hz), 2.25 (t, 2 H, J = 5.9 Hz), 1.75 (m, 6 H); MALDI-TOF-MS, 1298.4 (1298.3 calcd for M + H).

(15) Resin substitution has been corrected for the weight of the polyamide chain. The change in substitution during a specific coupling or for the entire synthesis can be calculated as $L_{\text{new}}(\text{mmol/g}) = L_{\text{old}}(1 + L_{\text{old}}(W_{\text{new}} - W_{\text{old}}) \times 10^{-3})$, where L is the loading (mmol of amine per gram of resin), and W is the weight (g mol⁻¹) of the growing polyamide attached to the resin. See: Barros, K.; Chatzi, O.; Gatos, D.; Stravropoulos, G. *Int. J. Peptide Protein Res.* 1991, 37, 513.

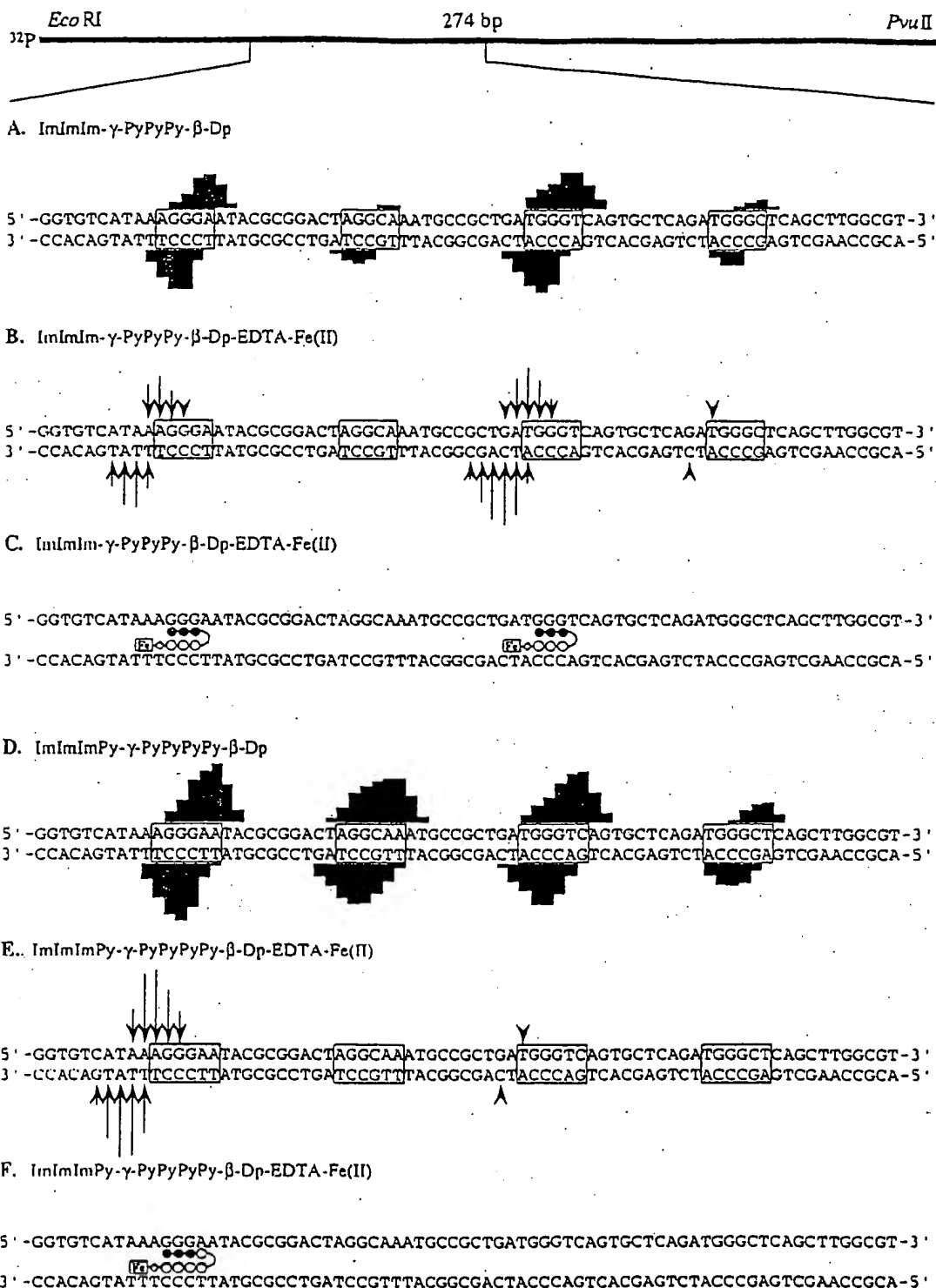


Figure 5. Results from MPE-Fe(II) footprinting of ImImIm- γ -PyPyPy- β -Dp and ImImImPy- γ -PyPyPyPy- β -Dp and affinity cleavage of ImImIm- γ -PyPyPy- β -Dp-EDTA-Fe(II) and ImImImPy- γ -PyPyPyPy- β -Dp-EDTA-Fe(II). (Top) Illustration of the 274 bp restriction fragment with the position of the sequence indicated. Boxes represent equilibrium binding sites determined by the published model. Only sites that were quantitated by DNase I footprint titrations are boxed. (A and D): MPE-Fe(II) protection patterns for polyamides at 10 μ M concentration. Bar heights are proportional to the relative protection from cleavage at each band. (B and E): Affinity cleavage patterns of ImImIm- γ -PyPyPy- β -Dp-EDTA-Fe(II) at 1 μ M and of ImImImPy- γ -PyPyPyPy- β -Dp-EDTA-Fe(II) at 100 nM, respectively. Arrow heights are proportional to the relative cleavage intensities at each base pair. (C and F): Ball and stick binding models for the single orientation binding to formal match sequences by the six-ring and eight-ring EDTA-Fe(II) analogs, respectively. Shaded and nonshaded circles denote imidazole and pyrrole carboxamides, respectively. Nonshaded diamonds represent the β -alanine residue. The boxed Fe denotes the EDTA-Fe(II) cleavage moiety.

ImImImPy- γ -PyPyPyPy- β -Dp-EDTA (2-E). Compound 2-E was prepared as described for compound 1-E (yield 3.8 mg, 40%). ^1H NMR (DMSO- d_6) δ 10.34 (s, 1 H), 10.11 (s, 1 H), 9.92 (s, 1 H), 9.90 (s, 1

H), 9.89 (s, 1 H), 9.84 (s, 1 H), 9.57 (s, 1 H), 8.42 (m, 1 H), 8.03 (m, 3 H), 7.64 (s, 1 H), 7.56 (s, 1 H), 7.44 (s, 1 H), 7.20 (m, 3 H), 7.15 (m, 2 H), 7.07 (d, 1 H, J = 1.6 Hz), 7.05 (m, 2 H), 6.99 (d, 1 H, J = 1.6

Table 1. Equilibrium Association Constants (M^{-1})^a

	match site		end mismatch	core mismatches
polyamide ImImIm- γ -PyPyPy- β -Dp	5'-AGGGA-3'	5'-TGGGT-3'	5'-TGGGC-3'	5'-AGGCA-3'
	4.6×10^6 (0.3)	7.6×10^6 (0.5)	1.3×10^6 (0.3)	8.6×10^5 (0.4)
	match site		end mismatch	core mismatches
polyamide ImImImPy- γ -PyPyPyPy- β -Dp	5'-AGGGAA-3'	5'-TGGGTC-3'	5'-TGGGCT-3'	5'-AGGCAA-3'
	3.7×10^6 (0.8)	1.4×10^7 (0.5)	1.7×10^6 (0.3)	2.9×10^6 (0.3)

^a Values reported are the mean values measured from a minimum of three DNase I footprint titration experiments, with the standard deviation for each data set indicated in parentheses. ^b The assays were performed at 22 °C at pH 7.0 in the presence of 10 mM Tris-HCl, 10 mM KCl, 10 mM MgCl₂, and 5 mM CaCl₂. ^c Base pairs that are in bold represent formal mismatches.

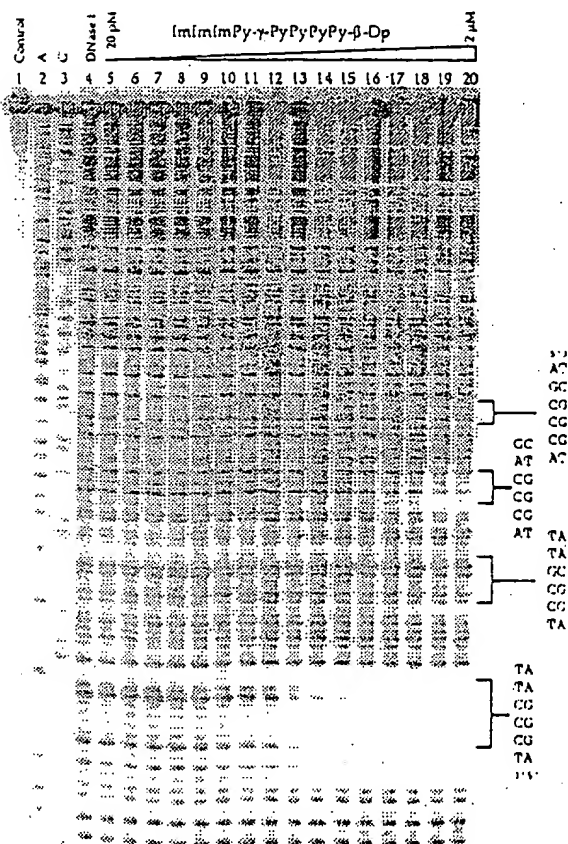


Figure 6. Quantitative DNase I footprint titration experiment with ImImImPy- γ -PyPyPyPy- β -Dp on the *EcoRI/PvuII* restriction fragment from plasmid pSES1: lane 1, intact DNA; lane 2, A reaction; lane 3, G reaction; lane 4, DNase I standard; lanes 5–20, 20 pM, 50 pM, 100 pM, 200 pM, 500 pM, 1 nM, 2 nM, 5 nM, 10 nM, 20 nM, 50 nM, 100 nM, 200 nM, 500 nM, 1 μ M, 2 μ M ImImImPy- γ -PyPyPyPy- β -Dp. The 5'-AGGGAA-3', 5'-AGGCAA-3', 5'-TGGGTC-3', and 5'-TGGGCT-3' sites that were analyzed are shown on the right side of the autoradiogram. All reactions contain 20 kbp restriction fragment, 10 mM Tris-HCl (pH 7.0), 10 mM KCl, 10 mM MgCl₂, and 5 mM CaCl₂.

Hz), 6.87 (m, 2 H), 4.00 (s, 3 H), 3.98 (s, 3 H), 3.97 (s, 3 H), 3.83 (m, 4 H), 3.82 (s, 6 H), 3.79 (s, 3 H), 3.78 (s, 6 H), 3.67 (m, 4 H), 3.4–3.0 (m, 16 H), 2.71 (d, 3 H, J = 4.2 Hz), 2.34 (t, 2 H, J = 5.4 Hz), 2.25 (t, 2 H, J = 5.9 Hz), 1.72 (m, 6 H); MALDI-TOF-MS, 1542.2 (1542.6 calcd for M + H).

DNA Reagents and Materials. Enzymes were purchased from Boehringer-Mannheim or New England Biolabs and were used with their supplied buffers. Deoxyadenosine and thymidine 5'-[α -³²P]-triphosphates and deoxyadenosine 5'-[γ -³²P]triphosphate were obtained from Amersham. Purified water was obtained by filtering doubly-distilled water through the MilliQ filtration system from Millipore. Sonicated, deproteinized calf thymus DNA was acquired from Pharmacia. All other reagents and materials were used as received. All DNA manipulations were performed according to standard protocols.¹⁶

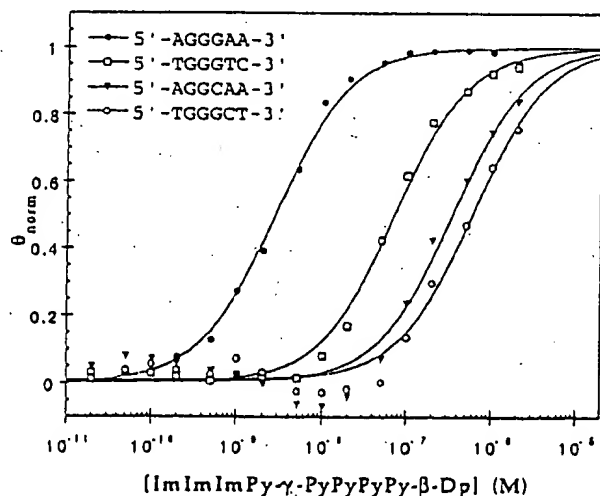
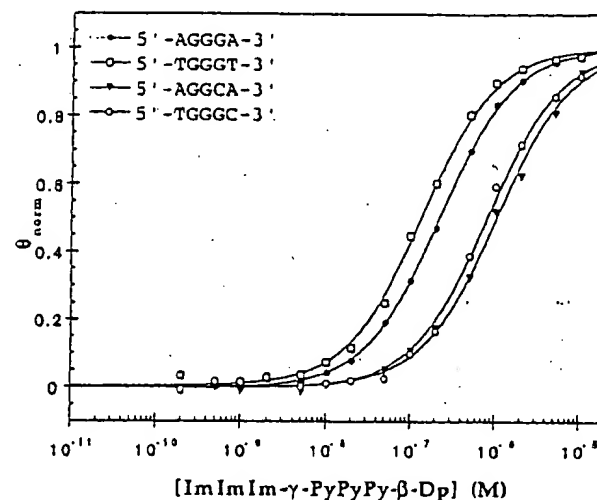


Figure 7. Data from the quantitative DNase I footprint titration experiments for the two polyamides, ImImImPy- γ -PyPyPyPy- β -Dp (top) and ImImImPy- γ -PyPyPyPy- β -Dp (bottom), in complex with the designated sites. The θ_{norm} points were obtained using photostimulable storage phosphor autoradiography and processed as described in the Experimental Section. The data points for 5'-AGGGA(A)-3', 5'-TGGGT(C)-3', 5'-AGGCA(A)-3', and 5'-TGGGC(T)-3' sites are indicated by filled circles (●), open squares (□), filled inverted triangles (▼), and open circles (○), respectively. The solid curves are the best-fit Langmuir binding titration isotherms obtained from the nonlinear least-squares algorithm using eq 2.

Construction of Plasmid DNA. The plasmid pSES1 was constructed by hybridization of the inserts, 5'-GATCCGGTGTCA-TAAAGGGAATACGCGGACTAGGCAAATGCCGC-TGATGGGTCAGTGCTCAGATGGGCTC-3' and 5'-AGCTGAGC-

(16) Sambrook, J.; Fritsch, E. F.; Maniatis, T. *Molecular Cloning*; Cold Spring Harbor Laboratory: Cold Spring Harbor, NY, 1989.

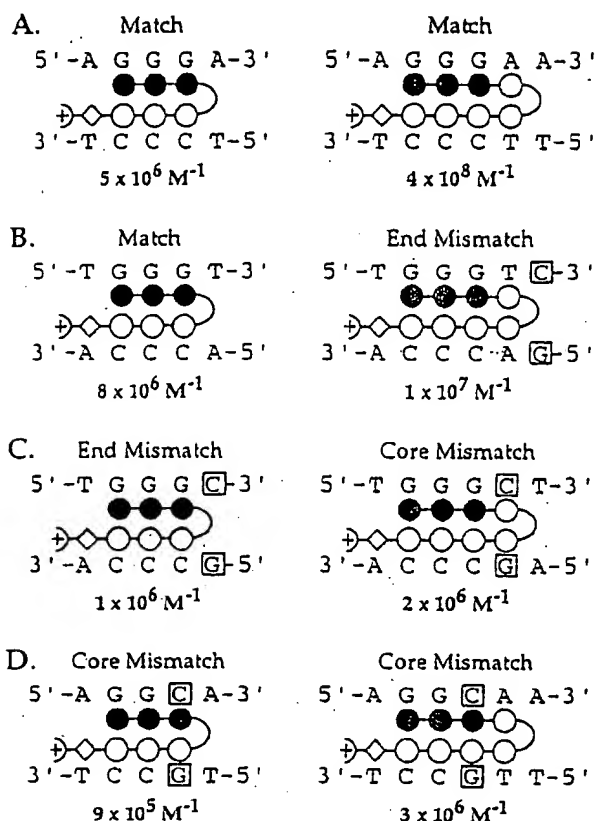


Figure 8. Ball and stick models of ImimIm- γ -PyPyPy- β -Dp (left) and ImimImPy- γ -PyPyPy- β -Dp (right) for each binding site, with the corresponding equilibrium association constants shown below each individual model. The binding sites shown are (a) 5'-AGGGA(A)-3', (b) 5'-TGGGT(C)-3', (c) 5'-TGGGC(T)-3', and (d) 5'-AGGCA(A)-3'. Shaded and nonshaded circles denote imidazole and pyrrole carboxamides, respectively. Nonshaded diamonds represent the β -alanine residue. Formally mismatched base pairs are boxed.

CCATCTGAGCACTGACCCATCAGCGGCATTTGCCTAGT-CCGCGTATTCCTTTATGACACCG-3'. The hybridized insert was ligated into linearized pUC19 *Bam*HI/*Hind*III plasmid using T4 DNA ligase. The resultant constructs were used to transform Epicurian Coli XL-2 Blue competent cells from Stratagene. Ampicillin-resistant white colonies were selected from 25 mL of Luria-Bertani medium agar plates containing 50 μ g/mL ampicillin and treated with XGAL and IPTG solutions. Large-scale plasmid purification was performed with Qiagen Maxi purification kits. Dideoxy sequencing was used to verify the presence of the desired insert. Concentration of the prepared plasmid was determined at 260 nm using the relationship of 1 OD unit = 50 μ g/mL of duplex DNA.

Preparation of 3'- and 5'-End-Labeled Restriction Fragments. The plasmid pSES1 was linearized with *Eco*RI and then treated with either Klenow fragment, deoxyadenosine 5'-(α - 32 P)triphosphate and thymidine 5'-(α - 32 P)triphosphate for 3' labeling, or calf alkaline phosphatase and then 5' labeled with T4 polynucleotide kinase and deoxyadenosine 5'-(γ - 32 P)triphosphate. The labeled fragment (3' or 5') was then digested with *Pvu*II and loaded onto a 5% non-denaturing polyacrylamide gel. The desired 274 base pair band was visualized by autoradiography and isolated. Chemical sequencing reactions were performed according to published methods.¹⁷

MPE-Fe(II) Footprinting. All reactions were carried out in a volume of 40 μ L. A polyamide stock solution or water (for reference lanes) was added to an assay buffer where the final concentrations were 25 mM Tris-acetate buffer (pH 7.0), 10 mM NaCl, 100 μ M base pair calf thymus DNA, and 15 kcpm 3'- or 5'-radiolabeled DNA. The solutions were allowed to equilibrate for 4 h. A fresh 50 μ M MPE-

Fe(II) solution was made from 100 μ L of a 100 μ M MPE solution and 100 μ L of a 100 μ M ferrous ammonium sulfate ($\text{Fe}(\text{NH}_4)_2(\text{SO}_4)_2 \cdot 6\text{H}_2\text{O}$) solution. After the 4 h equilibration, MPE-Fe(II) solution (5 μ M) was added, and the reactions were equilibrated for 5 min. Cleavage was initiated by the addition of dithiothreitol (5 mM) and allowed to proceed for 14 min. Reactions were stopped by ethanol precipitation, resuspended in 100 mM Tris-borate-EDTA/80% formamide loading buffer, denatured at 85 $^\circ\text{C}$ for 5 min, placed on ice, and immediately loaded onto an 8% denaturing polyacrylamide gel (5% crosslink, 7 M urea) at 2000 V.

Affinity Cleaving. All reactions were carried out in a volume of 400 μ L. A polyamide stock solution or water (for reference lanes) was added to an assay buffer where the final concentrations were 25 mM Tris-acetate buffer (pH 7.0), 200 mM NaCl, 50 μ g/mL of glycogen, and 15 kcpm 3'- or 5'-radiolabeled DNA. After the reactions were allowed to equilibrate for 4 h, ferrous ammonium sulfate ($\text{Fe}(\text{NH}_4)_2(\text{SO}_4)_2 \cdot 6\text{H}_2\text{O}$), 10 μ M final concentration, was added. After another 15 min, cleavage was initiated by the addition of dithiothreitol (5 mM) and allowed to proceed for 12 min. Reactions were stopped by ethanol precipitation, resuspended in 100 mM Tris-borate-EDTA/80% formamide loading buffer, denatured at 85 $^\circ\text{C}$ for 5 min, placed on ice, and immediately loaded onto an 8% denaturing polyacrylamide gel (5% cross-link, 7 M urea) at 2000 V.

DNase I Footprinting. All reactions were carried out in a volume of 40 μ L. We note explicitly that no carrier DNA was used in these reactions. A polyamide stock solution or water (for reference lanes) was added to an assay buffer where the final concentrations were 10 mM Tris-HCl buffer (pH 7.0), 10 mM KCl, 10 mM MgCl_2 , 5 mM CaCl_2 , and 20 kcpm 3'-radiolabeled DNA. The solutions were allowed to equilibrate for a minimum of 4 h at 22 $^\circ\text{C}$ (the four-ring hairpin was allowed to equilibrate for up to 12 h with no noticeable effect on the data set). Cleavage was initiated by the addition of 4 μ L of a DNase I stock solution (diluted with 1 mM DTT to give a stock concentration of 0.225 u/mL) and was allowed to proceed for 5 min at 22 $^\circ\text{C}$. The reactions were stopped by the addition of 3 M sodium acetate solution containing 50 mM EDTA and then ethanol precipitated. The cleavage products were resuspended in 100 mM Tris-borate-EDTA/80% formamide loading buffer, denatured at 85 $^\circ\text{C}$ for 5 min, placed on ice, and immediately loaded onto an 8% denaturing polyacrylamide gel (5% cross-link, 7 M urea) at 2000 V for 1 h. The gels were dried under vacuum at 80 $^\circ\text{C}$, then quantitated using storage phosphor technology.

Equilibrium association constants were determined as previously described.^{6,11} The data were analyzed by performing volume integrations of the 5'-AGGGA(A)-3', 5'-TGGGT(C)-3', 5'-TGGGC(T)-3', and 5'-AGGCA(A)-3' sites and a reference site. The apparent DNA target site saturation, θ_{app} , was calculated for each concentration of polyamide using the following equation:

$$\theta_{\text{app}} = 1 - \frac{I_{\text{tot}}/I_{\text{ref}}}{I_{\text{tot}}^0/I_{\text{ref}}^0} \quad (1)$$

where I_{tot} and I_{ref} are the integrated volumes of the target and reference sites, respectively, and I_{tot}^0 and I_{ref}^0 correspond to those values for a DNase I control lane to which no polyamide has been added. The $([L]_{\text{tot}}, \theta_{\text{app}})$ data points were fit to a Langmuir binding isotherm (eq 2, $n = 1$) by minimizing the difference between θ_{app} and θ_{fit} , using the modified Hill equation:

$$\theta_{\text{fit}} = \theta_{\text{min}} + (\theta_{\text{max}} - \theta_{\text{min}}) \frac{K_a^n [L]_{\text{tot}}^n}{1 + K_a^n [L]_{\text{tot}}^n} \quad (2)$$

where $[L]_{\text{tot}}$ corresponds to the total polyamide concentration, K_a corresponds to the apparent monomeric association constant, and θ_{min} and θ_{max} represent the experimentally determined site saturation values when the site is unoccupied or saturated, respectively. Data were fit using a nonlinear least-squares fitting procedure of Kaleidagraph software (version 2.1, Abelbeck software) with K_a , θ_{max} , and θ_{min} as the adjustable parameters. All acceptable fits had a correlation coefficient of $R > 0.97$. At least three sets of acceptable data were used in determining each association constant. All lanes from each gel were used unless visual inspection revealed a data point to be

(17) (a) Iverson, B. L.; Dervan, P. B. *Nucleic Acids Res.* 1987, 15, 7823. (b) Maxam, A. M.; Gilbert, W. S. *Methods Enzymol.* 1980, 65, 499.

obviously flawed relative to neighboring points. The data were normalized using the following equation:

$$\theta_{\text{norm}} = \frac{\theta_{\text{app}} - \theta_{\text{min}}}{\theta_{\text{max}} - \theta_{\text{min}}} \quad (3)$$

Quantitation by Storage Phosphor Technology Autoradiography. Photostimulable storage phosphorimaging plates (Kodak Storage Phosphor Screen S0230 obtained from Molecular Dynamics) were pressed flat against gel samples and exposed in the dark at 22 °C for 12–16 h. A Molecular Dynamics 400S PhosphorImager was used to

obtain all data from the storage screens. The data were analyzed by performing volume integrations of all bands using the ImageQuant v. 3.2.

Acknowledgment. This paper is dedicated to Nelson Leonard on the occasion of his 80th birthday. We are grateful to the National Institutes of Health (GM-2768) for research support, the National Institutes of Health for a research service award to S.E.S., and the Howard Hughes Medical Institute for a predoctoral fellowship to E.E.B. We would like to thank G. M. Hathaway for MALDI-TOF mass spectrometry.

JA9611598

Recognition of 5'-(A,T)GG(A,T)₂-3' Sequences in the Minor Groove of DNA by Hairpin Polyamides

Michelle E. Parks, Eldon E. Baird, and Peter B. Dervan*

Contribution from the Division of Chemistry and Chemical Engineering,
California Institute of Technology, Pasadena, California 91125

Received March 6, 1996

Abstract: A series of four hairpin pyrrole-imidazole polyamides, ImImPy- γ -PyPyPy- β -Dp, PyPyPy- γ -ImImPy- β -Dp, AcImImPy- γ -PyPyPy- β -Dp, and AcPyPyPy- γ -ImImPy- β -Dp (Im = *N*-methylimidazole-2-carboxamide, Py = *N*-methylpyrrole-2-carboxamide, Dp = *N,N*-dimethylaminopropylamide, γ = γ -aminobutyric acid, β = β -alanine, and Ac = acetyl), designed for recognition of 5'-(A,T)GG(A,T)₂-3' sequences in the minor groove of DNA were synthesized using solid phase methodology and analyzed with respect to DNA binding affinity and sequence specificity. Quantitative DNase I footprint titration experiments reveal that the optimal polyamide ImImPy- γ -PyPyPy- β -Dp binds a designated 5'-TGGTT-3' match site with an equilibrium association constant of $K_a = 1.0 \times 10^8 \text{ M}^{-1}$ and the single base pair mismatch sites, 5'-TGTTA-3' and 5'-GGGTA-3', with 50-fold and 100-fold-lower affinity, respectively (10 mM Tris-HCl, 10 mM KCl, 10 mM MgCl₂, and 5 mM CaCl₂, pH 7.0 and 22 °C). Polyamides of sequence composition AcImImPy- γ -PyPyPy- β -Dp and AcPyPyPy- γ -ImImPy- β -Dp, which differ only by the position of the γ -linker, bind with similar affinities and specificities. Recognition of sequences containing contiguous G-C base pairs expands the sequence repertoire available for targeting DNA with pyrrole-imidazole polyamides.

Introduction

Pyrrole-imidazole polyamides offer a general method for the design of non-natural molecules for sequence-specific recognition in the minor groove of DNA.¹⁻³ Within the 2:1 polyamide-DNA model, an imidazole (Im) on one ligand opposite a pyrrolicarboxamide (Py) on the second ligand recognizes a G-C base pair, while a pyrrolicarboxamide/imidazole combination targets a C-G base pair.^{1,3} A pyrrolicarboxamide/pyrrolicarboxamide pair is partially degenerate for A-T or T-A base pairs.¹⁻³ On the basis of this model, the recognition of the sequences 5'-(A,T)G(A,T)C(A,T)-3',¹ 5'-(A,T)G(A,T)₂-3',³ (A,T)₂G(A,T)₂-3',⁴ and 5'-(A,T)GCGC(A,T)-3'⁵ has been achieved. However, sequences containing contiguous G-C base pairs are notably absent from this list.

Formation of a hairpin polyamide by covalently linking a polyamide heterodimer with a γ -aminobutyric acid (γ) residue provides an approximate 300-fold enhancement in affinity over the unlinked polyamides, ImPyPy- and PyPyPy.⁶ Moreover, the specificity of the hairpin is greatly improved. The initial placement of the γ -amino acid turn was chosen for synthetic ease and was not varied. With the development of solid phase

methodology for polyamide synthesis, we now assess the effect of varying the position of the γ -turn monomer.⁷

In order to explore the recognition of 5'-(A,T)GG(A,T)₂-3' sequences, a series of four head-to-tail linked hairpin polyamides containing neighboring imidazole rings, ImImPy- γ -PyPyPy- β -Dp (1), PyPyPy- γ -ImImPy- β -Dp (2), AcImImPy- γ -PyPyPy- β -Dp (3), and AcPyPyPy- γ -ImImPy- β -Dp (4), were prepared using solid phase methods (Figures 1 and 2).⁷ The polyamides are all synthesized with Boc- β -alanine-Pam-resin, previously shown as optimal for polyamides.⁸ Each imidazole is expected to form a specific hydrogen bond with a guanine amino group allowing the recognition of contiguous G-C base pairs (Figure 1). In addition, the linker turn position is varied within the nonacetylated and acetylated pairs of polyamides to determine the effect on the sequence specificity and binding affinity. We report here the binding specificity and affinity of the polyamides as determined by the complementary techniques, MPE-Fe^{II} footprinting⁹ and quantitative DNase I footprinting.¹⁰ MPE-Fe^{II} footprinting verifies that sequence-specific recognition of the expected 5'-TGGTT-3' target site has been achieved. In addition, DNase I quantitative footprint titration experiments reveal that the position of the γ -linker does not dramatically affect either affinity or specificity of polyamides, especially the pair containing acetylated N-termini.

Results

Synthesis of Polyamides. The polyamides ImImPy- γ -PyPyPy- β -Dp (1), PyPyPy- γ -ImImPy- β -Dp (2), AcImImPy- γ -PyPyPy- β -Dp (3), and AcPyPyPy- γ -ImImPy- β -Dp (4) were

* Abstract published in *Advance ACS Abstracts*, June 15, 1996.

(1) (a) Wade, W. S.; Dervan, P. B. *J. Am. Chem. Soc.* 1987, 109, 1574-1575. (b) Wade, W. S.; Mrksich, M.; Dervan, P. B. *J. Am. Chem. Soc.* 1992, 114, 8783. (c) Mrksich, M.; Wade, W. S.; Dwyer, T. J.; Geierstanger, B. H.; Wemmer, D. E.; Dervan, P. B. *Proc. Natl. Acad. Sci. U.S.A.* 1992, 89, 7586. (d) Wade, W. S.; Mrksich, M.; Dervan, P. B. *Biochemistry* 1993, 32, 11385.

(2) (a) Pelton, J. G.; Wemmer, D. E. *Proc. Natl. Acad. Sci. U.S.A.* 1989, 86, 5723. (b) Pelton, J. G.; Wemmer, D. E. *J. Am. Chem. Soc.* 1990, 112, 1393. (c) Chen, X.; Ramiakrishnan, B.; Rao, S. T.; Sundaralingham, M. *Nature Struct. Biol.* 1994, 1, 169.

(3) (a) Mrksich, M.; Dervan, P. B. *J. Am. Chem. Soc.* 1993, 115, 2572. (b) Geierstanger, B. H.; Jacobsen, J.-P.; Mrksich, M.; Dervan, P. B.; Wemmer, D. E. *Biochemistry* 1994, 33, 3055.

(4) Geierstanger, B. H.; Dwyer, T. J.; Bathini, Y.; Lown, J. W.; Wemmer, D. E. *J. Am. Chem. Soc.* 1993, 115, 4474.

(5) (a) Geierstanger, B. H.; Mrksich, M.; Dervan, P. B.; Wemmer, D. E. *Science* 1994, 266, 646-650. (b) Mrksich, M.; Dervan, P. B.; *J. Am. Chem. Soc.* 1995, 117, 3325.

(6) Mrksich, M.; Parks, M. E.; Dervan, P. B. *J. Am. Chem. Soc.* 1994, 116, 7983.

(7) Baird, E. E.; Dervan, P. B. *J. Am. Chem. Soc.* 1996, 118, 6141-6146.

(8) Parks, M. E.; Baird, E. E.; Dervan, P. B. *J. Am. Chem. Soc.* 1996, 118, 6147-6152.

(9) (a) Van Dyke, M. W.; Dervan, P. B. *Biochemistry* 1983, 22, 2373. (b) Van Dyke, M. W.; Dervan, P. B. *Nucleic Acids Res.* 1983, 11, 5555.

(10) (a) Brenowitz, M.; Seneor, D. F.; Shea, M. A.; Ackers, G. K. *Methods Enzymol.* 1986, 130, 132. (b) Brenowitz, M.; Seneor, D. F.; Shea, M. A.; Ackers, G. K. *Proc. Natl. Acad. Sci. U.S.A.* 1986, 83, 8462. (c) Seneor, D. F.; Brenowitz, M.; Shea, M. A.; Ackers, G. K. *Biochemistry* 1986, 25, 7344.

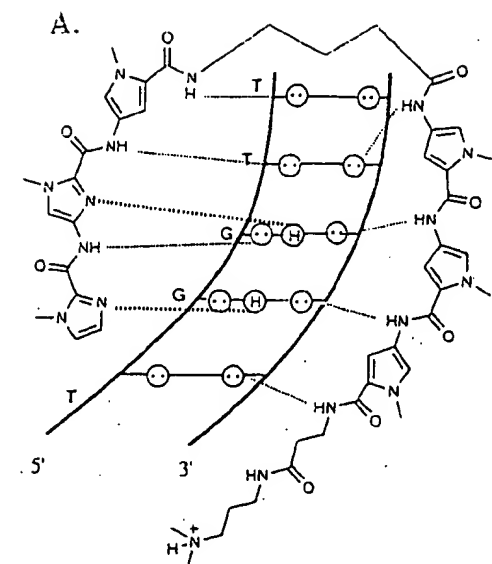
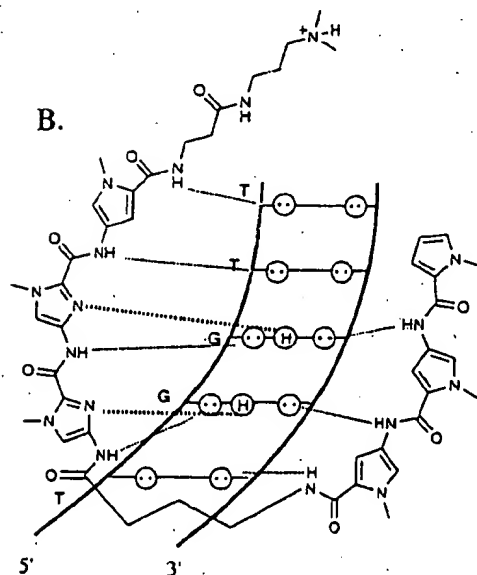
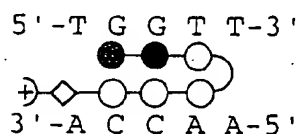
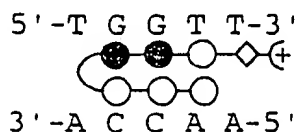
ImImPy- γ -PyPyPy- β -Dp • TGGTTPyPyPy- γ -ImImPy- β -Dp • TGGTT

Figure 1. Binding model for the complexes formed between polyamides ImImPy- γ -PyPyPy- β -Dp (1) (A) and PyPyPy- γ -ImImPy- β -Dp (2) (B) and a 5'-TGGTT-3' sequence. Circles with dots represent lone pairs of N3 of purines and O2 of pyrimidines. Circles containing an H represent the N2 hydrogen of guanine. Putative hydrogen bonds are illustrated by dotted lines. Ball and stick models are also shown. Shaded and nonshaded circles denote imidazole and pyrrole carboxamides, respectively. Nonshaded diamonds represent a β -alanine residue.

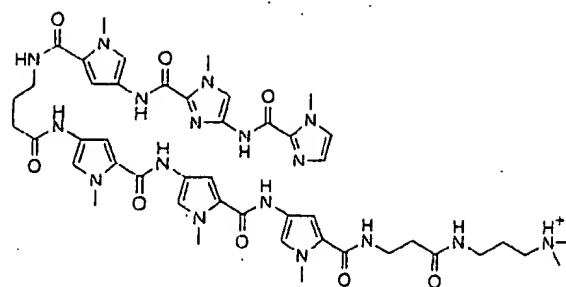
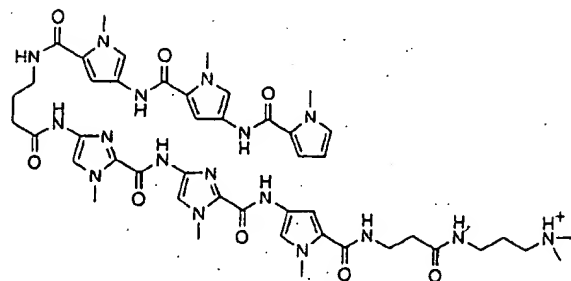
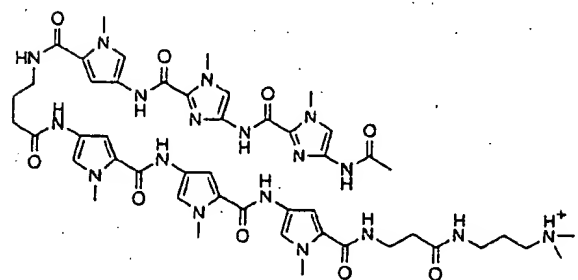
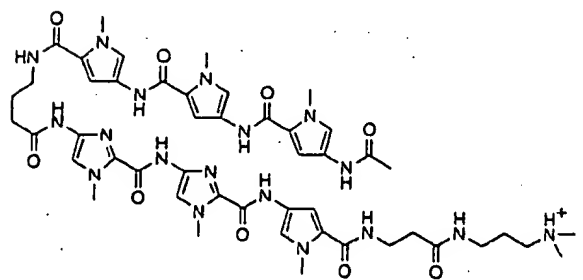
ImImPy- γ -PyPyPy- β -Dp (1)PyPyPy- γ -ImImPy- β -Dp (2)AcImImPy- γ -PyPyPy- β -Dp (3)AcPyPyPy- γ -ImImPy- β -Dp (4)

Figure 2. Series of polyamides synthesized using solid phase methodology.⁷

prepared by solid phase methodology (Figure 2). Four unique pyrrole and imidazole building blocks were combined in a stepwise manner on a solid support using Boc-chemistry protocols (Figure 3). For example, polyamide 2, PyPyPy- γ -ImImPy- β -Dp, was prepared in 14 steps on the resin, and then cleaved with a single-step aminolysis reaction (Figure 3). All polyamides were found to be soluble up to at least 1 mM concentration in aqueous solution.

Footprinting. MPE-Fe^{II} footprinting on a 3'- or 5'-³²P-end-labeled 266 base pair *EcoRI*/*PvuII* restriction fragment from plasmid pMEPGG (25 mM Tris-acetate, 100 μ M bp calf thymus DNA, 10 mM NaCl) reveals that the synthetic polyamides 1–4, at 10 μ M concentration, bind the designated target site 5'-

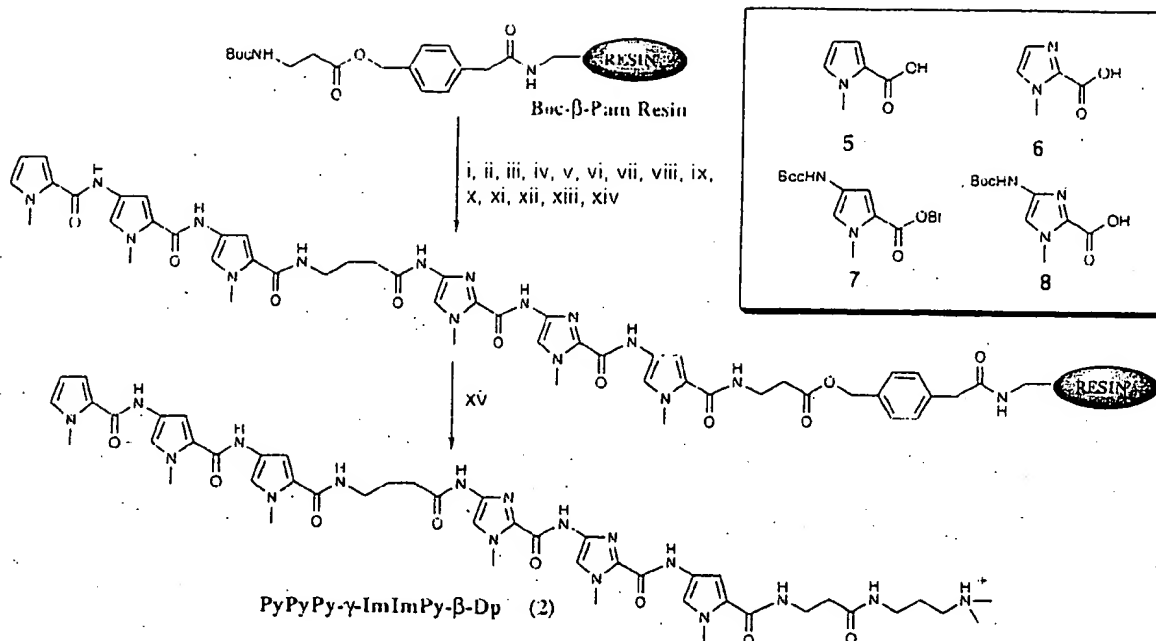


Figure 3. Solid phase synthetic scheme for PyPyPy-γ-ImImPy-β-Dp starting from commercially available Boc-β-Pam-resin: (i) 80% TFA/DCM, 0.4 M PhSH; (ii) Boc-Py-OBt, DIEA, DMF; (iii) 80% TFA/DCM, 0.4 M PhSH; (iv) Boc-Im-OBt (DCC/HOBt), DIEA, DMF; (v) 80% TFA/DCM, 0.4 M PhSH; (vi) Boc-Im-OBt (DCC/HOBt), DIEA, DMF; (vii) 80% TFA/DCM, 0.4 M PhSH; (viii) Boc-γ-aminobutyric acid (HBTU, DIEA); (ix) 80% TFA/DCM, 0.4 M PhSH; (x) Boc-Py-OBt, DIEA, DMF; (xi) 80% TFA/DCM, 0.4 M PhSH; (xii) Boc-Py-OBt, DIEA, DMF; (xiii) 80% TFA/DCM, 0.4 M PhSH; (xiv) pyrrole-2-carboxylic acid (HBTU/DIEA); (xv) (*N,N*-dimethylamino)propylamine, 55 °C. (Inset) Pyrrole and imidazole monomers for synthesis of all compounds described here: pyrrole-2-carboxylic acid 5, imidazole-2-carboxylic acid 6,^{1b} Boc-pyrrole-OBt ester 7,⁷ and Boc-imidazole acid 8.⁷

TGGTT-3' (Figures 4 and 5). In addition, several single base pair mismatch sites are bound with lower affinity. Quantitative DNase I footprint titration experiments (10 mM Tris-HCl, 10 mM KCl, 10 mM MgCl₂, and 5 mM CaCl₂, pH 7.0 and 22 °C) were performed to determine the equilibrium association constants of the four polyamides 1–4 for a designated match site, 5'-TGGTT-3', as well as for two single base pair mismatch sites, 5'-TGTTA-3' and 5'-GGGTA-3' (Table 1).¹⁰ The polyamide ImImPy-γ-PyPyPy-β-Dp binds the target site 5'-TGGTT-3' with the highest affinity (association constant $K_a = 1.0 \times 10^8 \text{ M}^{-1}$) (Figures 6 and 7). The remaining polyamides have lower but approximately equal association constants of $K_a = \sim 2 \times 10^7 \text{ M}^{-1}$ for the target site. The nonacetylated polyamides in this series are > 50-fold specific for the 5'-TGGTT-3' match site over either of the single base pair mismatch sites analyzed. The acetylated pair of polyamides exhibit lower sequence specificity for the analyzed sites.

Discussion

Each polyamide within this series specifically binds the five base pair designated target sequence 5'-TGGTT-3', as shown by MPE-Fe^{II} footprinting experiments, providing the first example of contiguous G-C recognition in the polyamide-DNA motif. Interestingly, the polyamides prefer different mismatch sequences, indicating that the position of the turn alters sequence selectivity, although only for the mismatches.

Quantitative DNase I footprint titration experiments reveal that ImImPy-γ-PyPyPy-β-Dp (1) is optimal within this series of four polyamides. This hairpin binds a 5'-TGGTT-3' match site with an equilibrium association constant of $K_a = 1 \times 10^8 \text{ M}^{-1}$, while the corresponding hairpin PyPyPy-γ-ImImPy-β-Dp (2), which differs only in the position of the γ turn, shows lower affinity ($K_a = \sim 2 \times 10^7 \text{ M}^{-1}$) for the 5'-TGGTT-3' site. Both unacetylated polyamides demonstrate good specificity (> 50-

fold) for the target match site over the single base pair mismatch sites. The acetylated polyamides are similar in affinity to PyPyPy-γ-ImImPy-β-Dp (2), but exhibit lower specificity. AcImImPy-γ-PyPyPy-β-Dp (3) and AcPyPyPy-γ-ImImPy-β-Dp (4) are virtually indistinguishable from each other on the basis of affinity and specificity for the analyzed target sequences, indicating little preference for turn position.

This series of contiguous imidazole-containing polyamides is remarkably similar in affinity and specificity to the single imidazole-containing hairpin polyamide, ImPyPy-γ-PyPyPy-β-Dp, indicating little or no energetic penalty in this system for adjacent imidazoles.⁸ Importantly, the position of the hairpin turn does not significantly affect the recognition of the target 5'-TGGTT-3' match site, although single base pair mismatch relative affinities are altered.

Implications for the Design of Minor Groove Binding Molecules. The 2:1 motif has been used to specifically target several sequences: 5'-TGTCA-3',¹ 5'-TGTTA-3',³ 5'-AAGTT-3',⁴ and 5'-TGCGCA-3'.⁵ The results reported herein add sequences containing two contiguous G-C base pairs to the list, expanding the sequence repertoire for DNA recognition by polyamides. Furthermore, turn position showed minimal effects on the specificity and affinity of the polyamides, indicating a new degree of flexibility within the 2:1 motif. The expansion of the polyamide sequence repertoire through contiguous G-C recognition coupled with solid phase synthetic advances allowing the rapid assembly and characterization of polyamides brings the goal of sequence-specific recognition of any DNA sequence by designed molecules closer to fruition.

Experimental Section

Materials. Boc-glycine-(4-carboxylaminomethyl)-benzyl-ester-copoly(styrene-divinylbenzene) resin (Boc-G-Pam-resin) (0.2 mmol/g) 0.2 mmol/g Boc-β-alanine-(4-carboxylaminomethyl)-benzyl-ester-co-

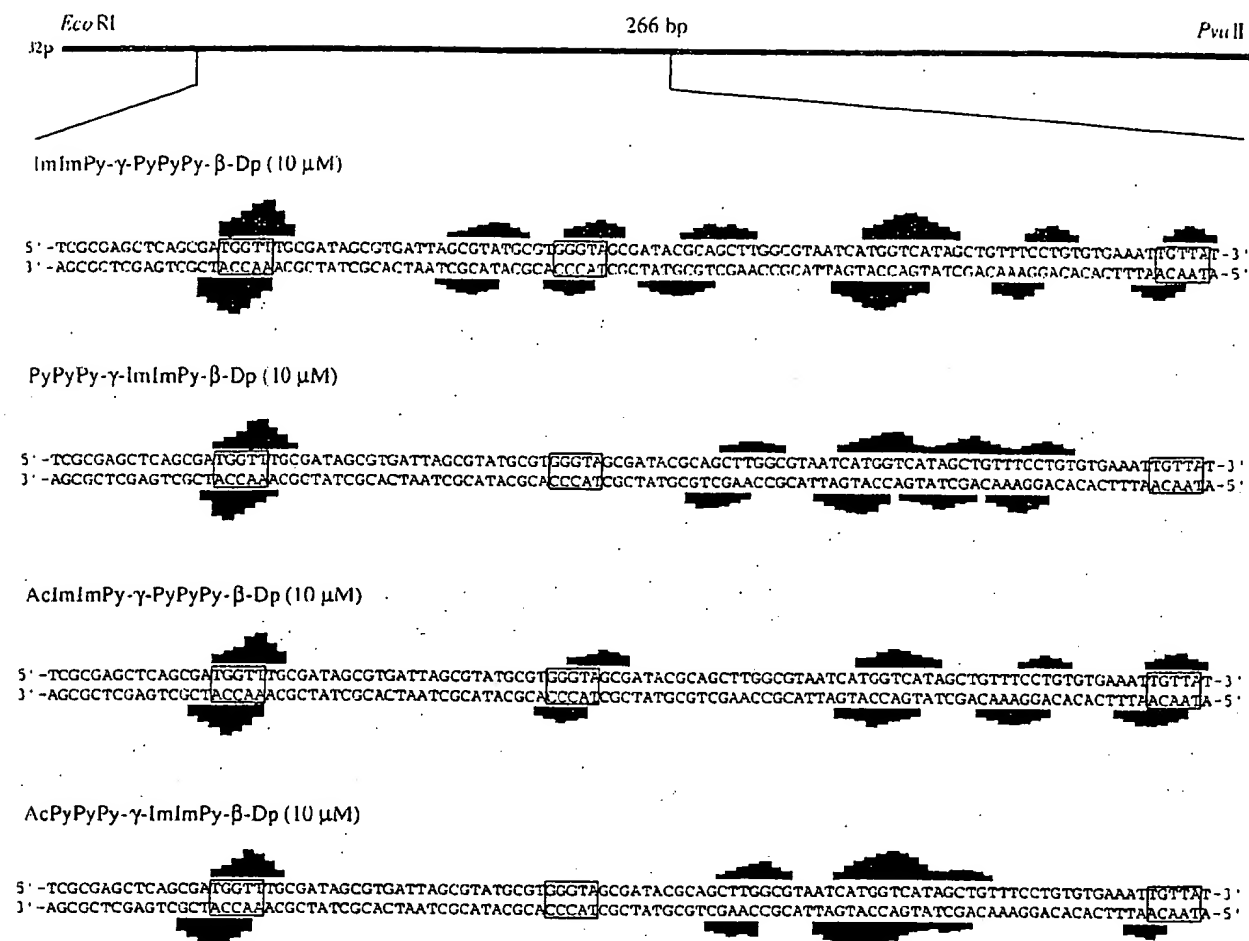


Figure 5. Histograms of cleavage protection (footprinting) data. (Top) Illustration of the 266 bp restriction fragment with the position of the sequence indicated. MPE-Fe^{II} protection patterns for polyamides at 10 μ M concentration. Bar heights are proportional to the relative protection from cleavage at each band. Boxes represent equilibrium binding sites determined by the published model.⁹ Only sites that were quantitated by DNase I footprint titrations are boxed.

Table 1. Equilibrium Association Constants (M^{-1})^{a,b}

polyamide	match site 5'-aTGGTTt-3'	single mismatch sites	
		5'-tGTtAt-3'	5'-tGGTAg-3'
ImImPy-γ-PyPyPy-β-Dp	1.0×10^4 (0.1)	1.7×10^6 (0.6)	$\leq 1 \times 10^6$
PyPyPy-γ-ImImPy-β-Dp	1.6×10^7 (0.2)	$< 1 \times 10^5$	$< 1 \times 10^4$
AcImImPy-γ-PyPyPy-β-Dp	1.3×10^7 (0.7)	1.6×10^6 (1.1)	1.3×10^6 (0.8)
AcPyPyPy-γ-ImImPy-β-Dp	2.0×10^7 (0.3)	1.3×10^6 (0.5)	$\leq 1 \times 10^6$

^a Values reported are the mean values measured from at least three footprint titration experiments, with the standard deviation for each data set indicated in parentheses. ^b The assays were performed at 22 °C at pH 7.0 in the presence of 10 mM Tris-HCl, 10 mM KCl, 10 mM MgCl₂, and 5 mM CaCl₂.

δ 10.31 (s, 1 H), 9.91 (s, 1 H), 9.90 (s, 1 H), 9.85 (s, 1 H), 9.75 (s, 1 H), 9.34 (br s, 1 H), 8.03 (m, 3 H), 7.56 (s, 1 H), 7.46 (s, 1 H), 7.21 (m, 2 H), 7.15 (m, 2 H), 7.07 (d, 1 H, J = 1.2 Hz), 7.03 (d, 1 H, J = 1.3 Hz), 6.98 (d, 1 H, J = 1.2 Hz), 6.87 (m, 2 H), 4.02 (m, 6 H), 3.96 (m, 6 H), 3.87 (m, 6 H), 3.75 (q, 2 H, J = 4.9 Hz), 3.36 (q, 2 H, J = 4.0 Hz), 3.20 (q, 2 H, J = 4.7 Hz), 3.01 (q, 2 H, J = 5.1 Hz), 2.71 (d, 6 H, J = 4.8 Hz), 2.42 (m, 4 H), 1.80 (m, 4 H) MALDI-TOF-MS 978.8 (979.1 calcd for M + H).

AcImImPy-γ-PyPyPy-β-Dp (3). Polyamide was prepared by manual solid phase protocols and isolated as a white powder (8 mg, 28% recovery): UV λ_{max} 246 (43 400), 312 (50 200); ¹H NMR (DMSO-*d*₆) δ 10.35 (s, 1 H), 10.30 (s, 1 H), 9.97 (s, 1 H), 9.90 (s, 1 H), 9.82 (s, 1 H), 9.30 (s, 1 H), 9.2 (br s, 1 H), 8.02 (m, 3 H), 7.52 (s, 1 H), 7.48 (s, 1 H), 7.21 (m, 2 H), 7.16 (d, 1 H, J = 1.1 Hz), 7.11 (d, 1 H, J = 1.2 Hz), 7.04 (d, 1 H, J = 1.1 Hz), 6.97 (d, 1 H, J = 1.3 Hz), 6.92 (d, 1 H, J = 1.4 Hz), 6.87 (d, 1 H, J = 1.2 Hz), 3.99 (s, 3 H), 3.97 (s, 3 H), 3.83 (s, 3 H), 3.82 (s, 3 H), 3.80 (s, 3 H), 3.79 (s, 3 H), 3.47 (q, 2 H, J = 4.7 Hz), 3.30 (q, 2 H, J = 4.6 Hz), 3.20 (q, 2 H, J = 5.0 Hz),

3.05 (q, 2 H, J = 5.1 Hz), 2.75 (d, 6 H, J = 4.1 Hz), 2.27 (m, 4 H), 2.03 (s, 3 H), 1.74 (m, 4 H); MALDI-TOF-MS 1036.4 (1036.1 calcd for M + H).

AcPyPyPy-γ-ImImPy-β-Dp (4). Polyamide was prepared by machine-assisted solid phase protocols⁷ as a white powder (14 mg, 48% recovery): UV λ_{max} 246 (44 400), 312 (52 300); ¹H NMR (DMSO-*d*₆) δ 10.32 (s, 1 H), 10.28 (s, 1 H), 9.89 (m, 2 H), 9.82 (s, 1 H), 9.18 (s, 1 H), 9.10 (br s, 1 H), 8.03 (m, 3 H), 7.55 (s, 1 H), 7.52 (s, 1 H), 7.21 (d, 1 H, J = 1.1 Hz), 7.18 (d, 1 H, J = 7.16 Hz), 7.15 (d, 1 H, J = 1.0 Hz), 7.12 (d, 1 H, J = 1.0 Hz), 7.02 (d, 1 H, J = 1.0 Hz), 6.92 (d, 1 H, J = 1.1 Hz), 6.87 (d, 1 H, J = 1.1 Hz), 6.84 (d, 1 H, J = 1.0 Hz), 3.97 (s, 3 H), 3.93 (s, 3 H), 3.87 (s, 3 H), 3.80 (s, 3 H), 3.78 (m, 6 H), 3.35 (q, 2 H, J = 5.6 Hz), 3.19 (q, 2 H, J = 5.3 Hz), 3.08 (q, 2 H, J = 5.7 Hz), 2.87 (q, 2 H, J = 5.8 Hz), 2.71 (d, 6 H, J = 4.0 Hz), 2.33 (m, 4 H), 1.99 (s, 3 H), 1.74 (m, 4 H); MALDI-TOF-MS 1036.2 (1036.1 calcd for M + H).

Construction of Plasmid DNA. Using T4 DNA ligase, the plasmid pMEPGG was constructed by ligation of an insert, 5'-GATCGC-

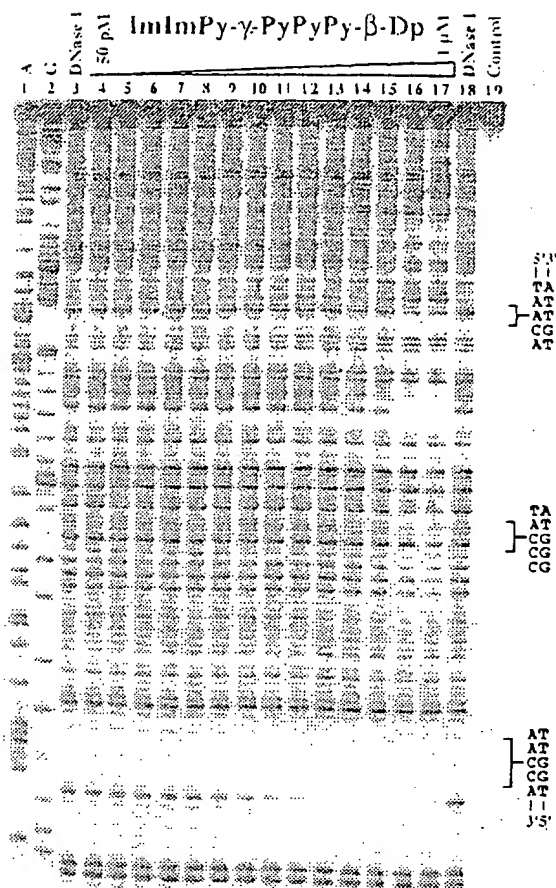


Figure 6. Quantitative DNase I footprint titration experiment with ImImPy- γ -PyPyPy- β -Dp (1) on the 3'- 32 P-labeled 266 base pair *EcoRI*/*PvuII* restriction fragment from plasmid pMEPGG. Lane 1: A reaction. Lane 2: G reaction. Lanes 3 and 18: DNase I standard. Lanes 4–17: 50 pM, 100 pM, 200 pM, 500 pM, 1 nM, 2 nM, 5 nM, 10 nM, 20 nM, 50 nM, 100 nM, 200 nM, 500 nM, 1 μ M ImImPy- γ -PyPyPy- β -Dp (1), respectively. Lane 19: intact DNA. The 5'-TGGTT-3', 5'-GGGTA-3', and 5'-TGTGA-3' sites which were analyzed are shown on the right side of the autoradiogram. All reactions contain 10 kpm restriction fragment, 10 mM Tris-HCl, 10 mM KCl, 10 mM MgCl₂, and 5 mM CaCl₂.

GAGCTCAGCGATGGTTTGGCATAGCGTGATTAGC-GTATGCGTGGGTAGCGATACGC-3' and 5'-GCGTATCGCTAC-CCACGATACGCTAAT-CACGCTATCGCAAACCATCGCTGAGCTCGCGATC-3', into pUC 19 previously cleaved with *Bam*HI and *Hind*III. Ligation products were used to transform Epicurian Coli XL 1 Blue competent cells (Stratagene). Colonies were selected for α -complementation on 25 mL Luria-Bertani medium agar plates containing 50 μ g/mL ampicillin and treated with XGAL and IPTG solutions. Large-scale plasmid purification was performed with Qiagen purification kits. Plasmid DNA concentration was determined at 260 nm using the relation 1 OD unit = 50 μ g/mL duplex DNA. The plasmid was linearized with *Eco*RI, followed by treatment with either Klenow, deoxyadenosine 5'-[α - 32 P]triphosphate (Amersham), and thymidine 5'-[α - 32 P]triphosphate for 3' labeling or calf alkaline phosphatase and subsequent 5' end labeling with T4 polynucleotide kinase and γ - 32 P]dATP. The 3'- or 5'-end-labeled fragment was then digested with *Pvu*II and isolated by nondenaturing gel electrophoresis. The 3'- or 5'- 32 P-end-labeled 266 base pair *Eco*RI/*Pvu*II restriction fragment was used in all experiments described here. Chemical sequencing reactions were performed according to published protocols.¹³ Standard protocols were used for all DNA manipulations.¹⁴

Identification of Binding Sites by MPE-Fe^{II} Footprinting. All reactions were carried out in a total volume of 40 μ L with final

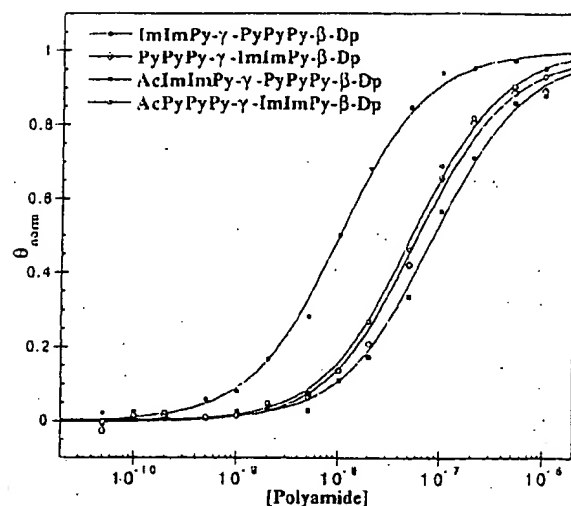


Figure 7. Data for the quantitative DNase I footprint titration experiments for the four polyamides 1–4 in complex with the designated 5'-TGGTT-3' site. The θ_{norm} points were obtained using photostimulable storage phosphor autoradiography and processed as described in the Experimental Section. The data points for ImImPy- γ -PyPyPy- β -Dp (1), PyPyPy- γ -ImImPy- β -Dp (2), AcImImPy- γ -PyPyPy- β -Dp (3), and AcPyPyPy- γ -ImImPy- β -Dp (4) are indicated by \bullet , \circ , \square , and \triangle , respectively. The solid curves are the best-fit Langmuir binding titration isotherms obtained from a nonlinear least squares algorithm using eq 2.

concentrations of species as indicated in parentheses. The ligands were added to solutions of radiolabeled restriction fragment (10 000 cpm), calf thymus DNA (100 μ M bp), Tris-acetate (25 mM, pH 7.0), and NaCl (10 mM) and incubated for 1 h at 22 $^{\circ}$ C. A 50 μ M MPE-Fe^{II} solution was prepared by mixing 100 μ L of a 100 μ M MPE solution with a freshly prepared 100 μ M ferrous ammonium sulfate solution. Footprinting reactions were initiated by the addition of MPE-Fe^{II} (5 μ M), followed 5 min later by the addition of dithiothreitol (5 mM), and allowed to proceed for 15 min at 22 $^{\circ}$ C. Reactions were stopped by ethanol precipitation, resuspended in 100 mM tris-borate-EDTA/80% formamide loading buffer, and electrophoresed on 8% polyacrylamide denaturing gels (5% cross-link, 7 M urea) at 2000 V for 1 h. The gels were analyzed using storage phosphor technology.

Analysis of Energetics by Quantitative DNase I Footprint Titration. All reactions were executed in a total volume of 40 μ L with final concentrations of each species as indicated. The ligands, ranging from 50 pM to 1 μ M, were added to solutions of radiolabeled restriction fragment (10 000 cpm), Tris-HCl (10 mM, pH 7.0), KCl (10 mM), MgCl₂ (10 mM), and CaCl₂ (5 mM) and incubated for 4 h at 22 $^{\circ}$ C. Footprinting reactions were initiated by the addition of 4 μ L of a stock solution of DNase I (0.025 unit/mL) containing 1 mM dithiothreitol and allowed to proceed for 6 min at 22 $^{\circ}$ C. The reaction mixtures were stopped by addition of a 3 M sodium acetate solution containing 50 mM EDTA and ethanol precipitated. The reactions were resuspended in 100 mM tris-borate-EDTA/80% formamide loading buffer and electrophoresed on 8% polyacrylamide denaturing gels (5% cross-link, 7 M urea) at 2000 V for 1 h. The footprint titration gels were dried and quantitated using storage phosphor technology.

Equilibrium association constants were determined as previously described.^{6,10} The data were analyzed by performing volume integrations of the 5'-TGGTT-3', 5'-TGTGA-3', and 5'-GGGTA-3' sites and a reference site. Binding sites are assumed to be independent and noninteracting as they are separated by at least one full turn of the double helix. The apparent DNA target site saturation, θ_{app} , was calculated for each concentration of polyamide using the following equation:

(13) (a) Iverson, B. L.; Dervan, P. B. *Nucleic Acids Res.* 1987, 15, 7823–7830. (b) Maxam, A. M.; Gilbert, W. S. *Methods Enzymol.* 1980, 65, 499–560.

(14) Sambrook, J.; Fritsch, E. F.; Maniatis, T. *Molecular Cloning*; Cold Spring Harbor Laboratory: Cold Spring Harbor, NY, 1989.

$$\theta_{\text{app}} = 1 - \frac{I_{\text{tot}} I_{\text{ref}}}{I_{\text{tot}}^0 I_{\text{ref}}^0} \quad (1)$$

where I_{tot} and I_{ref} are the integrated volumes of the target and reference sites, respectively, and I_{tot}^0 and I_{ref}^0 correspond to those values for a DNase I control lane to which no polyamide has been added. The $([L]_{\text{tot}}, \theta_{\text{app}})$ data points were fitted to a Langmuir binding isotherm (eq 2, $n = 1$) by minimizing the difference between θ_{app} and θ_{fit} using the modified Hill equation:

$$\theta_{\text{fit}} = \theta_{\text{min}} + (\theta_{\text{max}} - \theta_{\text{min}}) \frac{K_a [L]_{\text{tot}}}{1 + K_a [L]_{\text{tot}}} \quad (2)$$

where $[L]_{\text{tot}}$ corresponds to the total polyamide concentration, K_a corresponds to the association constant, and θ_{min} and θ_{max} represent the experimentally determined site saturation values when the site is unoccupied or saturated, respectively. The concentration of DNA used for quantitative footprint titrations is ≤ 50 pM, which justifies the assumption that free ligand concentration is approximately equal to total ligand concentration.¹⁰ Data were fitted using a nonlinear least squares fitting procedure of Kaleidagraph software (version 2.1, Abelbeck software) running on a Power Macintosh 6100/60AV computer with K_a , θ_{max} , and θ_{min} as the adjustable parameters. The goodness-of-fit of the binding curve to the data points is evaluated by the correlation coefficient, with $R > 0.97$ as the criterion for an acceptable fit. At least three sets of acceptable data were used in

determining each association constant. All lanes from each gel were used unless visual inspection revealed a data point to be obviously flawed relative to neighboring points. The data were normalized using the following equation:

$$\theta_{\text{norm}} = \frac{\theta_{\text{app}} - \theta_{\text{min}}}{\theta_{\text{max}} - \theta_{\text{min}}} \quad (3)$$

Quantitation by Storage Phosphor Technology Autoradiography. Photostimulable storage phosphorimaging plates (Kodak Storage Phosphor Screen S0230 obtained from Molecular Dynamics) were pressed flat against gel samples and exposed in the dark at 22 °C for 12–16 h. A Molecular Dynamics 400S PhosphorImager was used to obtain all data from the storage screens. The data were analyzed by performing volume integrations of all bands using the ImageQuant version 3.2 software running on an AST Premium 386/33 computer.

Acknowledgment. We are grateful to the National Institutes of Health (GM-27681) for research support, the National Institutes of Health for a research service award to M.E.P., and the Howard Hughes Medical Institute for a predoctoral fellowship to E.E.B.

JA9607289

Extension of Sequence-Specific Recognition in the Minor Groove of DNA by Pyrrole-Imidazole Polyamides to 9-13 Base Pairs

John W. Trauger, Eldon E. Baird, Milan Mrksich, and Peter B. Dervan*

Contribution from the Division of Chemistry and Chemical Engineering, California Institute of Technology, Pasadena, California 91125

Received March 6, 1996⁹

Abstract: The sequence-specific recognition of the minor groove of DNA by pyrrole-imidazole polyamides has been extended to 9-13 base pairs (bp). Four polyamides, ImPyPy-Py-PyPyPy-Dp, ImPyPy-G-PyPyPy-Dp, ImPyPy- β -PyPyPy-Dp, and ImPyPy- γ -PyPyPy-Dp (Im = *N*-methylimidazole, Py = *N*-methylpyrrole, Dp = *N,N*-dimethylaminopropylamide, G = glycine, β = β -alanine, and γ = γ -aminobutyric acid), were synthesized and characterized with respect to their DNA-binding affinities and specificities at sequences of composition 5'-(A,T)G-(A,T)₂C(A,T)-3' (9 bp) and 5'-(A,T)₂G(A,T)C(A,T)₂-3' (13 bp). In both sequence contexts, the β -alanine-linked compound ImPyPy- β -PyPyPy-Dp has the highest binding affinity of the four polyamides, binding the 9 bp site 5'-TGTTAAACA-3' ($K_a = 8 \times 10^8 \text{ M}^{-1}$) and the 13 bp site 5'-AAAAAGACAAAA-3' ($K_a = 5 \times 10^9 \text{ M}^{-1}$) with affinities higher than the formally *N*-methylpyrrole-linked polyamide ImPyPy-Py-PyPyPy-Dp by factors of ~ 8 and ~ 85 , respectively (10 mM Tris-HCl, 10 mM KCl, 10 mM MgCl₂, and 5 mM CaCl₂, pH 7.0). The binding data for ImPyPy- γ -PyPyPy-Dp, which has been shown previously to bind DNA in a "hairpin" conformation, indicates that γ -aminobutyric acid does not effectively link polyamide subunits in an extended conformation. These results expand the binding site size targetable with pyrrole-imidazole polyamides and provide structural elements that will facilitate the design of new polyamides targeted to other DNA sequences.

Introduction

The development of 2:1 pyrrole-imidazole polyamide-DNA complexes provides a new model for the design of molecules for sequence-specific recognition in the minor groove of DNA. The polyamide ImPyPy-Dp was shown to specifically bind the mixed A,T/G,C sequence 5'-(A,T)G(A,T)C(A,T)-3' as a side-by-side antiparallel dimer.¹ In this complex, each polyamide makes specific contacts with one strand on the floor of the minor groove such that the sequence specificity depends on the sequence of side-by-side amino acid pairings. A side-by-side pairing of imidazole opposite pyrrole recognizes G-C base pairs, while a side-by-side pairing of pyrrole opposite imidazole recognizes C-G base pairs.¹ A side-by-side pyrrole-pyrrole pairing is partially degenerate and targets both A-T and T-A base pairs.^{1,2} The generality of the 2:1 model has been demonstrated by targeting other sequences of mixed A,T/G,C composition.³⁻⁵ ImPyPy-Dp and distamycin (PyPyPy) bind simultaneously to a 5'-(A,T)G(A,T)₂-3' site as an antiparallel

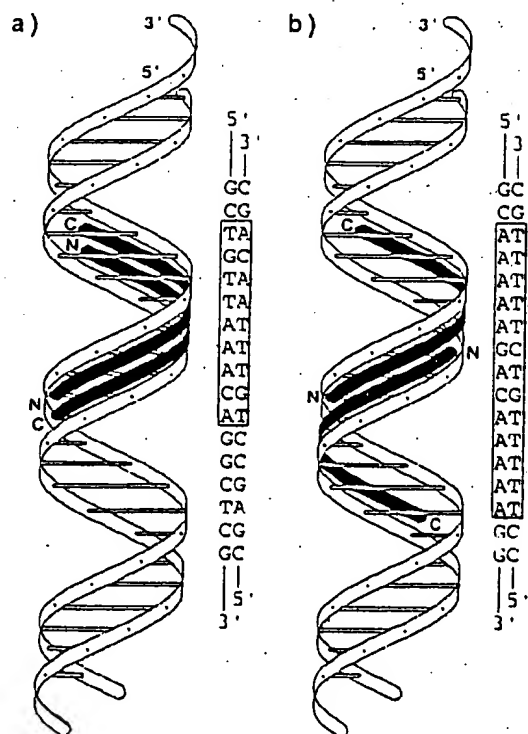


Figure 1. Ribbon models of (a) 9 bp "overlapped" and (b) 13 bp "slipped" 2:1 polyamide-DNA complexes.

heterodimer.³ A PyImPy polyamide and distamycin bind 5'-(A,T)₂G(A,T)₂-3'⁴ and ImPyImPy-Dp targets 5'-(A,T)GCGC-(A,T)-3'.⁵

The binding affinity and sequence specificity of a noncovalent antiparallel homodimeric or heterodimeric polyamide-DNA

* Abstract published in *Advance ACS Abstracts*, June 15, 1996.

(1) (a) Wade, W. S.; Mrksich, M.; Dervan, P. B. *J. Am. Chem. Soc.* 1992, 114, 5783. (b) Mrksich, M.; Wade, W. S.; Dwyer, T. J.; Geierstanger, B. H.; Wemmer, D. E.; Dervan, P. B. *Proc. Natl. Acad. Sci. U.S.A.* 1992, 89, 7586. (c) Wade, W. S.; Mrksich, M.; Dervan, P. B. *Biochemistry* 1993, 32, 11385.

(2) (a) Pelton, J. G.; Wemmer, D. E. *Proc. Natl. Acad. Sci. U.S.A.* 1989, 86, 5723. (b) Pelton, J. G.; Wemmer, D. E. *J. Am. Chem. Soc.* 1990, 112, 1393. (c) Chen, X.; Ramakrishnan, B.; Rao, S. T.; Sundaralingam, M. *Nature Struct. Biol.* 1994, 1, 169.

(3) (a) Mrksich, M.; Dervan, P. B. *J. Am. Chem. Soc.* 1993, 115, 2572-2576. (b) Geierstanger, B. H.; Jacobsen, J.-P.; Mrksich, M.; Dervan, P. B.; Wemmer, D. E. *Biochemistry* 1994, 33, 3055.

(4) Geierstanger, B. H.; Dwyer, T. J.; Battilini, Y.; Lowin, J. W.; Wemmer, D. E. *J. Am. Chem. Soc.* 1993, 115, 4474.

(5) (a) Geierstanger, B. H.; Mrksich, M.; Dervan, P. B.; Wemmer, D. E. *Science* 1994, 266, 646. (b) Mrksich, M.; Dervan, P. B. *J. Am. Chem. Soc.* 1995, 117, 3525.

4.9.97

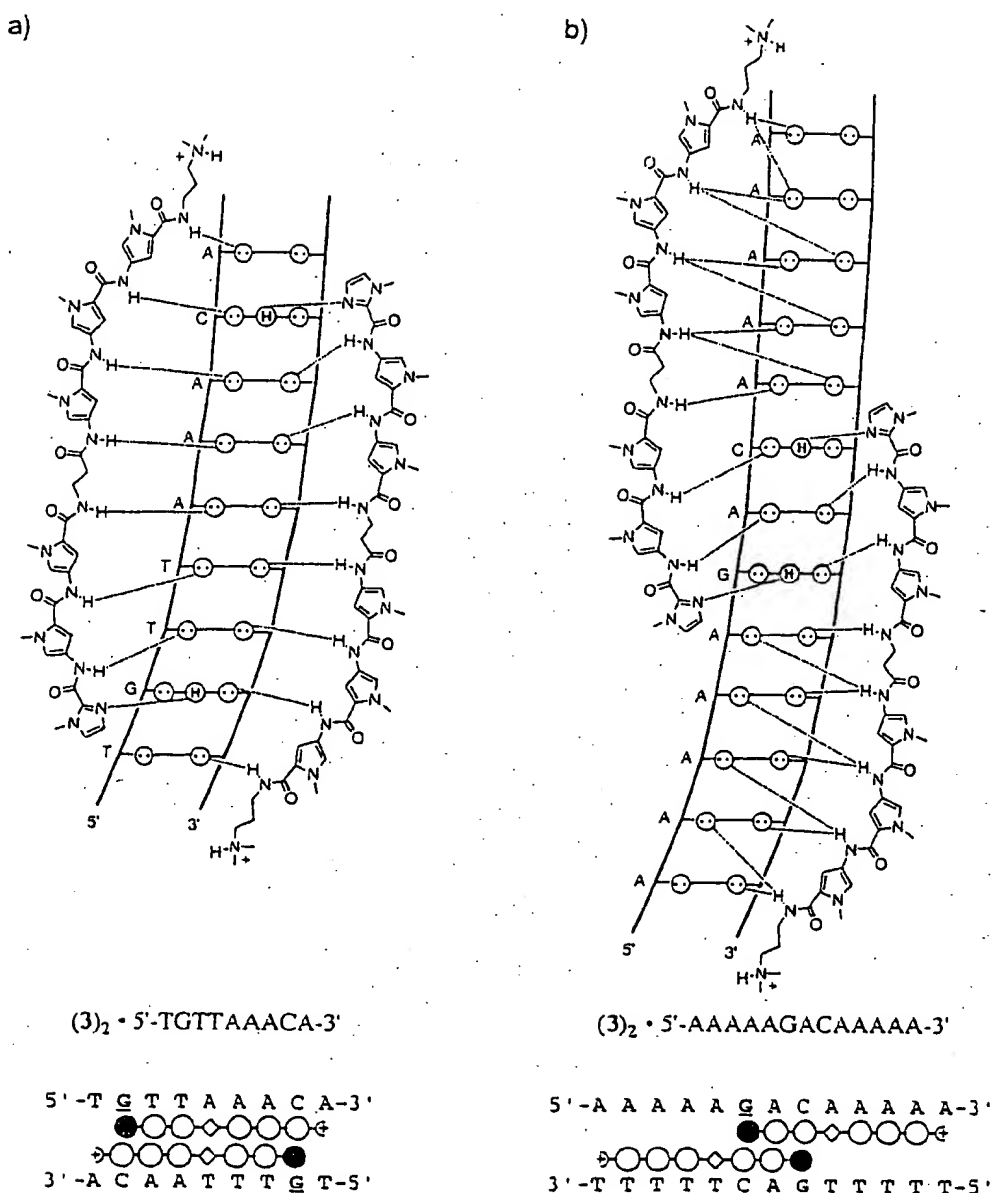


Figure 2. (Top) Complexes of ImPyPy- β -PyPyPy-Dp with the targeted sites (a) 5'-TGTTAAACA-3' (9 bp "overlapped") and (b) 5'-AAAAAGACAAAA-3' (13 bp "slipped"). Circles with dots represent lone pairs on N3 of purines and O2 of pyrimidines. Circles containing an H represent the N2 hydrogen of guanine. Putative hydrogen bonds are illustrated by dashed lines. (Bottom) Complexes of ImPyPy-X-PyPyPy-Dp, where X = Py, G, and β , with (a) 5'-TGTTAAACA-3' and (b) 5'-AAAAAGACAAAA-3'. The shaded and light circles represent imidazole and pyrrole rings, respectively, and the diamond represents the internal amino acid X. The specifically targeted guanines are highlighted.

complex can be increased by covalently linking the two polyamides.^{6,7} The DNA-binding properties of the polyamides ImPyPy-G-PyPyPy-Dp, ImPyPy- β -PyPyPy-Dp, and ImPyPy- γ -PyPyPy-Dp, in which the terminal carboxyl group of ImPyPy and the terminal amine of PyPyPy-Dp are connected with glycine (G), β -alanine (β), and γ -aminobutyric acid (γ), respectively, were recently reported.^{7,8} The γ -aminobutyric acid-linked polyamide bound the designated target site 5'-TGTTA-3' with high affinity and sequence specificity and

exhibited a binding isotherm in quantitative footprinting experiments consistent with formation of an intramolecular "hairpin" complex in which the polyamide folds back on itself.⁷ Modeling suggested that the glycine- and β -alanine-linked polyamides do not favorably bind as "hairpins" in the minor groove of DNA. Moreover, these polyamides exhibited cooperative binding isotherms in quantitative footprinting experiments, consistent with two polyamides binding in extended conformations as *intermolecular dimers*.^{7,8} It appears that the glycine- and β -alanine-linked polyamides disfavor binding in the hairpin conformation and prefer to bind in an extended conformation.^{7,8} In a formal sense, there are multiple extended binding motifs (and hence multiple binding site sequences) for polyamides of sequence composition Im(Py)_x-Dp, as discussed below.

"Overlapped" and "Slipped" Binding Modes. We report here the DNA-binding affinities of four polyamides having the

(6) (a) Mrksich, M.; Dervan, P. B. *J. Am. Chem. Soc.* 1993, 115, 9892-9899. (b) Dwyer, T. J.; Geierstanger, B. H.; Mrksich, M.; Dervan, P. B.; Wemmer, D. E. *J. Am. Chem. Soc.* 1993, 115, 9900. (c) Mrksich, M.; Dervan, P. B. *J. Am. Chem. Soc.* 1994, 116, 3663. (d) Singh, M. P.; Plouvier, B.; Hill, G. C.; Gueck, J.; Pon, R. T.; Lown, J. W. *J. Am. Chem. Soc.* 1994, 116, 2006.

(7) Mrksich, M.; Parks, M. E.; Dervan, P. B. *J. Am. Chem. Soc.* 1994, 116, 7983.

(8) Mrksich, M. Ph.D. Thesis, California Institute of Technology, 1994.

general sequence $\text{ImPyPy-X-PyPyPy-Dp}$, where $X = \text{Py, G, } \beta,$ or γ , to the 9 bp site 5'-TGTTAAACA-3' and to the 13 bp sites 5'-AAAAAGACAAAAA-3' and 5'-ATATAGACATATA-3'. The polyamides having internal *N*-methylpyrrole, glycine, and β -alanine residues were anticipated to bind the 9 and 13 bp sites in an extended conformation. It was not clear at the outset if the γ -aminobutyric acid-linked polyamide $\text{ImPyPy-}\gamma\text{-PyPyPy-Dp}$ would bind exclusively in an extended or "hairpin" conformation to the targeted sites. For $\text{ImPyPy-X-PyPyPy-Dp}$ polyamides binding in an extended conformation, the polyamide-DNA complexes expected to form at the 9 bp and 13 bp target sites represent two distinct binding modes, which we refer to as "overlapped" and "slipped", respectively. In the "overlapped" (9 bp) binding mode, two $\text{ImPyPy-X-PyPyPy-Dp}$ polyamides bind directly opposite one another (Figures 1a and 2a). The "slipped" (13 bp) binding mode integrates the 2:1 and 1:1 polyamide-DNA binding motifs at a single site. In this binding mode, the ImPyPy moieties of two $\text{ImPyPy-X-PyPyPy-Dp}$ polyamides bind the central 5'-AGACA-3' sequence in a 2:1 manner as in the ImPyPy homodimer,¹ and the PyPyPy moieties of the polyamides bind the all-A,T flanking sequences as in the 1:1 complexes of distamycin (Figures 1b and 2b). The structure of the complex formed by the polyamide $\text{ImPyPy-G-PyPyPy-Dp}$ with a 13 bp target site has been characterized by 2D NMR.⁹

In the 9 bp "overlapped" and 13 bp "slipped" binding sites described above, the G-C and C-G base pairs are separated by one and five A,T base pairs, respectively. While we have concentrated here on these sites, we note that "partially slipped" sites of 10, 11, and 12 bp in which the G-C and C-G base pairs are separated by two, three, and four A,T base pairs, respectively, are also potential binding sites of the polyamides studied here.

Studies of the energetics of distamycin binding have shown that while the binding affinities are similar for complexation to $\text{poly}[\text{d}(\text{A-T})]\cdot\text{poly}[\text{d}(\text{A-T})]$ and $\text{poly}[\text{d}(\text{A})]\cdot\text{poly}[\text{d}(\text{T})]$, the origins of these binding affinities are different.¹⁰ Binding to the alternating copolymer is enthalpy driven, while binding to the homopolymer is entropy driven.¹⁰ However, not all 5 bp sites (A,T)₅ are bound with equal affinity. By quantitative footprinting experiments, the distamycin analog Ac-PyPyPy-Dp (Ac = acetyl) was shown to bind the sites 5'-AATAA-3' and 5'-TTAAT-3' with 2-fold and 14-fold lower affinity, respectively, relative to the site 5'-AAAAA-3'.¹⁶ On the basis of this result, we anticipated that the 13 bp site 5'-AAAAAGACAAAAA-3' may be bound with higher affinity than the 13 bp site 5'-ATATAGACATATA-3'.

The binding affinities of polyamides 1-4 (Figure 3) for the three targeted sites 5'-TGTTAAACA-3', 5'-AAAAAGACAAAAA-3', and 5'-ATATAGACATATA-3' were determined by quantitative DNase I footprint titration experiments.

Results

Synthesis of Polyamides. The polyamides $\text{ImPyPy-Py-PyPyPy-Dp}$ (1),¹¹ $\text{ImPyPy-G-PyPyPy-Dp}$ (2),⁷ $\text{ImPyPy-}\beta\text{-PyPyPy-Dp}$ (3),⁷ and $\text{ImPyPy-}\gamma\text{-PyPyPy-Dp}$ (4)⁷ were prepared as described previously.

(9) Geierstanger, B. H.; Mirskich, M.; Dervan, P. B.; Wemmer, D. E. *Nature Struct. Biol.* 1996, 3, 321.

(10) Breslauer, K. J.; Remeta, D. P.; Chou, W.-Y.; Ferrante, R.; Curry, J.; Zaunzowski, D.; Snyder, J. G.; Marky, L. A. *Proc. Natl. Acad. Sci. U.S.A.* 1987, 84, 8922. (b) Marky, L. A.; Breslauer, K. J. *Proc. Natl. Acad. Sci. U.S.A.* 1987, 84, 4359. (c) Marky, L. A.; Kupke, K. I. *Biochemistry* 1989, 28, 9982.

(11) Kelly, J. J.; Baird, E. E.; Dervan, P. B. *Proc. Natl. Acad. Sci. U.S.A.*, in press.

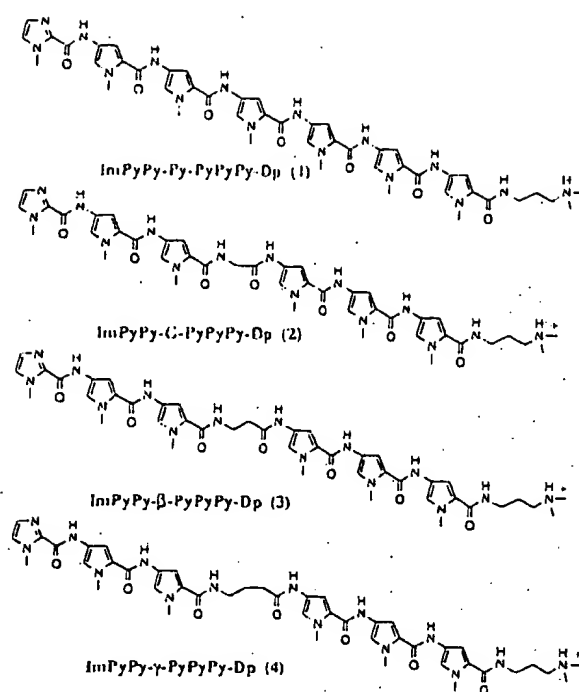


Figure 3. Structures of the four polyamides $\text{ImPyPy-X-PyPyPy-Dp}$, where $X = \text{N-methylpyrrole (Py), glycine (G), } \beta\text{-alanine } (\beta), \text{ and } \gamma\text{-aminobutyric acid } (\gamma)$.

Footprinting. Quantitative DNase I footprinting^{12,13} on the 3'-³²P-labeled 281 bp pJT3 *A/III/FspI* restriction fragment (Figures 4 and 5) (10 mM Tris-HCl, 10 mM KCl, 10 mM MgCl_2 , 5 mM CaCl_2 , pH 7.0, 22 °C) reveals that, of the four polyamides $\text{ImPyPy-X-PyPyPy-Dp}$, three ($X = \text{Py, G, } \beta$) bind to both the 9 bp "overlapped" site 5'-TGTTAAACA-3' and the 13 bp "slipped" site 5'-AAAAAGACAAAAA-3' with equilibrium association constants (K_a) greater than $5 \times 10^7 \text{ M}^{-1}$ (Table 1) and display cooperative binding isotherms (eq 2, $n = 2$) at these sites consistent with binding as intermolecular dimers (Figure 6). The fact that the polyamides $\text{ImPyPy-G-PyPyPy-Dp}$ and $\text{ImPyPy-}\beta\text{-PyPyPy-Dp}$ bind in the 9 bp "overlapped" binding mode indicates that the internal glycine and β -alanine amino acids are accommodated opposite a second ligand in a 2:1 polyamide-DNA complex.

The polyamide $\text{ImPyPy-}\gamma\text{-PyPyPy-Dp}$ binds the site 5'-TGTTAAACA-3' with an equilibrium association constant K_a $1 \times 10^8 \text{ M}^{-1}$ and also binds the site 5'-AAAAAGACAAAAA-3' with lower affinity ($K_a = 6 \times 10^6 \text{ M}^{-1}$). This compound displays binding isotherms (eq 2, $n = 1$) at these sites (Figure 6), consistent with binding as an intramolecular hairpin to the 5 bp "matched" sites 5'-TGTTA-3' and 5'-AAACA-3' (Figure 7) and to the 5 bp "single base pair mismatch" site 5'-AGACA-3'.⁷ Significantly, it appears from these results that $\text{ImPyPy-}\gamma\text{-PyPyPy-Dp}$ does not effectively link polyamide subunits in an extended conformation.

Binding Affinities. Comparison of the binding affinities of the four polyamides $\text{ImPyPy-X-PyPyPy-Dp}$, where $X = \text{Py, G, } \beta,$ and γ , reveals that the internal amino acid X has a dramatic effect on complex stabilities (Table 1, Figure 6). The formally *N*-methylpyrrole-linked polyamide $\text{ImPyPy-Py-PyPyPy-Dp}$ binds

(12) (a) Galas, D.; Schmitz, A. *Nucleic Acids Res.* 1978, 5, 3157. (b) Fox, K. R.; Waring, M. J. *Nucleic Acids Res.* 1984, 12, 9271.

(13) (a) Brenowitz, M.; Seneac, D. F.; Shea, M. A.; Ackers, G. K. *Methods Enzymol.* 1986, 130, 132. (b) Brenowitz, M.; Seneac, D. F.; Shea, M. A.; Ackers, G. K. *Proc. Natl. Acad. Sci. U.S.A.* 1986, 83, 8462. (c) Seneac, D. F.; Brenowitz, M.; Shea, M. A.; Ackers, G. K. *Biochemistry* 1986, 25, 7344.

5'-GCAACTGTGGGAAGGCGATCGGTGCGGGCCTCTTCGCTATTACGCCAGCTGGCGAAGGGGGATGTGCTGCAAGGCGATTAGTTGGGTAACG
 3'-CGTTACAAACCTTCCCGTAGCCACGCCGAGAGCGATAATGCGGTGACCGCTTTCCCTACACGACGTTCCGCTAATTCAACCCATTGC

CCAGGGTTTTTCCACTCACGACGTTGTAAACGACGGCCAGTGAATTCGAGCTCGGTACCCGGGAACGATAGCGTACCGGTGCAAAAAGACAAAAAGGC
 GTGCCAAAAGGGTCAGTGTGCAACATTTGCTGCGGGTCACTTAAGCTCGAGCATGGGCTTTGCAATCGCATGCGCACTTTTCTGTTTTCGG

TGCAGCCCGCATATAGACATATAGGGCCGTCGACGCTGTTAAACAGGCTCGACGCCAGCTGCTCTAGCTAGCGTCTAGCGTTTAA-3'
 AGCTCCGCCGCTATATCTGTATATCCCGCAGCTGCGACAATTTCGAGCTGCGGTGAGCAGGATCGATCGACCATCGCAGAATT-5'

Figure 4. Sequence of the 281 bp pJT3. *Afl*III/*Esp*I restriction fragment. The three binding sites that were analyzed in quantitative footprint titration experiments are indicated.

Table 1. Association Constants (M^{-1}) for Polyamides ImPyPy-X-PyPyPy-Dp, Where X = *N*-Methylpyrrole (Py), Glycine (G), β -Alanine (β), and γ -Aminobutyric Acid (γ).^{a,b}

binding site	polyamide			
	ImPyPy-Py-PyPyPy-Dp	ImPyPy-G-PyPyPy-Dp	ImPyPy- β -PyPyPy-Dp	ImPyPy- γ -PyPyPy-Dp
5'-TGTTAAACA-3'	$9.7 (\pm 2.3) \times 10^7$	$1.4 (\pm 0.1) \times 10^8$	$7.8 (\pm 0.6) \times 10^8$	$1.4 (\pm 0.3) \times 10^8$
5'-AAAAAGACAAAAA-3'	$5.4 (\pm 1.5) \times 10^7$	$1.1 (\pm 0.1) \times 10^8$	$\geq 4.7 (\pm 0.7) \times 10^8$	$6.4 (\pm 0.6) \times 10^6$
5'-ATATAGACATATA-3'	$3.6 (\pm 0.5) \times 10^7$	$6.6 (\pm 0.4) \times 10^6$	$1.0 (\pm 0.1) \times 10^8$	$4.6 (\pm 0.5) \times 10^6$

^a The reported association constants are the mean values obtained from three DNase I footprint titration experiments. The standard deviation for each value is indicated in parentheses. ^b The assays were carried out at 22 °C at pH 7.0 in the presence of 10 mM Tris-HCl, 10 mM KCl, 10 mM MgCl₂, and 5 mM CaCl₂.

5'-TGTTAAACA-3' and 5'-AAAAAGACAAAAA-3' with equilibrium association constants $K_a = 1 \times 10^8 M^{-1}$ and $5 \times 10^7 M^{-1}$, respectively. The glycine-linked polyamide ImPyPy-G-PyPyPy-Dp binds both 5'-TGTTAAACA-3' and 5'-AAAAAGACAAAAA-3' with affinities similar (equal and 2-fold higher, respectively) to those of ImPyPy-Py-PyPyPy-Dp. In contrast, the β -alanine linked polyamide ImPyPy- β -PyPyPy-Dp binds 5'-TGTTAAACA-3' and 5'-AAAAAGACAAAAA-3' with affinities higher than those of ImPyPy-Py-PyPyPy-Dp by factors of approximately 8 ($K_a = 8 \times 10^8 M^{-1}$) and 85 ($K_a = 5 \times 10^9 M^{-1}$), respectively. Relative to ImPyPy-Py-PyPyPy-Dp, the hairpin-forming polyamide ImPyPy- γ -PyPyPy-Dp binds 5'-TGTTAAACA-3' (a matched hairpin binding site) and 5'-AAAAAGACAAAAA-3' (a mismatched hairpin binding site) with equal and 8-fold-lower affinities, respectively.

Specificity for 5'-AAAAAGACAAAAA-3' versus 5'-ATATAGACATATA-3'. Comparison of the binding affinities of the four polyamides at the 13 bp sites 5'-AAAAAGACAAAAA-3' and 5'-ATATAGACATATA-3' indicates that the specificity between the sites depends on the internal amino acid (Table 1). ImPyPy-G-PyPyPy-Dp and ImPyPy- β -PyPyPy-Dp are approximately 20-fold and ≥ 5 -fold specific respectively for 5'-AAAAAGACAAAAA-3' versus 5'-ATATAGACATATA-3'. The polyamides ImPyPy-Py-PyPyPy-Dp and ImPyPy- γ -PyPyPy-Dp bind 5'-AAAAAGACAAAAA-3' and 5'-ATATAGACATATA-3' with similar affinities.

Discussion

Implications for the Design of Minor Groove Binding Molecules. The results presented here reveal that β -alanine is an optimal linker for joining two three-ring subunits in an extended conformation, providing a useful structural motif for the design of new polyamides targeted to sites longer than 8 bp. Recently, it has been shown that as the length of a polyamide having the general sequence Im(Py)_x-Dp increases beyond five rings (corresponding to a 7 bp binding site), the binding affinity ceases to increase with increasing polyamide length, indicating that the *N*-methylimidazole and *N*-methylpyrrole residues fail to maintain an appropriate base-pair register across the entire length of the polyamide-DNA complex.¹¹ The higher binding affinities observed here for ImPyPy- β -PyPyPy-Dp relative to ImPyPy-Py-PyPyPy-Dp indicate that the flexible β -alanine linker relieves the register mismatch, allowing both three-ring subunits to bind optimally. Notably, higher binding affinities are observed for ImPyPy- β -PyPyPy-Dp versus Im-

PyPy-Py-PyPyPy-Dp despite the higher conformational entropy and lower aromatic surface area of the β -alanine-linked polyamide. The observation here that β -alanine effectively links polyamide subunits within 2:1 polyamide-DNA complexes is consistent with the previously reported finding that β -alanine effectively links polyamide subunits within 1:1 polyamide-DNA complexes.¹⁴

From the standpoint of binding specificity, the observation here that a single compound can bind in multiple binding modes is problematic. The next generation of pyrrole-imidazole polyamides targeted to binding sites greater than 8 bp in length should incorporate constraints that specify a single binding mode.

The previously described γ -aminobutyric acid-based "hairpin" motif⁷ complements the β -alanine-based "extended" motif described here. For ImPyPy- γ -PyPyPy-Dp, the binding isotherms and affinities observed here are consistent with the previous report that γ -aminobutyric acid effectively links polyamide subunits in a "hairpin" conformation⁷ and indicate that γ -aminobutyric acid does not effectively link polyamide subunits in an extended conformation. Significantly, these observations indicate that (1) extended binding modes will not compromise the sequence specificity of hairpin-forming, γ -aminobutyric acid-linked polyamides, and (2) β -alanine and γ -aminobutyric acid linkers could be used within a single polyamide with predictable results.

The results reported here expand the binding site size targetable with pyrrole-imidazole polyamides and provide structural motifs that will facilitate the design of new pyrrole-imidazole polyamides targeted to other sequences.

Experimental Section

Materials. Restriction endonucleases were purchased from either New England Biolabs or Boehringer-Mannheim and used according to the manufacturer's protocol. *Escherichia coli* XL-1 Blue competent cells were obtained from Stratagene. Sequenase (version 2.0) was obtained from United States Biochemical, and DNase I was obtained from Pharmacia. [α -³²P]Thymidine 5'-triphosphate (≥ 3000 Ci/mmol) and [α -³²P]deoxyadenosine 5'-triphosphate (≥ 6000 Ci/mmol) were purchased from DuPont NEN.

Construction of Plasmid DNA. Plasmid pJT3 was prepared by standard methods. Briefly, plasmid pJT1 was prepared by hybridization of two complementary sets of synthetic oligonucleotides: 5'-CCGG-

(14) (a) Youngquist, R. S.; Dervan, P. B. *J. Am. Chem. Soc.* 1987, 109, 7564. (b) Griffin, J. H.; Dervan, P. B. Unpublished results.

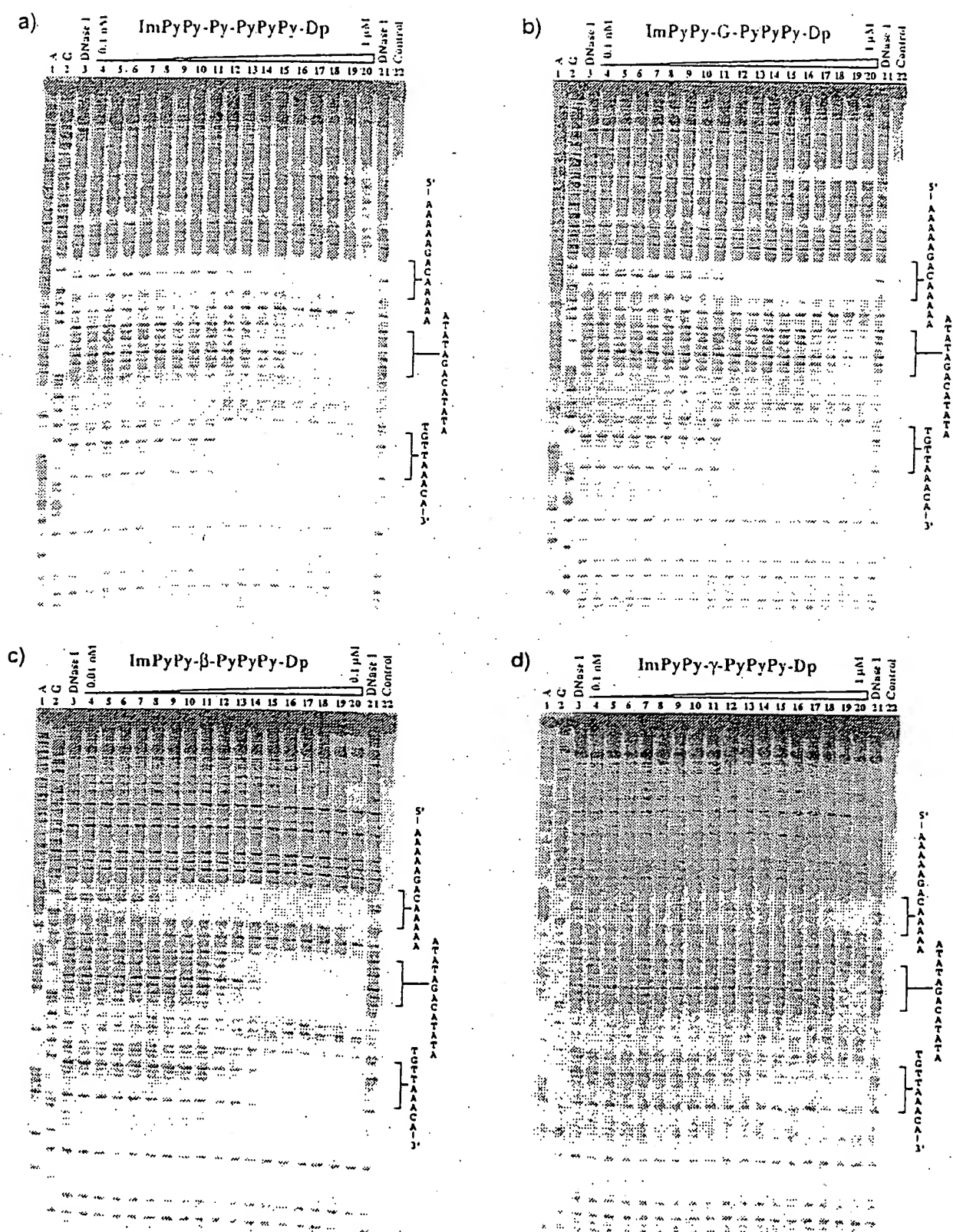


Figure 5. Storage phosphor autoradiograms of 8% denaturing polyacrylamide gels used to separate the fragments generated by DNase I digestion in quantitative footprint titration experiments. Lanes 1 and 2, A and G sequencing lanes. Lanes 3 and 21: DNase I digestion products obtained in the absence of polyamide. Lanes 4-20: DNase I digestion products obtained in the presence of 0.1 nM (0.01 nM), 0.2 nM (0.02 nM), 0.5 nM (0.05 nM), 1 nM (0.1 nM), 1.5 nM (0.15 nM), 2.5 nM (0.25 nM), 4 nM (0.4 nM), 6.5 nM (0.65 nM), 10 nM (1 nM), 15 nM (1.5 nM), 25 nM (2.5 nM), 40 nM (4 nM), 65 nM (6.5 nM), 100 nM (10 nM), 200 nM (20 nM), 300 nM (30 nM), 1 μM (0.1 μM) (concentrations used for polyamide ImPyPy-β-PyPyPy-Dp only are in parentheses). Lane 22: intact DNA. The targeted binding sites are indicated on the right side of the autoradiograms. All reactions contain 15 kbp restriction fragment, 10 mM Tris-HCl, 10 mM KCl, 10 mM MgCl₂, and 5 mM CaCl₂.

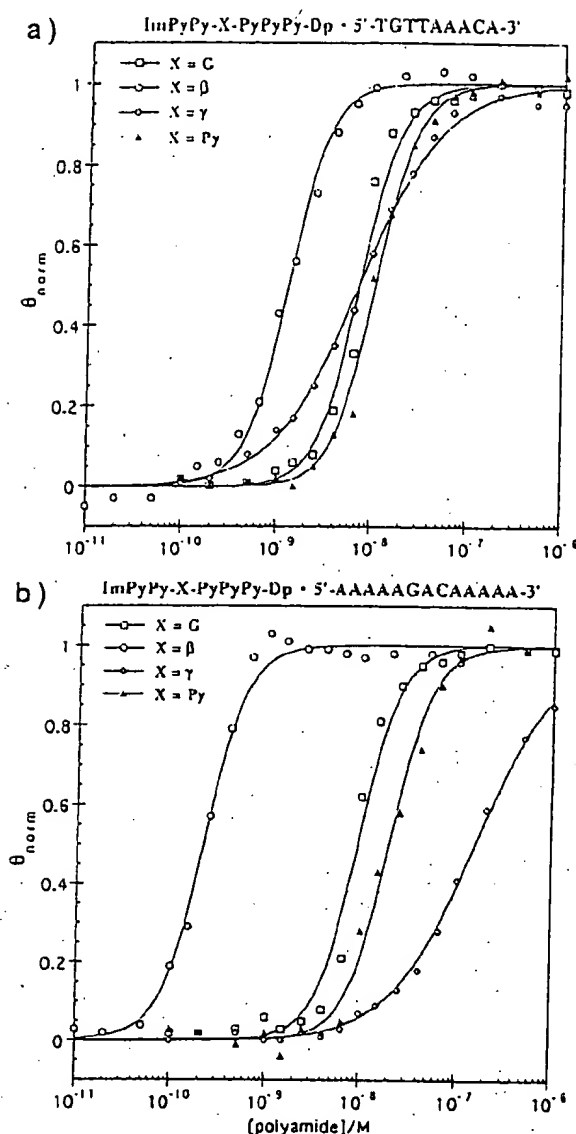


Figure 6. Data obtained from quantitative DNase I footprint titration experiments showing the effect of the internal amino acid X on binding of the polyamides ImPyPy-X-PyPyPy-Dp to the sites (a) 5'-TGT-TAAACA-3' and (b) 5'-AAAAAGACAAAA-3', where X = G (\square), β (\bullet), γ (\diamond), and Py (\blacktriangle). The $(\theta_{\text{norm}}, [L]_{\text{tot}})$ data points were obtained as described in the Experimental Section. Each data point is the average value obtained from three quantitative footprint titration experiments.

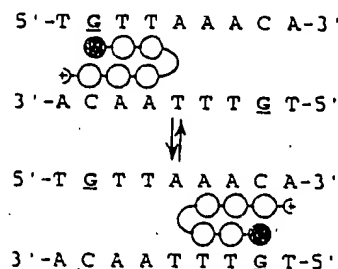


Figure 7. Model for the complex formed by ImPyPy- γ -PyPyPy-Dp with 5'-TGTTAAACA-3' (5 bp, "hairpin").

GAACGTAGCGTACCGGTGCAAAAAGACAAAAAGG-CTCGA-3' and 5'-GGCGTCGAGCCTTTTGTCTTTTGCACCGTACGTACGTTT-3', and 5'-CGCCGCATATAGACATATAGGGCCGAGCTCGTCTAGCTAGCGTCTAGCGTCTTAAG-3' and 5'-TCGACTTAAGACGCTACGACGCTAGCTAGGACGAGCT-

GGGCTTATATGCTTATATGC-3'. The resulting oligonucleotide duplexes were phosphorylated with ATP and T4 polynucleotide kinase and ligated to the large pUC19 *AbaI/SalI* restriction fragment using T4 DNA ligase. *E. coli* XL-1 Blue competent cells were then transformed with the ligated plasmid, and plasmid DNA from ampicillin-resistant white colonies isolated using a Promega Maxi-Prep kit. Plasmid pJT3 was prepared in a similar manner, except that the following synthetic oligonucleotides were hybridized and cloned into the large *ApaI/SalI* fragment of pJT1: 5'-GTGACGCTGTTAAACAGGCTCGACGCCAGCTCGTCTAGCTAGCGTCTAGCGTCTTAAGAG-3' and 5'-TCGACTTAAAGACGCTACGACGCTAGCTAGGACGAGCTGGCGTCCGAGCCTGTTAAACAGGCTCGACGCC-3'. The presence of the desired insert was determined by restriction analysis and dideoxy sequencing. Plasmid DNA concentration was determined at 260 nm using the relation 1 OD unit = 50 $\mu\text{g/mL}$ duplex DNA.

Preparation of ^{32}P -End-Labeled Restriction Fragments. Plasmid pJT3 was digested with *AflIII*, labeled at the 3'-end using Sequenase (version 2.0), and digested with *FspI*. The 281 bp restriction fragment was isolated byondenaturing gel electrophoresis and used in all quantitative footprinting experiments described here. Chemical sequencing reactions were performed as described.^{15,16} Standard techniques were employed for DNA manipulations.¹⁷

Quantitative DNase I Footprint Titration.^{12,15} All reactions were executed in a total volume of 40 μL . We note explicitly that no carrier DNA was used in these reactions. A polyamide stock solution or H_2O (for reference lanes) was added to an assay buffer containing radiolabeled restriction fragment (15 000 cpm), affording final solution conditions of 10 mM Tris-HCl, 10 mM KCl, 10 mM MgCl_2 , 5 mM CaCl_2 , pH 7.0, and either (i) 0.1 nM to 1 μM polyamide, for all polyamides except ImPyPy- β -PyPyPy-Dp, (ii) 0.01 nM to 0.1 μM polyamide for ImPyPy- β -PyPyPy-Dp, or (iii) no polyamide (for reference lanes). The solutions were allowed to equilibrate for 5 h at 22 $^\circ\text{C}$. Footprinting reactions were initiated by the addition of 4 μL of a DNase I stock solution (at the appropriate concentration to give ~55% intact DNA) containing 1 mM dithiothreitol and allowed to proceed for 7 min at 22 $^\circ\text{C}$. The reactions were stopped by the addition of 10 μL of a solution containing 1.25 M NaCl, 100 mM EDTA, and 0.2 mg/mL glycogen, and ethanol precipitated. The reaction mixtures were resuspended in 1X TBE/80% formamide loading buffer, denatured by heating at 85 $^\circ\text{C}$ for 10 min, and placed on ice. The reaction products were separated by electrophoresis on an 8% polyacrylamide gel (5% cross-link, 7 M urea) in 1X TBE at 2000 V. Gels were dried and exposed to a storage phosphor screen (Molecular Dynamics).

Quantitation and Data Analysis. Data from the footprint titration gels were obtained using a Molecular Dynamics 400S PhosphorImager followed by quantitation using ImageQuant software (Molecular Dynamics). Background-corrected volume integration of rectangles encompassing the footprint sites and a reference site at which DNase I reactivity was invariant across the titration generated values for the site intensities (I_{site}) and the reference intensity (I_{ref}). The apparent fractional occupancies (θ_{app}) of the sites were calculated using the equation

$$\theta_{\text{app}} = 1 - \frac{I_{\text{site}}/I_{\text{ref}}}{I_{\text{site}}^0/I_{\text{ref}}^0} \quad (1)$$

where I_{site} and I_{ref} are the site and reference intensities, respectively, from a control lane to which no polyamide was added.

The $([L]_{\text{tot}}, \theta_{\text{app}})$ data points were fitted to a general Hill equation (eq 2) by minimizing the difference between θ_{app} and θ_{fit} :

$$\theta_{\text{fit}} = \theta_{\text{min}} + (\theta_{\text{max}} - \theta_{\text{min}}) \frac{K_a^n [L]_{\text{tot}}^n}{1 + K_a^n [L]_{\text{tot}}^n} \quad (2)$$

where $[L]_{\text{tot}}$ is the total polyamide concentration, K_a is the apparent association constant, and θ_{min} and θ_{max} are the experimentally deter-

(15) Iverson, B. L.; Dervan, P. B. *Nucleic Acids Res.* 1987, 15, 7823-7830.

(16) Maxam, A. M.; Gilbert, W. S. *Methods Enzymol.* 1980, 65, 499-560.

(17) Sambrook, J.; Fritsch, E. F.; Maniatis, T. *Molecular Cloning*; Cold Spring Harbor Laboratory: Cold Spring Harbor, NY, 1989.

nmed site saturation values when the site is unoccupied or saturated, respectively. The data were fitted using a nonlinear least squares fitting procedure with K_a , θ_{\max} , and θ_{\min} as the adjustable parameters, and with either $n = 2$ or $n = 1$ depending on which value of n gave the better fit. We note explicitly that treatment of the data in this manner does not represent an attempt to model a binding mechanism. Rather, we have chosen to compare values of the association constant, a parameter that represents the concentration of polyamide at which the binding site is half-saturated. The binding isotherms were normalized using the following equation:

$$\theta_{\text{norm}} = \frac{\theta_{\text{app}} - \theta_{\min}}{\theta_{\max} - \theta_{\min}} \quad (3)$$

Three sets of data were used in determining each association constant.

The method for determining association constants used here involves the assumption that $[L]_{\text{tot}} \approx [L]_{\text{free}}$, where $[L]_{\text{free}}$ is the concentration of

polyamide free in solution (unbound). For very high association constants this assumption becomes invalid, resulting in underestimated association constants. In the experiments described here, the DNA concentration is estimated to be ~ 50 pM. As a consequence, measured association constants of $1 \times 10^9 \text{ M}^{-1}$ and $5 \times 10^9 \text{ M}^{-1}$ underestimate the true association constants by factors of approximately ± 1.5 and $1.5-2$, respectively.

Acknowledgment. We are grateful to the National Institutes of Health (Grant GM-27681) for research support, to the National Science Foundation for a predoctoral fellowship to J.W.T., and to the Howard Hughes Medical Institute for a predoctoral fellowship to E.E.B.

JA960726C

Hin Recombinase Bound to DNA: The Origin of Specificity in Major and Minor Groove Interactions

Jin-An Feng, Reid C. Johnson, Richard E. Dickerson*

The structure of the 52-amino acid DNA-binding domain of the prokaryotic Hin recombinase, complexed with a DNA recombination half-site, has been solved by x-ray crystallography at 2.3 angstrom resolution. The Hin domain consists of a three- α -helix bundle, with the carboxyl-terminal helix inserted into the major groove of DNA, and two flanking extended polypeptide chains that contact bases in the minor groove. The overall structure displays features resembling both a prototypical bacterial helix-turn-helix and the eukaryotic homeodomain, and in many respects is an intermediate between these two DNA-binding motifs. In addition, a new structural motif is seen: the six-amino acid carboxyl-terminal peptide of the Hin domain runs along the minor groove at the edge of the recombination site, with the peptide backbone facing the floor of the groove and side chains extending away toward the exterior. The x-ray structure provides an almost complete explanation for DNA mutant binding studies in the Hin system and for DNA specificity observed in the Hin-related family of DNA invertases.

The Hin recombinase catalyzes a DNA inversion reaction in the *Salmonella* chromosome (1, 2). This site-specific recombination reaction controls the alternate expression of two flagellin genes by reversibly switching the orientation of a promoter. During the process of inverting the 1-kb segment of DNA, Hin proteins bind to left and right recombination sites (*hixL* and *hixR*, respectively) located at the boundaries of the invertible DNA segment. The *hixL* and *hixR* sites with their bound Hin protein then form a synaptic complex with a third *cis*-acting site, a recombinational enhancer, which itself is bound by two dimers of the 98-amino acid Fis protein. Formation of this invertasome complex (3–5) aligns the two recombination sites correctly and activates the Hin protein to initiate the exchange of DNA strands, leading to inversion of the intervening DNA.

Hin belongs to a family of bacterial DNA invertases or recombinases that includes Gin from phage Mu, Cin from phage P1, and Pin from the ϕ 14 prophage of *Escherichia coli*. In addition to sharing 66 to 80 percent sequence identity between pairs of sequences, this family of proteins can substitute functionally for one another in each biological system (1). These DNA invertases most likely constitute an evolutionary family not unlike the c-type cytochromes. The availability of DNA sequence information from the binding sites of all four systems makes the present study of Hin-DNA binding es-

pecially informative in elucidating principles of protein-DNA recognition.

Hin binds to each *hixL* and *hixR* recom-

bination site as a dimer. The final 52 amino acids of the two chains (Fig. 1A) are involved in binding to a 26-bp recombination site (Fig. 1B) built from two 12-bp imperfect inverted repeats separated by a 2-bp core region where DNA strand exchange occurs (6–8). The amino-terminal 138-amino acid "catalytic" domain is positioned in part over the core nucleotides. Although the monomeric 52-amino acid peptide by itself can bind to a recombination half-site with low-to-moderate affinity (dissociation constant $K_d \approx 10^{-7}$), cooperative interactions between the amino-terminal domains of two intact Hin molecules are required for high-affinity binding ($K_d \approx 10^{-9}$) (8–10).

A large body of footprinting, mutation, and chemical derivatization data has indicated features of Hin-DNA interaction which are distinctive to prokaryotic DNA-binding proteins (8–13). Specific binding requires both major groove interactions involving a helix-turn-helix (HTH) α -helix motif and minor groove interactions involving the sequence Gly¹³⁹-Arg¹⁴⁰-Pro¹⁴¹-Arg¹⁴². If residues 139 and 140 are deleted from the carboxyl-terminal domain, for example, then sequence-specific binding to DNA is abolished. As Fig. 1A shows, these

A. Amino Acid Sequences of DNA-Binding Domains of Enteric Invertases

α -Helix	1-----1	2-----2	3-----3
Hin	GRPRAITKH.EQEISRLLEK.GHP.RQQLAIF.GIG.VSTLYRY7.PASSIXKRMN		
Gin	GRPPKLTKA.EQEAGRLLAQ.GIP.RKQVALIY.DVA.LSTLYKKH.PAKRAHIENDDRIN		
Cin	GRPPKYQEE.TQCOMRLLEK.GIP.RKQVALIY.DVA.VSTLYKKF.PASSFQS		
Pin	GRPPKLTPE.QQAQAGRLIAA.GTP.RKQVALIY.DVG.VSTLYKRF.PAGDK		
	139 148	162	173 181

B. *hixL* binding site for Hin protein:

-13 -8 -1+1 +8 +13
 5'-T-T-C-T-T-G-A-A-A-C-C-A-A-G-G-T-T-T-T-T-G-A-T-A-A-3'
 3'-A-A-G-A-A-C-T-T-T-T-G-G-T-T-C-C-A-A-A-A-C-T-A-T-T-5'

C. Synthetic *hixL* half-site for crystallography

Strand 1: 2 3 4 5 6 7 8 9 10 11 12 13 14 15
 5'-T--G--T--T--T--T--T--G--A--T--A--A--G--A
 Strand 2: C--A--A--A--A--A--C--T--A--T--T--C--T--A--5'
 29 28 27 26 25 24 23 22 21 20 19 18 17 16

Fig. 1. Amino acid and DNA base sequences in the Hin recombinase family (1, 34). (A) Amino acid sequence of the DNA-binding domain (the 52 carboxyl-terminal residues) of the Hin protein and corresponding regions in Gin, Cin, and Pin. Residues in boldface are identical in all four sequences at least in three of the four α helices 1 to 3 as located in our Hin structure analysis are marked above the Hin sequence. For crystallography, this Hin fragment was synthesized manually or on an ABI 430 synthesizer by the solid-phase method as described previously (8). (B) Base sequence of the left DNA inversion site, *hixL*. Numbering is to either direction from the center of the inverted repeat. Asterisks mark purine bases that are protected from methylation by the binding of Hin. (C) The 14-bp synthetic *hixL* half-site as cocrystallized with the Hin 52-mer. Strand 1 of the duplex is numbered 2 through 15 to match the right half of the entire *hixL* site in (B). Bases in strand 2 are numbered separately. For ease of reference, note that base *n* in strand 1 is paired with base (32 - *n*) in strand 2. Base pairs will be referenced by strand 1 numbers alone; that is, "base pair 9" is understood to signify base pair G9-C23. Phosphates always are numbered according to the base that follows: Phosphate P9 occurs between T and G9, whereas across the helix on the other strand, phosphate P24 lies between C23 and A24. Hence phosphate *n* on strand 1 lies opposite phosphate (33 - *n*) on strand 2. Asterisks mark bases that were iodinated for purposes of multiple isomorphous replacement phase analysis.

The authors are with the Molecular Biology Institute and Department of Biological Chemistry, University of California, Los Angeles, CA 90024.

*To whom correspondence should be addressed at the Molecular Biology Institute.

two residues also are invariant among all four of the DNA invertases.

By comparison with pairwise amino acid sequence identities of 66 to 80 percent in the entire protein sequences, the carboxyl-terminal peptides shown in Fig. 1A have somewhat fewer identities, 49 to 62 percent, but still are obviously homologous proteins. The Hin interactions resemble those in the binding of DNA by the homeo-domain in eukaryotes. Indeed, as noted by Affolter *et al.* (14), the amino acid sequence of the Hin binding domain can be

aligned with that of the homeodomain of the *Drosophila* engrailed protein with a 27 percent sequence identity, sufficient to suggest a class resemblance.

We report here the 2.3 Å resolution crystal structure analysis of the 52-amino acid carboxyl-terminal DNA-binding domain of Hin complexed with a 14-bp DNA oligomer containing a half-hixl binding site (Fig. 1C). The Hin peptide forms a three- α -helix core with an extended chain at each end. The core interacts with the major groove of DNA, whereas the flanking ami-

no- and carboxyl-terminal chains extend along two regions of the minor groove. The carboxyl-terminal eight-residue tail of the Hin peptide crosses the phosphodiester backbone and is inserted in the minor groove in a manner that has not heretofore been encountered in DNA-protein complexes. The crystal structure provides a virtually complete explanation of base specificity experiments in solution, including mutant studies.

Structure of the complex. The structure of the Hin-DNA complex was solved by multiple isomorphous replacement with the use of three iodine derivatives (Table 1). A typical section of the final ($2F_o - F_c$) map is shown in Fig. 2. One 52-amino acid Hin domain binds to each 14-bp DNA half-site (Fig. 3). DNA helices consisting of the 13 complete base pairs are stacked end-to-end in the crystal, as in figure 2 of (15). The unpaired base T2 on strand 1 (Fig. 1C) swings up to make a Hoogsteen-like interaction with base pair 3, G3-C29. At the other end, unpaired base A16 on strand 2 is not defined in the electron density map and presumably is disordered. The *a* axis of the crystal, the direction of stacking of two DNA helices, has a length at room temperature of 86.4 Å = 26 × 3.32 Å. The 12-base pair steps along the helix produce a total rotation of 407° (average 33.9° per step), so that the nonbonded interhelix junction between base pair 15 (A15-T17) of one helix and base pair 3 (G3-C29) of the next requires a reverse twist of 360° - 407° = -47°.

The DNA half-site is a standard B-DNA helix, with the usual local variation in helix parameters (16, 17). The helix is relatively straight and not curved around the protein domain as in CAP, α p repressor, 434 repressor, and Met repressor (18-22), and has been proposed for the Fis-DNA complex (23, 24). However, an unusually large amount of DNA surface area is contacted by Hin. Upon binding Hin peptide, the DNA half-site monomer loses 1816 Å² of static solvent-accessible surface area.

The DNA half-site contains a short run of five AT base pairs (numbers 4 through 8) that could be regarded as a segment of A-tract DNA. Three frequent characteristics of A-tract DNA are a straight and unbent helix axis, narrow minor groove, and large propeller twist, large enough for the formation of bifurcated hydrogen bonds within the major groove between adjacent base pairs (25-27). However, in the Hin-DNA complex the minor groove maintains a uniform width of approximately 6.5 to 8.5 Å (minimal P-P atom separation across the groove, less 5.8 Å for two phosphate group radii), rather than the 3.5 to 4.5 Å typical of most A-tracts. Propeller twist is large all along the Hin-DNA complex, averaging

Table 1. Summary of crystallographic analysis. Crystals of Hin domain/DNA complex were grown by vapor diffusion against 15 to 18 percent PEG1500 as described elsewhere (15). The structure was determined initially to 3.2 Å resolution by multiple isomorphous replacement (MIR). Heavy atom parameters were refined and MIR phases calculated with the program HEAVY (44). The initial MIR map generated after solvent flattening (45) revealed clear density for B-form DNA and for most of the protein backbone density. This map was improved further by refining heavy atom parameters against solvent-flattened phases (46). After two additional cycles of phasing, solvent flattening, and heavy atom parameter refinement, the final MIR map, with mean phasing figure of merit of 0.55 for data between 20.0 and 3.2 Å, was used to build a model of the complex. However, it still was difficult to fit the amino acid sequence into many regions of the map. Only after phases were extended and modified to 2.8 Å by the method of Zhang and Main (47) did the map show clear density for side chains of some "marker" residues. At that point, all residues could be fitted unambiguously with the exception of the final eight carboxyl-terminal amino acids. Conventional positional refinement then was carried out to 2.8 Å with X-PLOR (48, 49). To refine the model further against a new 2.3 Å data set collected at -150°C, rigid-body refinements were carried out in successive steps to 2.5 Å. After positional refinement and simulated annealing, the ($2F_o - F_c$) map was of sufficient quality to allow the last eight residues to be built into the minor groove of the DNA, following a clear and continuous density. Electron density for residues Ser¹⁴³ and Ser¹⁴⁴, however, remained poorly defined. Refinement was extended to 2.3 Å in four cycles of simulated annealing with X-PLOR prior to tightly restrained B-factor refinement. At the present stage of refinement, the agreement of the atomic model to crystallographic data is $R = 0.228$ for 8.0 to 2.3 Å resolution data. Coordinates have been deposited with the Brookhaven Protein Data Bank and are available for immediate distribution.

Parameter	Native	Native (-150°C)	IdU ^a	IdC ^{1b}	IdU ^a + IdC ^{1b}
<i>Unit cell dimensions^c</i>					
<i>a</i> (Å)	86.4	84.9	85.9	86.0	86.6
<i>b</i> (Å)	84.7	81.4	82.6	82.6	83.5
<i>c</i> (Å)	47.4	44.0	47.0	46.4	47.2
<i>Data collection statistics</i>					
Resolution (Å)	2.8	2.3	3.2	3.2	3.5
Measured reflections	11673	17839	10387	7578	7578
Unique reflections	4177	5645	2703	2501	2020
Reflections > 2 σ (<i>F</i>)	2653	5346			
Completeness (%)	92.6	80.1	92.1	87.5	87.0
<i>R</i> _{int} (%)	5.7	5.6	7.5	7.8	8.4
Mean isomorphous difference ^d (%)			18.4	16.9	18.3
<i>Phasing statistics</i>					
Resolution (Å)			20-3.2	20-3.2	20-3.5
Cullis <i>R</i> factor			0.59	0.58	0.54
Phasing power ^g			1.80	1.74	2.42
<i>Refinement</i>					
Resolution (Å)		8.0-2.3			
<i>R</i> factor ^h		0.228			
Reflections with <i>F</i> > 2 σ		5346			
Total number of atoms		978			
Water molecules	18				
<i>Rms deviations</i>					
Bond lengths (Å)		0.024			
Bond angles (deg.)	3.97				

^aSpace group C222, with one Hin-DNA complex per asymmetric unit. [†] $R_{\text{int}} = \sum (|I| - \langle I \rangle) / \sum \langle I \rangle$, where *I* is the observed intensity and $\langle I \rangle$ is the averaged intensity obtained from multiple observations of symmetry-related reflections.

^hThe mean isomorphous difference is $\sum (|F_o| - |F_c|) / \sum (|F_o| + |F_c|)$, where $|F_o|$ and $|F_c|$ are structure factor amplitudes of protein and heavy atom derivative of the protein, respectively. ^gPhasing power is the mean amplitude of heavy atom structure factors, F_H , divided by E , the root-mean-square lack-of-closure error. The mean figure of merit, 20.0 to 3.2 Å, is 0.55.

^dCrystallographic *R* factor = $\sum (|F_o| - |F_c|) / \sum (|F_o| + |F_c|)$, where F_o and F_c are the observed and calculated structure magnitudes, respectively.

-16°, but is not systematically larger in the A-A-A-A region than elsewhere. Hence the five AT base pairs do not constitute a classical A-tract structure, perhaps because of binding to Hin.

Overall protein folding. The 52-amino acid DNA-binding domain of Hin consists of a compact bundle of three α -helices, with extended amino-terminal arm and carboxyl-terminal tail (Fig. 3). α -Helix 1 (Glu¹⁴⁸ to Lys¹⁵⁸) lies parallel to the axis of the DNA, α -helix 2 (Arg¹⁶² to Phe¹⁶⁹) is nearly antiparallel to helix 1 with an angle of -25° between helix axes, and α -helix 3 (Val¹⁷³ to Phe¹⁸⁰) is inserted in the major DNA groove parallel to the base pairs (not to the floor of the groove itself). The HTH motif formed by helices 2 and 3 is similar to those found in other prokaryotic regulatory DNA-binding proteins. The Hin HTH region can be superimposed on equivalent regions of Fis (23, 24) and λ repressor (28) with root-mean-square deviations in C α atomic positions of only 0.61 and 0.76 Å, respectively.

All three α helices are amphipathic, with hydrophobic residues packed tightly against one another in a hydrophobic core (Fig. 3A). Ile¹⁵² and Leu¹⁵⁶ of helix 1 interdigitate with Leu¹⁶⁵ and Phe¹⁶⁹ of helix 2. Val¹⁷³, Leu¹⁷⁶, and Phe¹⁸⁰ of helix 3 also point into the hydrophobic core, which is delineated by the blue polypeptide backbone regions in Fig. 3A. At the bottom in that view, Ile¹⁴⁴ on the amino-terminal arm closes the hydrophobic pocket. These hydrophobic interactions appear to be the main forces stabilizing the folding of the Hin protein. They also are strongly conserved among the other DNA invertases, Gin, Cin, and Pin (Fig. 1A), supporting the inference that all four of these proteins are folded in the same way. Hydrophobic interactions are supplemented by hydrogen bonds between side chains: Arg¹⁶² (invariant among the four invertases), at the beginning of helix 2, is hydrogen-bonded to main chain carbonyl oxygens of Phe¹⁸⁰ (the final residue of helix 3) and Pro¹⁸¹. Most charged side chains of the protein are either in contact with DNA or exposed to the solvent.

Major groove protein-DNA interactions. α -Helix 3 is the DNA recognition helix for the Hin protein; helices 1 and 2 are too far from the DNA to permit direct interactions. Only Gln¹⁶³ at the amino terminus of helix 2 makes an indirect DNA contact through a hydrogen bond to residue Tyr¹⁷⁷ (invertase invariant) in helix 3, which in turn contacts phosphate P19 (Fig. 3B). Five interactions between helix 3 and DNA backbone phosphates position the recognition helix properly, and two-amino acid side chains, Ser¹⁷⁴ and Arg¹⁷⁸, make specific bonds to the edges of base pairs

G9-C23 and A10-T22, as detailed below. It is significant that four of the eight amino acids in helix 3 are completely invariant among the four DNA invertases, and another three are semi-invariant, with the same residue in three sequences and a closely related one in the fourth.

The five nonspecific interactions with DNA backbone phosphates are depicted in Fig. 3B. The side chain of Tyr¹⁷⁷ reaches up to phosphate P19 on one edge of the major groove, whereas Tyr¹⁷⁹ on the other side of the α helix reaches down to phosphate P8 directly across the groove on the other wall. One of the terminal -NH₂ groups of the Arg¹⁷⁸ side chain donates a hydrogen bond to the remaining oxygen of phosphate P8. The side chain of Thr¹⁷⁵ and the main chain amide of Gly¹⁷² anchor helix 3 even further by donating hydrogen bonds to phosphate P9. In contrast to other HTH DNA-binding proteins, all of these nonspecific anchoring contacts to DNA phosphates are made by residues of helix 3; the "three-point contact" made by residues Gly¹⁷², Thr¹⁷⁵, Tyr¹⁷⁷, and Tyr¹⁷⁹ efficiently braces helix 3 against the opening of the major groove of DNA in a position to make specific recognition interactions.

Specific base sequence recognition uses only two Hin side chains, Ser¹⁷⁴ and Arg¹⁷⁸, and in part involves the mediation of water molecules (Fig. 4) in a manner that has been proposed for the trp repressor (29). The side chain of Ser¹⁷⁴ donates a hydrogen bond to the N-7 atom of A10. One turn of α helix away from this position, the terminal -NH₂ of Arg¹⁷⁸ that is not involved

with P8 donates a similar hydrogen bond to the N-7 of G9. The Arg¹⁷⁸ ϵ -imino nitrogen donates another hydrogen bond to bound water molecule 1, which in turn donates a bond to the O-4 of T22, essentially "reading" the fact that this base pair is indeed A10-T22 and not a G-C pair. The other proton of this water molecule bonds to water molecule 2, which receives another hydrogen bond from the N-6 amine of A21 (recognizing this as an A-T pair and not G-C), and donates hydrogen bonds to N-7 of the same base and to the main chain carbonyl oxygen of Ser¹⁷⁴. Ser¹⁷⁴ is invariant among all four DNA invertases. Arg¹⁷⁸ is substituted only by Lys, and when this happens, two basic side chains always appear adjacent at positions 178 and 179 (Fig. 1A), meaning that some of the hydrogen bonds of the Hin structure could well be preserved. Both of the bound waters have the tetrahedral geometry expected for water molecules, donating two hydrogen bonds and accepting two others. The fourth bond to water 1, not shown explicitly in Fig. 4B, must be to another water molecule not well localized in the electron-density map.

All of these specific interactions are drawn in Fig. 4, A and B. Together they recognize base pairs 9, 10, and 11 of the half recombination site. Indeed, the binding of Hin is particularly sensitive to alterations of base pairs 9 and 10 (13). Dimethyl sulfate modification of the N-7 position of G9 inhibits Hin binding (8, 10). Methylation at the N-6 position of A10 by the deoxyadenosine methylase of *Salmonella* decreases binding affinity (13). Hin binding

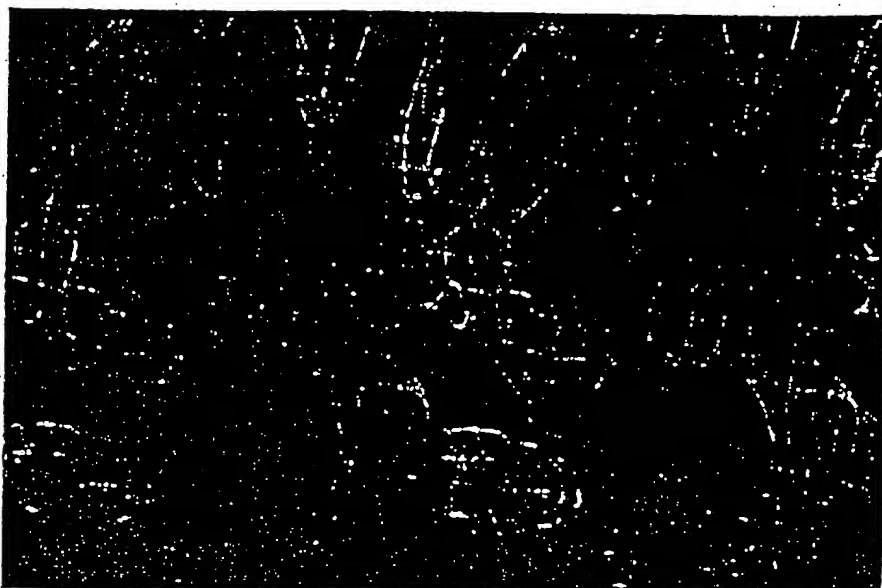


Fig. 2. Stereo view of the ($2F_o - F_c$) electron density map at 2.3 Å resolution (blue contours) showing portions of DNA base pairs 8 to 11 (top) and the region of helix 3 around Arg¹⁷⁸ and Tyr¹⁷⁹ (marked). Contour level is 1 σ . The protein framework is in red, and DNA is in green.

also is strongly and adversely affected by mutations at these sites, being inhibited by substitution of C at positions 9 and 11 or either C or T at position 10.

Minor groove protein-DNA interactions—the amino-terminal arm. Genetic and biochemical studies have demonstrated that contacts made by the amino-terminal

arm of the Hin DNA-binding domain are at least as critical to DNA recognition as are those of helix 3 (10, 12, 13). Indeed, merely deleting Gly¹³⁹ and Arg¹⁴⁰ from the Hin DNA-binding peptide is sufficient to abolish specificity of binding to *hixL* (12). These residues are invariant in all of the DNA invertases.

The amino-terminal arm, Gly¹³⁹-His¹⁴⁷, adopts an extended conformation (Fig. 5). Clear electron density (Fig. 5A) allows Gly¹³⁹ and Arg¹⁴⁰ to be located unambiguously within the minor groove. The ϵ -imine of the Arg¹⁴⁰ side chain donates a hydrogen bond to N-3 of A26. The unusually high 26° propeller twist of base pair 6 (T6-A26) permits a second hydrogen bond from the main chain amide of Arg¹⁴⁰ to the O-2 of T6. If a G-C pair were to be substituted, this latter bond would become impossible, and the N-2 amine of guanine would push the Arg¹⁴⁰ side chain away. Although the neighboring A-T base pairs are less propeller-twisted, the ability of an A-T pair to adopt such a large propeller contributes to the recognition process (25–27). Gly¹³⁹ rests in close van der Waals contact with base pair 5; the main chain C α atom of that residue is only 3.4 Å from the O-2 of T5 and 4.1 Å from the C-2 of A27. Introduction of an amine group at that locus, as in guanine, would push the Hin polypeptide chain up and away from the floor of the minor groove at that point. Each base pair substitution of A-T by G-C at positions 5 and 6 abolishes the binding affinity of Hix (13). Indeed, A-T base pairs at positions 5 and 6 are universally present in all of the recombination sites of various enteric inversion systems: *hixL* and *hixR*; *gixL* and *gixR*; *cixL* and *cixR*; and *pixL* and *pixR* (1) (Fig. 6). Biochemical footprinting experiments also show that both intact Hin and the Hin peptide protect adenines 5 and 6 from methylation (10).

Pro¹⁴¹ arches across one wall of the minor groove, and the ϵ -imino of Arg¹⁴² is hydrogen-bonded to phosphate P8, an interaction that may be important in directing the amino-terminal arm into the minor groove of the DNA: Hin, Gin, Cin, and Pin all have Pro at position 141 or 142, followed immediately by a basic Arg or Lys. A significant role may be played by Ile¹⁴⁴, which interacts with the hydrophobic core formed by packing helices 1 to 3 against one another. Ile¹⁴⁴ may restrict movement of the amino-terminal arm, thus bringing Arg¹⁴² into proximity to phosphate P8. In other DNA invertases, position 144 is always a bulky hydrophobic side chain, either Leu or Tyr (Fig. 1A).

Minor groove protein-DNA interactions—the carboxyl-terminal tail. The carboxyl-terminal tail of the Hin polypeptide crosses the phosphodiester backbone at the

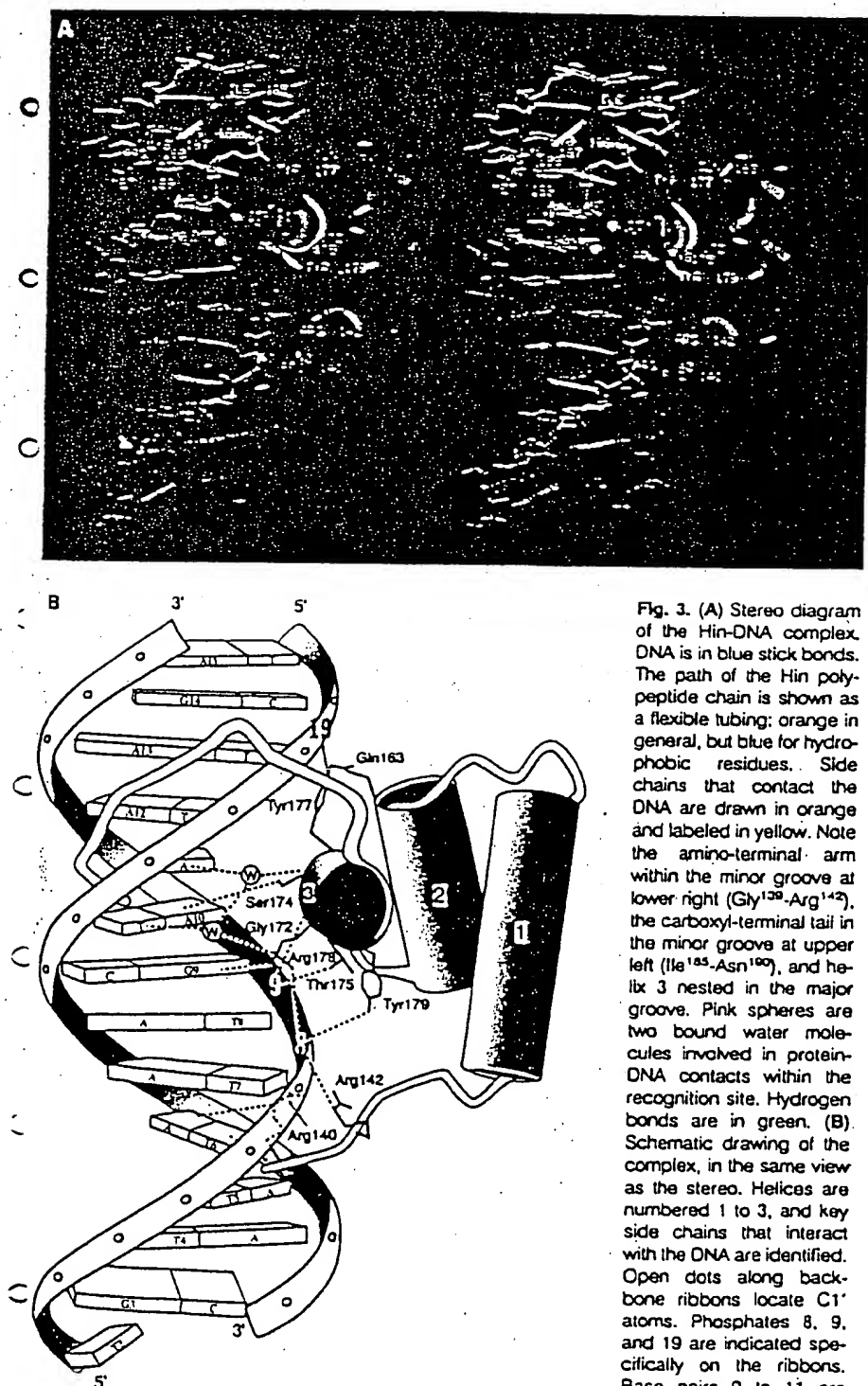


Fig. 3. (A) Stereo diagram of the Hin-DNA complex. DNA is in blue stick bonds. The path of the Hin polypeptide chain is shown as a flexible tubing: orange in general, but blue for hydrophobic residues. Side chains that contact the DNA are drawn in orange and labeled in yellow. Note the amino-terminal arm within the minor groove at lower right (Gly¹³⁹-Arg¹⁴²), the carboxyl-terminal tail in the minor groove at upper left (Ile¹⁴⁴-Asn¹⁶⁰), and helix 3 nested in the major groove. Pink spheres are two bound water molecules involved in protein-DNA contacts within the recognition site. Hydrogen bonds are in green. (B) Schematic drawing of the complex, in the same view as the stereo. Helices are numbered 1 to 3, and key side chains that interact with the DNA are identified. Open dots along backbone ribbons locate C1' atoms. Phosphates 8, 9, and 19 are indicated specifically on the ribbons. Base pairs 9 to 11 are shown in stereo close-up in Fig. 4A, base pairs 4 to 8 in Fig. 5B, and pairs 9 to 15 in Fig. 7.

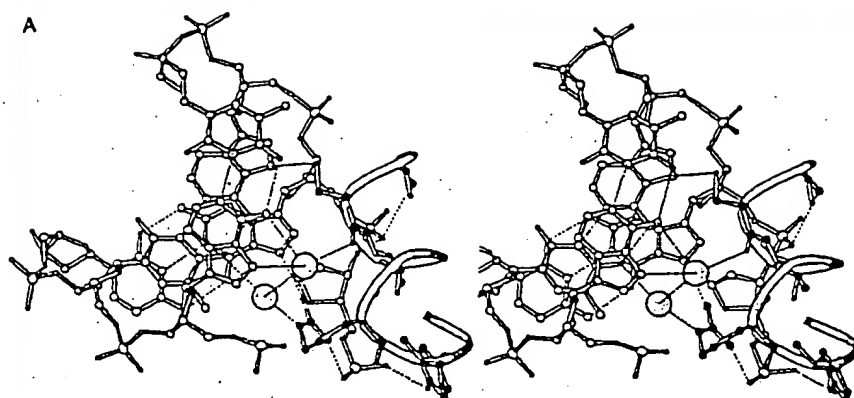
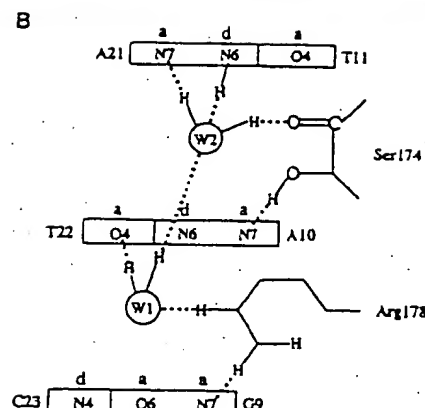


Fig. 4. (A) Stereo close-up of the interaction between DNA and helix 3 in the major groove, viewed approximately down the DNA helix axis. Base pair T11-A21 is nearest the viewer, with A10-T22 beneath, and G9-C23 farthest away. Strand 1 backbone continues to lower right through P9 and P8. Helix 3 is drawn as a smooth curve, with specific depiction, from top to bottom,



of residues Gly¹⁷², Ser¹⁷⁴, Thr¹⁷⁵, Arg¹⁷⁸, and Tyr¹⁷⁹. Two shaded spheres are bound water molecules. (B) Schematic of specific base pair recognition involving Ser¹⁷⁴, Arg¹⁷⁸, and two bound water molecules. Along base edges, "a" marks a hydrogen bond acceptor (ring N-7, or carbonyl O-4 or O-6) and "d" marks a hydrogen bond donor (N-4 or N-6 amine group).

outer edge of the recombination site and then follows the minor groove back toward the center of the 13-bp DNA helix (Figs. 3 and 7). The final six residues of the Hin polypeptide, Ile¹⁸⁵-Lys¹⁸⁶-Lys¹⁸⁷-Arg¹⁸⁸-Met¹⁸⁹-Asn¹⁹⁰, adopt an extended conformation and lie within the minor groove, but the side chains themselves make no contacts with the floor of the groove. Instead, they point outward, with the polypeptide backbone resting against base edges. At the point where the final six-amino acid residues dip into the minor groove, the main chain CO of Ile¹⁸⁵ hydrogen bonds to the N-2 of G14. The main chain NH of Lys¹⁸⁷ bonds to the O-2 of T20, and a little farther along, the main chain amide of Asn¹⁹⁰ interacts with the O-2 of T22 while the side chain of the carboxyl-terminal residue bonds to the N-3 of A10. These interactions may be responsible for the large propeller twist and roll angles of base pairs 10 and 12 and the $\sim 16^\circ$ bend of DNA toward the major groove. Consistent with the interactions just discussed, the N-3 of A10 is partially protected from dimethyl sulfate attack by Hin binding (10). In addition, Mack *et al.* (11) have noted that a Hin peptide lacking the last eight residues, when modified with EDTA-Fe, cleaved DNA with reduced efficiency as compared with a peptide containing the complete carboxyl terminus. This portion of the chain is variable among the DNA invertases: whereas Hin has six final amino acids, Gin has ten, Cin has three, and Pin has a lone Lys (Fig. 1A). This carboxyl-terminal tail is presumably supportive but not essential.

The hydrogen-bonded extension of the last six residues along the floor of the minor groove recalls AT-specific binding of minor groove drugs such as netropsin and distamycin (30, 31). Such binding involves an

element of base specificity: if any of the base pairs 10 to 13 were G-C rather than A-T, then the tail of the Hin peptide would be pushed away from the floor of the groove. In another context, it has been proposed (32, 33) that an extended polypeptide containing repeats of SPKK (34) sequence may interact with DNA minor groove in a sim-

ilar fashion to netropsin, with main chain amide nitrogen forming hydrogen bonds with base pairs in the minor groove. Our structure seems to provide a concrete example of such a model.

The molecular basis of specificity. Two aspects of the Hin system make it especially conducive to an understanding of the ef-

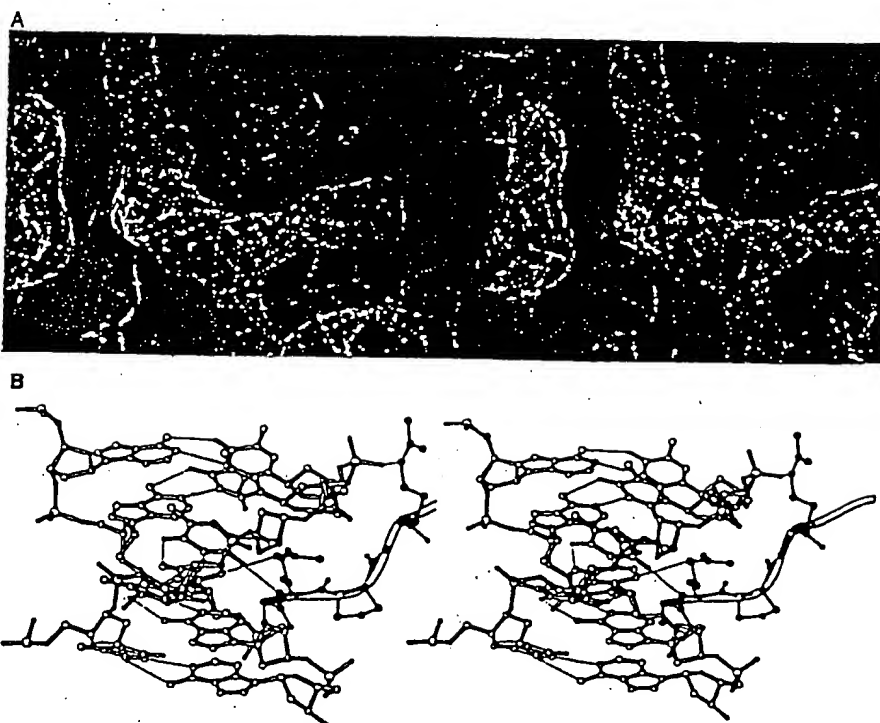


Fig. 5. Stereo views of the amino-terminal arm of the Hin peptide, in the minor groove of DNA. (A) The refined ($2F_o - F_c$) electron density map (blue framework) with minor groove vertical, showing Arg¹⁴⁰-Pro¹⁴¹-Arg¹⁴² looping over the phosphate backbone toward the right. Protein is in red, and DNA is in green. (B) View along the minor groove, from the top in (A), showing the entire "A-trail" region, from T4-A28 at bottom through T8-A24 at top. This view is approximately that of the lower half of Fig. 3B. The ribbon extending from center toward upper right is the Hin peptide region Gly¹³⁸-Arg¹⁴⁰-Pro¹⁴¹-Arg¹⁴², with side chains drawn explicitly.

Fig. 6. Base sequences in enteric bacterial inversion sites: the left and right inversion sites from the *Hin* inversion system of *Salmonella*, the *Gin* inversion elements from bacteriophage Mu, *Cin* from phage P1, and *Pin* from the ϕ 14 prophage of *Escherichia coli* (1). Only one chain from each complex is shown; the other is complementary as in Fig.

1B. Each of the eight sites is built from two roughly symmetrical half-sites. Asterisks at bottom indicate positions that are especially important in site recognition by invertases.

	Left half-site	Right half-site
	-11 -6 -1-1 -6 -11	
<i>hixL</i>	5'-T-T-C-T-T-G-A-A-A-C-C-A-A-G-G-T-T-T-T-G-A-T-A-A-3'	3'-A-A-T-A-A-G-C-C-A-A-G-G-T-T-T-T-G-A-T-A-A-5'
<i>hixR</i>	5'-T-T-T-T-C-C-T-T-T-T-G-G-A-A-G-G-T-T-T-T-G-A-T-A-A-3'	3'-A-A-T-A-A-G-C-C-A-A-G-G-T-T-T-T-G-A-T-A-A-5'
<i>gixL</i>	5'-T-T-C-C-T-G-T-A-A-A-C-C-G-A-G-G-T-T-T-T-G-A-T-A-A-3'	3'-A-A-T-A-A-G-C-C-A-A-G-G-T-T-T-T-G-A-T-A-A-5'
<i>gixR</i>	5'-T-T-C-C-T-G-T-A-A-A-C-C-G-A-G-G-T-T-T-T-G-A-T-A-A-3'	3'-A-A-T-A-A-G-C-C-A-A-G-G-T-T-T-T-G-A-T-A-A-5'
<i>cinL</i>	5'-T-T-C-T-C-T-T-A-A-A-C-C-A-A-G-G-T-T-T-T-G-A-T-A-A-3'	3'-A-A-T-A-A-G-C-C-A-A-G-G-T-T-T-T-G-A-T-A-A-5'
<i>cinR</i>	5'-T-T-C-T-C-T-T-A-A-A-C-C-A-A-G-G-T-T-T-T-G-A-T-A-A-3'	3'-A-A-T-A-A-G-C-C-A-A-G-G-T-T-T-T-G-A-T-A-A-5'
<i>pinL</i>	5'-T-T-C-T-C-C-C-A-A-A-C-C-A-A-G-G-T-T-T-T-G-A-T-A-A-3'	3'-A-A-T-A-A-G-C-C-A-A-G-G-T-T-T-T-G-A-T-A-A-5'
<i>pinR</i>	5'-T-T-C-T-C-C-C-A-A-A-C-C-A-A-G-G-T-T-T-T-G-A-T-A-A-3'	3'-A-A-T-A-A-G-C-C-A-A-G-G-T-T-T-T-G-A-T-A-A-5'

the *Hin*-DNA complex account for this wealth of data, and provide a molecular basis for DNA-protein specificity?

The *Hin*-DNA crystal structure shows that all three components of the *Hin* peptide, the amino-terminal arm, the HTH region, and the carboxyl-terminal tail, contribute to base sequence recognition. The phosphate backbone contacts of helix 3 help position *Hin* on the DNA, but one could easily imagine that *Hin* could slide along the DNA in a nonspecific manner until it encounters the correct local base sequence.

Interactions of *Hin* residues Ser¹⁷⁴ and Arg¹⁷⁸, both direct and through intermediate water molecules (Fig. 4B) place restrictions on base pairs 9, 10, and 11. Some latitude in base sequence is possible if different arrangements of hydrogen bond donors and acceptors are permitted. Those rearrangements that are possible without losing the total number of hydrogen bonds are shown in Fig. 8. Base 9 is restricted to being a purine (G or A) by virtue of the hydrogen bond donated to ring atom N-7. In complete agreement with this model, of the 16 half-sites shown in Fig. 6 and listed in Table 2, G occurs 13 times at position 9 and A occurs 3 times. No pyrimidine is ever found at that locus. Replacement of G at position 9 by A or T (and C at position -9 by T or A) in the mutant studies of Hughes *et al.* (13) is acceptable, but C at position 9 reduces binding significantly. Our crystal structure shows why: G, A, or T at position 9 offer a hydrogen bond acceptor to Arg¹⁷⁸, whereas C offers a N-4 amine donor instead, and hence is disfavored. Even T is less favorable, because it positions the hydrogen bond acceptor differently and partially blocks it with its own C-5 methyl group.

Position 10 also must be a purine for the same reason as 9. The choice in 14 of the

fects of sequence on specificity. The first is the availability of binding data on 39 different base substitution mutations generated by Hughes *et al.* (13). They constructed a symmetrized *hixC* sequence in which the left half is given the complementary sequence to the right half shared by both *hixL* and *hixR* and established that this symmetrized *hixC* binds *Hin* fully as well as the wild-type *hixL* and *hixR*. (It is the *hixC* sequence that we used for crystallographic analysis.) They then constructed an ex-

haustive set of symmetrical mutants in the two halves of *hixC*, varying each of the 13 positions among all three of the other bases. Hence we have complete information about the strength of *Hin* binding with every possible single-base change in the optimal *hixC* sequence. The second favorable aspect is the existence of four homologous DNA inversion systems: *Hin*, *Gin*, *Cin*, and *Pin*. Taken together, these provide 8 complete recombination sites or 16 binding half-sites (Fig. 6). How far can our x-ray analysis of

Table 2. Frequency of occurrence of bases at key positions in bacterial inversion sites. Sequences are read in a 5'-to-3' direction from the center of the inversion site as shown in Fig. 6. Hence, for left half-sites the other chain, not shown in Fig. 6, is tabulated. Allowed substitution data derive from the frequency of lysogenization in a P22 challenge phage assay at 100 μ M isopropyl- β -D-thiogalactopyranoside (IPTG) concentration, table 1 of (13).

Position	Natural <i>hix</i> , <i>gix</i> , <i>cin</i> , and <i>pin</i> sites				Acceptable mutations in symmetrized <i>hixC</i> site (13)	DNA groove
	G	A	T	C		
5		2	14		Not G, not C	Minor
6		1	15		Not G, not C	Minor
9	13	3			Not C	Major
10	2	14			Not T, not C	Major
11	8	2	6		Not C	Major
12		15	1		Not C	Minor
13	2	14			All equivalent	Minor

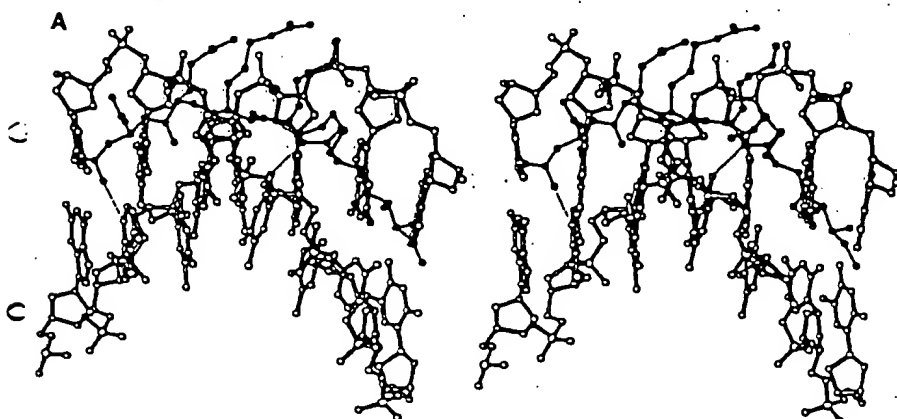
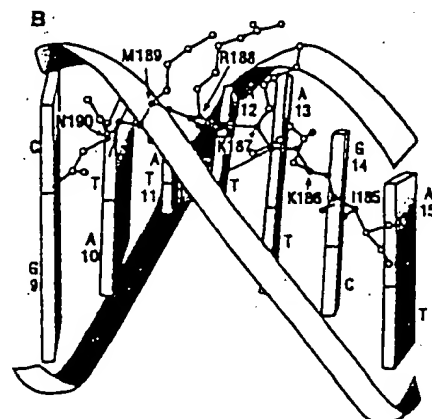


Fig. 7. Linear extension of carboxyl-terminal residues 185 to 190 down the minor groove. (A) Stereo pair representation. DNA base pair G9-C23 is at left, and A15-T17 at right. Amino acid side chains are identified in (B).

which is a sketch from the same orientation. The main polypeptide chain atoms are in black dots; side chains are in open circles.



16 half-site sequences is A10, resulting in T22 at the other end of the base pair, with a hydrogen bond-accepting O-4 atom (Fig. 8A). However, G10-C22 is an acceptable minority choice in two sequences, and in that case the N-4 amine of C22 must donate a hydrogen bond to water 1 (Fig. 8B). Water 1 then would donate a hydrogen bond to another water molecule not shown here.

Base pair 11 is more variable than might have been expected, and for an interesting reason. Water molecule 2 in Fig. 8A accepts a hydrogen bond from the N-6 of A21 and donates a bond to N-7, but all that is required for a hydrogen balance is that this water molecule should donate one hydrogen and accept another. The two base atoms could just as easily be thymine O-4 and adenine N-6 as in Fig. 8A or cytosine N-4 and guanine O-6 as in Fig. 8B. The only combination not permitted would be guanine at position 21, with dual acceptors N-7 and O-6. For in that case, water 2 would not have enough protons to form the bond with the main chain carbonyl of Ser¹⁷⁴. In other words, the requirement on the strand 1 side of base pair 11 is "not-C," and indeed this requirement is borne out in Table 2 both by the invertase family sequence comparisons and mutational substitutions.

The direction of the hydrogen bond between water molecules—water 1 donating to water 2—actually is firmly established. As Fig. 8C shows, if water 2 were to donate a bond both to water 1 and to the Ser¹⁷⁴ main chain carbonyl, then the two positions on base pair 11 would have to be adjacent donors, and no base pair shows this behavior. The full pattern of hydrogen bonds can be maintained only by arrangements as in Fig. 8, A and B.

A-T base pairs are favored at positions 12 and 13 because of a netropsin-like extension of the carboxyl-terminal six Hin residues down the floor of the minor groove (Fig. 7). Table 2 shows that A-T pairs indeed are overwhelmingly favored at these two loci, although mutant studies show position 13 to be more permissive. It could be that the similarity of sequences at this point among all of the enteric recombinases is a matter of evolutionary divergence from a common ancestral sequence, rather than convergence on function.

At the other end of the recognition domain, positions 4, 5, and 6 universally are A-T base pairs in all of the DNA inversion sites, and G-C pairs are strongly disfavored at positions 5 and 6 in the mutant studies. The x-ray structure shows the reason: Hin residues Gly¹³⁹ and Arg¹⁴⁰ are so intimately linked to the floor of the minor groove that there simply is no room for the C-2 amine group of guanine. As noted above, Gly¹³⁹ and Arg¹⁴⁰ are abso-

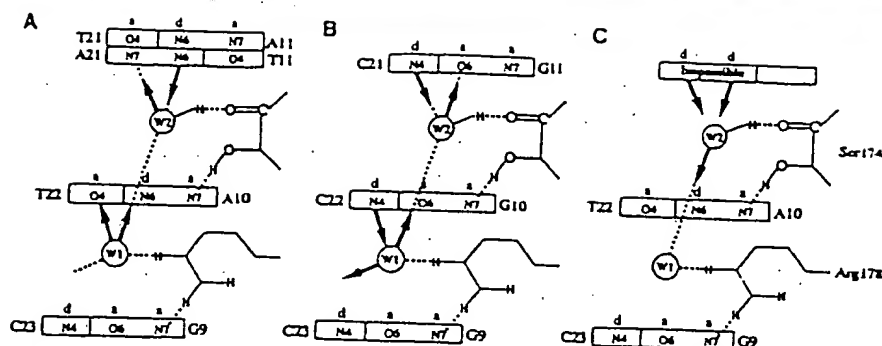


Fig. 8. The molecular basis for specificity, in the form of possible patterns of hydrogen bond donors and acceptors. (A) The pattern actually observed in the crystal structure. Base pair 11 could be reversed end-for-end without altering the pattern of hydrogen bond acceptor-donor-acceptor along its edge. (B) Hydrogen bond donors and acceptors could be reversed at base pair 11, allowing G11-C21. However, base 21 could not be G, with dual acceptors without breaking the bond between water 2 and the Ser¹⁷⁴ carbonyl. Hence C11-G21 is strongly disfavored. The acceptor at the central base pair can independently be replaced by a donor, permitting G10-C22 in place of A10-T22, but base 10 is still required to be a purine. (C) The hydrogen bond connecting the two water molecules cannot be reversed, for then, if the donation to Ser¹⁷⁴ carbonyl is maintained, base pair 11 would have to contribute two adjacent donors, which is chemically impossible for any of the base pairs.

Fig. 9. Optimal base sequence for enteric inversion half-sites. Numbers mark the distance out from the center of the site as in Fig. 6. A/T = an A-T base pair in either orientation. N = any base.

5 6 7 8 9 10 11 12 13
(A/T)-(A/T)-N-N-(purine)-A-(not-C)-(A/T)-(weak A)

lutely essential for sequence-specific binding of Hin to its DNA site.

In summary, the recognition element of the enteric inversion half-sites appears to involve two A-T base pairs (5 and 6) recognized by amino acid residues Gly¹³⁹ and Arg¹⁴⁰ in the minor groove, two non-specific base pairs (7 and 8), and then a five base sequence (9 to 13) recognized by helix 3 and the carboxyl-terminal tail in major and minor grooves, respectively. The optimal binding sequence is shown in Fig. 9. The Hin dimer has ~100-fold higher binding affinity to the full recombination site than does the Hin peptide binding to a half-site, and hence cooperative interactions by the Hin dimer may also contribute to recognition.

Hin-DNA versus other HTH DNA-binding complexes. The HTH motif occurs frequently in DNA-binding proteins, including prokaryotic regulators (18, 20, 28, 35), eukaryotic homeodomains (36-38), eukaryotic transcription factors such as HNF-3γ (39), the Oct-1 POU-specific domain, POU (40), the third tandem repeat of the cMyb protein (41), and the globular domain of histone H5, GH5 (42). Complexes of these proteins with DNA show two principal variants that are represented in Fig. 10 by the λ repressor and the engrailed homeodomain. In all cases, recognition helix 3 fits into the major groove and helix 2 runs across the width of the groove. In homeodomain structures, helix 1

lies essentially antiparallel to helix 2, which also spans the width of the major groove. The residues preceding helix 1 are positioned to interact with the minor groove, and recognition helix 3 is oriented along the floor of the major groove. This pattern is persistent; the cluster of three helices is virtually superimposable from one homeodomain complex to the next. In contrast, prokaryotic regulatory proteins (18, 20, 28, 35) have similar dispositions of helices 2 and 3, but with the exception of *trp* repressor, helix 1 is swung out and away from the DNA (Fig. 10A). Helix 3, on the other hand, tends to lie parallel to the edges of base pairs in the prokaryotic regulators, rather than along the floor of the groove as in homeodomains.

The present Hin-DNA complex is intermediate between these two structures. Recognition helix 3 is parallel to base pair edges rather than to the groove itself, as with prokaryotic repressors, but helix 1 is nearly antiparallel to 2, with its amino terminus extending toward the minor groove where a nonhelical chain continuation contributes interactions essential to specific recognition. The alignment of helix 3 parallel to base pairs in Hin and repressors is functional: comparison of the structures of 434 repressor-operator, 434 Cro-operator, λ repressor-operator, and CAP-DNA complexes, shows that amino acids at positions 1, 2, and 6 of the helix make specific contacts with bases in the major groove in each case.



λ repressor

Hin

Engrailed homeodomain

Fig. 10. Comparative interactions of a three-helix unit with the DNA double helix in the λ repressor-operator complex (left), the Hin-DNA complex (center), and the engrailed homeodomain complex (right). In each case, the carboxyl-terminal helix of the three is inserted into the major groove.

(43). Similarly, Hin uses positions 2 and 6 (Ser¹⁷⁴ and Arg¹⁷⁸) for its primary recognition process.

The disposition of helix 1 with respect to the DNA is not completely identical in Hin and homeodomains; in the latter, helix 1 crosses perpendicular to the walls of the major groove, whereas Hin has helix 1 aligned parallel with the overall DNA axis. The two loops connecting helices are shorter in Hin than in the homeodomain proteins and more like those of prokaryotic repressors. In addition, the α helices themselves are shorter than their homeodomain equivalents, especially helix 3, which in both yeast α2 and *Drosophila* engrailed homeodomains are 17 amino acids long.

There also is a remarkable difference in minor groove binding by the sequence Arg-Pro-Arg in the amino-terminal arm of Hin and in the engrailed homeodomain. In Hin, Arg¹⁴⁰ makes specific base contacts, whereas Arg¹⁴² anchors the two-pronged fork by binding to the phosphate backbone of DNA. In the engrailed homeodomain, Arg¹-Pro⁴-Arg³ inserts both Arg side chains into the minor groove and makes specific base contacts, and it is the adjacent Thr⁴ that interacts with phosphate backbone. Thus, the same three-amino acid recognition module can interact with the minor groove in two profoundly different ways to generate contacts essential for protein-DNA binding.

In another significant difference, the amino-terminal arms of homeodomain pro-

teins run along the minor groove in the direction of the HTH unit itself, whereas the amino-terminal arm of the Hin protein runs in an opposite direction (Figs. 3A and 9); toward what would be the center of the recombination site. Model-building of an intact recombinase bound to a complete *hix* site suggests that the positions cleaved by Hin during recombination are located on the opposite face of *hix* from the DNA-binding domains. It is likely that residues preceding the amino-terminal arm within an intact Hin protomer may continue running along the minor groove around the DNA and link with the catalytic domain that presumably is positioned over the cleavage site.

REFERENCES AND NOTES

1. A. C. Glasgow, K. T. Hughes, M. I. Simon, in *Mobile DNA*, D. E. Berg and M. M. Howe, Eds. (American Society for Microbiology, Washington, DC, 1989), pp. 637-659.
2. R. C. Johnson, *Curr. Opin. Genet. Dev.* 1, 404 (1991).
3. K. A. Heichman and R. C. Johnson, *Science* 249, 511 (1990).
4. K. A. Heichman, I. P. G. Moskowitz, R. C. Johnson, *Genes Dev.* 5, 1822 (1991).
5. I. P. G. Moskowitz, K. A. Heichman, R. C. Johnson, *ibid.*, p. 1835.
6. R. C. Johnson and M. I. Simon, *Cell* 41, 781 (1985).
7. R. C. Johnson and M. F. Bruijs, *EMBO J.* 8, 1581 (1989).
8. M. F. Bruijs, S. J. Horvath, L. E. Hood, T. A. Steitz, M. I. Simon, *Science* 235, 777 (1987).
9. J. P. Sluka, S. J. Horvath, M. F. Bruijs, M. I. Simon, P. B. Dervan, *ibid.* 238, 1129 (1987).
10. A. C. Glasgow, M. F. Bruijs, M. I. Simon, *J. Biol. Chem.* 264, 10072 (1989).
11. D. P. Mack et al., *Biochem. J.* 29, 6561 (1990).
12. J. P. Sluka, S. J. Horvath, A. C. Glasgow, M. I. Simon, P. B. Dervan, *ibid.*, p. 6551.
13. K. T. Hughes, P. C. W. Gaines, J. E. Karlinsky, R. Vinayak, M. I. Simon, *EMBO J.* 11, 2695 (1992).
14. M. Affolter et al., *Cell* 64, 879 (1991).
15. J.-A. Feng et al., *J. Mol. Biol.* 232, 982 (1993).
16. G. G. Privé, K. Yanagi, R. E. Dickerson, *ibid.* 217, 177 (1991).
17. K. Grzeskowiak, K. Yanagi, G. G. Privé, R. E. Dickerson, *J. Biol. Chem.* 266, 8861 (1991).
18. S. C. Schultz, G. C. Shields, T. A. Steitz, *Science* 253, 1001 (1991).
19. Z. Otwinowski et al., *Nature* 335, 321 (1988).
20. A. K. Aggarwal, D. W. Rodgers, M. Drott, M. Ptashne, S. C. Harrison, *Science* 242, 899 (1988).
21. W. S. Somers and S. E. V. Phillips, *Nature* 359, 387 (1992).
22. T. A. Steitz, *Q. Rev. Biophys.* 23, 205 (1990).
23. H. S. Yuan et al., *Proc. Natl. Acad. Sci. U.S.A.* 88, 9558 (1991).
24. D. Kostrewa et al., *Nature* 349, 178 (1991).
25. H. R. Drew et al., *Proc. Natl. Acad. Sci. U.S.A.* 78, 2179 (1981).
26. H. C. M. Nelson, J. T. Finch, B. F. Luisi, A. Klug, *Nature* 330, 221 (1987).
27. M. Coll, C. A. Frederick, A. H.-J. Wang, A. Rich, *Proc. Natl. Acad. Sci. U.S.A.* 84, 8385 (1987).
28. S. R. Jordan and C. O. Pabo, *Science* 242, 893 (1988).
29. T. E. Haran, A. Joachimiak, P. B. Sigler, *EMBO J.* 11, 3021 (1992).
30. M. L. Kopka, C. Yoon, D. Goodsell, P. Pjura, R. E. Dickerson, *Proc. Natl. Acad. Sci. U.S.A.* 82, 1376 (1985).
31. ———, *J. Mol. Biol.* 183, 553 (1985).
32. M. Suzuki, *EMBO J.* 8, 797 (1989).
33. M. E. Churchill and A. A. Travers, *Trends Biochem. Sci.* 16, 92 (1991).
34. Abbreviations for the amino acid residues are: A, Ala; C, Cys; D, Asp; E, Glu; F, Phe; G, Gly; H, His; I, Ile; K, Lys; L, Leu; M, Met; N, Asn; P, Pro; Q, Gln; R, Arg; S, Ser; T, Thr; V, Val; W, Trp; and Y, Tyr.
35. A. Mondragon and S. C. Harrison, *J. Mol. Biol.* 219, 321 (1991).
36. C. R. Klassinger, B.-S. Liu, E. Martin-Blanco, T. B. Kornberg, C. O. Pabo, *Cell* 63, 579 (1990).
37. C. Wolberger, A. K. Vershon, B. Liu, A. D. Johnson, C. O. Pabo, *ibid.* 67, 517 (1991).
38. G. Otting et al., *EMBO J.* 9, 3085 (1990).
39. K. L. Clark, E. D. Halay, E. Lai, S. K. Burley, *Nature* 364, 412 (1993).
40. N. Dekker et al., *ibid.* 372, 852 (1993); N. Assa-Munt, R. J. Mortishire-Smith, R. Aurora, W. Herr, P. E. Wright, *Cell* 73, 193 (1993).
41. K. Ogata, *Proc. Natl. Acad. Sci. U.S.A.* 89, 6428 (1992).
42. V. Ramakrishnan, J. T. Finch, V. Graziano, P. L. Lee, R. M. Sweet, *Nature* 362, 219 (1993).
43. S. C. Harrison and A. K. Aggarwal, *Annu. Rev. Biochem.* 59, 933 (1990).
44. T. C. Terwilliger, S.-H. Kim, D. Eisenberg, *Acta Crystallogr. A* 43, 1 (1987).
45. B.-C. Wang, *Methods Enzymol.* 115, 90 (1985).
46. M. A. Rould, J. J. Perona, T. A. Steitz, *Acta Crystallogr. A* 48, 751 (1992).
47. K. Y. J. Zhang and P. Main, *ibid.* 48, 377 (1991).
48. A. T. Brünger, J. Kuriyan, M. Karplus, *Science* 235, 458 (1987).
49. A. T. Brünger, *X-PLOR Manual*, version 3.1 (Yale Univ. Press, New Haven, CT, 1992).
50. We thank M. I. Simon and P. B. Dervan for providing Hin peptide, S. Finkel for help with DNA synthesis and purification, K. Zhang for many helpful discussions on phasing, and D. S. Goodsell for help with schematic drawings. Supported by NIH Program Project Grant GM-31299 (R.E.D.) and by GM-38509 (R.C.J.).

17 August 1993; accepted 15 December 1993

The Dictionary of
CELL BIOLOGY

Second Edition

EDITED BY

J. M. Lackie and J. A. T. Dow

*Yamanouchi Research Institute, Littlemore Hospital,
Oxford OX4 4XN, UK*

and

*Laboratory of Cell Biology, Institute of Biomedical
and Life Sciences, University of Glasgow,
Glasgow G12 8QQ, UK*

AUTHORS

S. E. Blackshaw¹
C. T. Brett
A. S. G. Curtis
J. A. T. Dow
J. G. Edwards²
J. M. Lackie
A. J. Lawrence
G. R. Moores

¹ Second edition only

² First edition only



ACADEMIC PRESS

Harcourt Brace & Company, Publishers
London San Diego New York
Boston Sydney Tokyo Toronto

ACADEMIC PRESS LIMITED
24-28 Oval Road
London NW1 7DX

US Edition published by
ACADEMIC PRESS INC.
San Diego, CA 92101

Copyright © 1995 by
ACADEMIC PRESS LIMITED
First published 1989

This book is printed on acid-free paper

All Rights Reserved

No part of this book may be reproduced in any form by photostat, microfilm, or any other means,
without written permission from the publishers

A CIP record for this book is available from the British Library

Cased edition ISBN 0-12-432562-9
Paperback edition ISBN 0-12-432563-7

Cover illustration

NIH 3T3 cells were incubated in our fixable dye **MitoTracker™ CMXRos** (M-7512), which stains mitochondria red, and then treated with aldehyde fixatives. After the fixed cells were permeabilized with acetone, they were stained with **BODIPY® FL phalloidin** (B-607), which labels actin green, and with **POPO™-1** (P-3580), which labels nuclei blue. This photomicrograph was obtained with a single exposure through the Omega® Optical triple-band filter set (O-5855), available directly from Molecular Probes. Photo contributed by Ian Clements and Sam Wells, Molecular Probes.

Typeset by Fakenham Photosetting Limited, Fakenham, Norfolk
Printed and bound in Great Britain by Mackays of Chatham, PLC, Chatham, Kent

In the preface
static", and we
progress and
biology. In thi
molecular biolo
the emergence
overtaken "int
chemokines ha
the G-proteins
proteins are le
include more t
deleting entrie
names that hav

As before, th
tried to be bro
has written ent
the neurobiolo
with molecular
to send us th
response. We
suggestions for

Several peop
particular we v
with typing. M
nevertheless be
We hope that ti
faster. On past
keep this proje
making a searc
undoubtedly le
changes and up
the third editio
back of the boo

A note regardi
The main entry
the definition
usefully to the
may well have

Generally, sp
have been alph

our comment
perhaps
this purpose

contains large identifiable cells and is consequently, like *Hirudo* and *Aplysia*, a favourite preparation for studying neural mechanisms at the cellular level, and in particular for studying isolated neurons in culture.

helix-coil transition See *random coil*.

helix-destabilising proteins (single-stranded binding proteins) Proteins involved in DNA replication. They bind cooperatively to single-stranded DNA, preventing the reformation of the duplex and extending the DNA backbone, thus making the exposed bases more accessible for base pairing.

helix-loop-helix A motif associated with *transcription factors*, allowing them to recognise and bind to specific DNA sequences. Two α -*helices* are separated by a loop. Examples: myoblast *MyoD1*, *c-myc*, *Drosophila* genes *daughterless*, *hairy*, *twist*, *scute*, *achaete*, *asense*. Not the same as helix-turn-helix.

helix-turn-helix A motif associated with *transcription factors*, allowing them to bind to and recognise specific DNA sequences. Two *amphipathic* α -*helices* are separated by a short sequence with a β -*sheet*. One helix lies across the major groove of the DNA, while the recognition helix enters the major groove and interacts with specific bases. An example in *Drosophila* is the *homeotic* gene *fushi tarazu*, that binds to the sequence TCAATTAAATGA. Not the same as helix-loop-helix.

helodermin See *exendin*.

helospectin See *exendin*.

helper factor A group of factors apparently produced by helper T-lymphocytes that act specifically or non-specifically to transfer T-cell help to other classes of lymphocytes. The existence of specific T-cell helper factor is uncertain.

helper T-cell See *T-helper cells*.

helper virus A virus that will allow the replication of a co-infecting defective virus by producing the necessary protein.

hema-, hemo- See *haema*, *haemo*.

heme See *haem*.

hemicellulose Class of plant cell-wall polysaccharide that cannot be extracted from the wall by hot water or chelating agents, but can be extracted by aqueous alkali. Includes *xylan*, *glucuronoxylan*, *arabinoxylan*, *arabinogalactan II*, *glucomannan*, *xyloglucan* and galactomannan. Part of the cell-wall matrix.

hemidesmosome Specialised junction between an epithelial cell and its basal lamina. Although morphologically similar to half a desmosome (into which intermediate cytokeratin filaments are also inserted), different proteins are involved.

hemizygote Nucleus, cell or organism that has only one of a normally *diploid* set of genes. In mammals the male is hemizygous for the *X-chromosome*.

Hensen's node (primitive knot) Thickening of the avian blastoderm at the cephalic end of the primitive streak. Presumptive notochord cells become concentrated in this region. May well be a source of retinoic acid that is acting as a morphogen in the developing embryo.

heparan sulphate (glycosaminoglycan) Constituent of membrane-associated *proteoglycans*. The heparan sulphate-binding domain of NCAM is proposed to augment NCAM-NCAM interactions, suggesting that cell-cell bonds mediated by NCAM may involve interactions between multiple ligands. The putative heparin-binding site on NCAM is a 28 amino acid peptide shown to bind both heparin and retinal cells, as well as to inhibit retinal cell adhesion to NCAM. This strengthens the argument that that this site contributes directly to NCAM-mediated cell-cell adhesion.

heparin Sulphated mucopolysaccharide, found in granules of mast cells, that inhibits the action of thrombin on fibrinogen by potentiating anti-thrombins, thereby interfering with the blood-clotting cascade. Platelet factor IV will neutralise heparin.

oxygen, and thus oxygen-fixing enzyme, oxygen sensitive.

of *Gram-negative* bacteria. Most species are aerobic, causing pneumonia, e.g. Legionnaires' disease. An outbreak in most members of an infection.

major protein of the cell wall of legumes.

gig cells.

muscle analogue of opionin. Two subunits, A and C, the latter homologous to calmodulin.

anovsky-type stain; used with acidic dyes used in histology and which differ in classes of leucocytes.

se caused by protozoan genus *Leishmania*. It is intracellularly in various forms of the disease, depending upon the site of infection (particular visceral leishmaniasis and mucocutaneous).

usually of non-oncogenic origin. It causes "slowly" characterised by horizontal growth.

NAc
GlcNAc

GlcNAc
GlcNAc
GlcNAc
GlcNAc

-Gal > α-D-Gal
-GalNAc

acetyl neuraminic acid
; Man = mannose.

zonal transmission, long incubation periods and chronic progressive phases. Visna virus is in this group, and there are similarities between visna, equine infectious anaemia virus and HIV.

lentoid Spherical cluster of retinal cells, formed by aggregation *in vitro*, that has a core of lens-like cells inside which accumulate proteins characteristic of normal lens. The cells concerned derive from retinal glial cells.

Lepore haemoglobin Variant haemoglobin in a rare form of *thalassaemia*; there is a composite δ-β chain as a result of an unequal *crossing-over* event. The composite chain is functional but synthesised at a reduced rate.

leprosy Disease caused by *Mycobacterium leprae*, an obligate intracellular parasite that survives lysosomal enzyme attack by possessing a waxy coat. Leprosy is a chronic disease associated with depressed cellular (but not humoral) immunity; the bacterium requires a temperature lower than 37°C, and thrives particularly in peripheral Schwann cells and macrophages. Only humans and the nine-banded armadillo are susceptible.

leptonema See *leptotene*.

Leptospira Genus of *spirochaete* bacteria that cause a mild chronic infection in rats and many domestic animals. The bacteria are excreted continuously in the urine, and contact with infected urine or water can result in infection of humans via cuts or breaks in the skin. Infection causes leptospirosis or Weil's disease, a type of jaundice, which is an occupational hazard for sewerage and farm workers.

leptospirosis Weil's disease, caused by infection with *Leptospira*.

leptotene Classical term for the first stage of *prophase I* of *meiosis*, during which the chromosomes condense and become visible.

Lesch-Nyhan syndrome A sex-linked recessive inherited disease in humans that results from mutation in the gene for

the purine salvage enzyme HGPRT, located on the X-chromosome. Results in severe mental retardation and distressing behavioural abnormalities, such as compulsive self-mutilation.

lethal mutation Mutation that eventually results in the death of an organism carrying the mutation.

LETS (large extracellular transformation/trypsin-sensitive protein) Originally described as a cell surface protein that was altered on transformation *in vitro*; now known to be *fibronectin*.

Leu enkephalin A natural peptide neurotransmitter; see *enkephalins*.

leucine (leu; L; 2-amino-4-methylpentanoic acid; 131 D) The most abundant amino acid found in proteins. Confers hydrophobicity and has a structural rather than a chemical role. See Table A2.

leucine aminopeptidase An *exopeptidase* that removes neutral amino acid residues from the N-terminus of proteins.

leucine zipper Motif found in certain *DNA-binding proteins*. In a region of approximately 35 amino acids, every seventh is a leucine. This facilitates dimerisation of two such proteins to form a functional *transcription factor*. Examples of proteins containing leucine zippers are products of the *proto-oncogenes myc, fos* and *jun*. See also *AP-1*.

leucinopine (dicarboxypropyl leucine) An analogue of *nopaline* found in crown gall tumours (induced by *Agrobacterium tumefaciens*) that do not synthesise octopine or nopaline.

leucocidin Exotoxins from staphylococcal and streptococcal species of bacteria that cause leucocyte killing or lysis.

leucocyte (USA leukocyte) Generic term for a white blood cell. See *basophil, eosinophil, lymphocyte, monocyte, neutrophil*.

leucocytosis An excess of leucocytes in the circulation.

Z

rus A togavirus (class I) genome responsible for the name whose disease is fever and haemorrhagic sepsis. It is transmitted by the mosquitoes of *Haemagogus*. Only one strain of the virus is known.

Yersinia of Gram-negative bacteria, *Yersinia enterocolitica*; all are pathogens. *Y. pestis* (for bubonic plague) was the cause of the plague.

tyrosine identified in avian yolk, containing a tyrosine protein called O1.

telolecithal eggs in which the yolk is distributed evenly (telolecithal) formed when cleavage occurs in the animal region can be termed

extra-embryonic the set of extra-embryonic tissues, growing out from the yolk surface, in birds the extra-embryonic cavity is the splanchnopleure, an extra-embryonic cavity, and the extra-embryonic cavity is the endoderm.

Z scheme of photosynthesis A schematic representation of the *light reactions of photosynthesis*, in which the photosynthetic reaction centres and electron carriers are arranged according to their electrode potential (free energy) in one dimension and their reaction sequence in the second dimension. This gives a Z shape, the two reaction centres (of photosystems I and II) being linked by the photosynthetic electron transport chain.

Z-disc Region of the *sarcomere* into which *thin filaments* are inserted. Location of α -actinin in the *sarcomere*.

Z-DNA See *DNA*.

zeatin A naturally occurring *cytokinin*, originally isolated from maize seeds. Its riboside is also a *cytokinin*.

zebrafish *Brachydanio rerio*; fish with a transparent embryo making it possible to follow progeny of single cells until quite late stages of development. This, together with the availability of mutant lines, makes it an important preparation for the study of vertebrate *cell lineage*.

zeta potential The electrostatic potential of a molecule or particle, e.g. cell measured at the plane of hydrodynamic slippage outside the surface of the molecule or cell. Usually measured by electrophoretic mobility. Related to the surface potential and a measure of the electrostatic forces of repulsion the particle or molecule is likely to meet when encountering another of the same sign of charge. See *cell electrophoresis*.

Zigmond chamber See *orientation chamber*.

zinc An essential "trace" element being an essential component of the active site of a variety of enzymes. Zn^{2+} has high affinity for the side-chains of cysteine and histidine. Zinc is present in tissues at

levels of ca. 0.1 mM; but intracellular levels must be much lower.

zinc finger A motif associated with *DNA-binding proteins*. A loop of 12 amino acids contains either two cysteine and two histidine groups (a "cysteine-histidine" zinc finger), or four cysteines (a "cysteine-cysteine" zinc finger), that directly coordinate a zinc atom. The loops (usually present in multiples) intercalate directly into the DNA helix. Originally identified in the RNA polymerase III transcription factor TFIIIA.

zipper See *leucine zipper*.

zippering Process suggested to occur in phagocytosis in which the membrane of the phagocyte covers the particle by a progressive adhesive interaction. The evidence for such a mechanism comes from experiments in which capped B-cells are only partially internalised, whereas those with a uniform opsonising coat of anti-IgG are fully engulfed.

ZO-1 High molecular weight protein (225 kD in mouse, 210 kD in MDCK cells) associated with *zonula occludens* (tight junction) in many vertebrate epithelia. *Cingulin*, which is distinct, is found in the same region.

zona pellucida A translucent non-cellular layer surrounding the ovum of many mammals.

zone of polarising activity The small group of mesenchyme cells in avian limb buds that is located at the posterior margin of the developing bud and that produces a substance, possibly retinoic acid, which provides positional information to the developing limb bud.

zonula adhaerens Specialised intercellular junction in which the membranes are separated by 15–25 nm, and into which are inserted microfilaments. Similar in structure to two apposed *focal*

The Penguin Dictionary of

Biology

M. Thain

M. Hickman

TENTH EDITION

being the Tenth Edition of the work originally compiled by
M. ABERCROMBIE, C. J. HICKMAN, M. L. JOHNSON

Diagrams by
RAYMOND TURVEY



PENGUIN BOOKS

For Wendy, Avril and Harry, and Margaret

PENGUIN BOOKS

Published by the Penguin Group
Penguin Books Ltd, 27 Wrights Lane, London W8 5TZ, England
Penguin Putnam Inc., 375 Hudson Street, New York, New York 10014, USA
Penguin Books Australia Ltd, Ringwood, Victoria, Australia
Penguin Books Canada Ltd, 10 Alcorn Avenue, Toronto, Ontario, Canada M4V 3B2
Penguin Books (NZ) Ltd, Private Bag 102902, NSMC, Auckland, New Zealand
Penguin Books Ltd, Registered Offices: Harmondsworth, Middlesex, England

First published as *The Penguin Dictionary of Biology*, 1951
Second edition 1954
Third edition 1957
Fourth edition 1961
Fifth edition 1966
Sixth edition 1973
Seventh edition 1980
Eighth edition, entitled *The New Penguin Dictionary of Biology*, 1990
Reprinted with amendments 1991, 1992
Reprinted, with amendments, as *The Penguin Dictionary of Biology*, 1992
Ninth edition 1994
Reprinted with minor revisions 1995, 1996
Tenth edition 2000
10 9 8 7 6 5 4 3 2 1

Copyright © M. Abercrombie, C. J. Hickman and M. L. Johnson, 1951, 1954, 1957, 1961, 1966, 1973, 1980
Copyright © Michael Thain, the Estate of M. Abercrombie, the Estate of C. J. Hickman and the Estate of M. L. Johnson, 1990, 1991, 1992, 1994, 1995, 1996, 2000
All rights reserved

The acknowledgements on pages vii–x constitute an extension of this copyright page

Set in 7/9 pt ITC Stone
Typeset by Rowland Phototypesetting Ltd, Bury St Edmunds, Suffolk
Printed in England by Clays Ltd, St Ives plc

Except in the United States of America, this book is sold subject to the condition that it shall not, by way of trade or otherwise, be lent, re-sold, hired out, or otherwise circulated without the publisher's prior consent in any form of binding or cover other than that in which it is published and without a similar condition including this condition being imposed on the subsequent purchaser

In the Preface to the Ninth Edition, I expressed the hope that advances in fields which have not, on this need is even more strongly, ever before for a trainee biologist, sciences, and in mathematics are up this belief and hope that, in colleges will encourage their students demands. In addition to providing we hope that this dictionary still suggestions (in SMALL CAPITALS) for

In our efforts to keep the Dictionary remains unaltered and thereby minority of new and modified especially unstable minefield when continue to ebb and flow, and within the entry on FISH has its own. Especially problematic is plant life chosen to include will not meet is that the lists of organisms make fluid at present. In part, this is due groups place upon the various for on anatomical features, others are of DNA sequences. Still others turn to some extent the continuing 'cladistic' schools of biological classification.

To illustrate the controversies current issues, both involving floral plant taxonomy has been to split Liliopsida) and dicotyledons (not the clustering of several orders; some research groups evaluating flowering plants lies elsewhere. C identifies the major morphological cotyledons but with the anatomical magnolia – traditionally a 'primitive' than the three pollen grain furrows traditional monocots such as b

holoblastic Form of CLEAVAGE.

holocarpic (Of fungi) having the mature thallus converted in its entirety to a reproductive structure. Compare EUCARPIC.

Holocene (recent) The present, post-Pleistocene, epoch (system) of the QUATERNARY period.

holocentric Of chromosomes with diffuse CENTROMERE activity, or a large number of centromeres. Common in some insect orders (Heteroptera, Lepidoptera) and a few plants (*Spirogyra*, *Luzula*).

Holocephali Subclass of the CHONDRICTHYES, including the ratfish *Chimaera*. First found in Jurassic deposits. Palatoquadrate fused to cranium (*autostylic* jaw suspension). Grouped with elasmobranchs because of their common loss of bone.

holocrine gland Gland in which entire cells are destroyed with discharge of contents (e.g. sebaceous gland). Compare APOCRINE GLAND, MEROCRINE GLAND.

holoenzyme Enzyme/cofactor complex. See ENZYME, APOENZYME.

hologamodeme See DEME.

Holometabola Those insects with a pupal stage in their life history. See ENDOPTERYGOTA. Compare THYSANOPTERA.

holophytic Having plant-like nutrition; i.e. synthesizing organic compounds from inorganic precursors, using solar energy trapped by means of chlorophyll. Effectively a synonym of photoautotrophic. Compare HOLOZOIC; see AUTOTROPHIC.

Holostei Grade of ACTINOPTERYGII which succeeded the chondrosteans as dominant Mesozoic fishes. Oceanic forms became extinct in the Cretaceous, but living freshwater forms include the gar pikes, *Lepisosteus*, and bowfins, *Amia*. Superseded in late Triassic and Jurassic by TELEOSTEI. Tendency to lose GANOINE covering to scales.

Holothuroidea Sea cucumbers. Class of ECHINODERMATA. Body cylindrical, with mouth at one end and anus at the other; soft, muscular body wall with skeleton of

scattered, minute plates; no spines or pedicillariae; suckered TUBE FEET; bottom-dwellers, often burrowing; tentacles (modified tube feet) around mouth for feeding. Lie on their sides.

holotype (type specimen) Individual organism upon which naming and description of new species depends. See NEOTYPE, BINOMIAL NOMENCLATURE.

holozoic Feeding in an animal-like manner. Generally involves ingestion of solid organic matter, its subsequent digestion within and assimilation from a food vacuole or gut, and egestion of undigested material via an anus or other pore. Compare HOLOPHYTIC.

homeobox Conserved DNA sequence MOTIF of ~180 base pairs, encoding DNA-binding regions of many proteins, specifically HMG boxes, $\alpha 1$ domains and homeodomains. Most proteins containing these regions are transcriptional regulators, and a single amino acid alteration can change the promoters to which they bind, potentially altering the downstream activation pattern of genes. First identified in 1984 within several HOMEOTIC GENES of *Drosophila*, the homeobox product confers the helix-turn-helix motif upon a protein, giving it its DNA-binding properties (see DNA-BINDING PROTEINS, REGULATORY GENE). Mating-type genes in ascomycete fungi control sexual development and contain homeobox motifs, and the rapidly evolving homeobox gene, *Odysseus*, is responsible for reproductive isolation (see SPECIATION) between sibling species of *Drosophila*.

homeodomain See HOMEBOX.

homeogenes HOMEBOX-containing genes whose protein products are all TRANSCRIPTION FACTORS; of wide (possibly universal) occurrence in animals, from cnidarians to vertebrates, but also present in other eukaryotes (plants, fungi and slime moulds, at least). Homeogenes include all homeotic and some SEGMENTATION GENES. One subset of HOMEOTIC GENES, the *Hox* (Antennapedia-like) homeogene family, is involved in encoding the relative positions of structures

along the antero-posterior bc (possibly all) animals and has re suggested as the defining charac morphy) of the kingdom (see Z HOX GENES are themselves re upstream genes whose product the rough axial specification early embryos, in *Drosophila* by cascade of gene expression (see The same colinear order of e) *Hox* gene clusters and their ho found in embryos as distant etically as those of fruit flies an expression at the 3' end of eac the chromosome starts in ant onic regions, each next gene is in the 5' direction along the c being expressed in progressive terior embryonic parts. Genes i ter are numbered accordin positions within it. The ANTEN PLEX and BITHORAX COMPLEX *phila* form a single (split) *Hox*. Some homeogenes contain D domains other than the ho encode transcription factors t differentiation of specific tiss *Pit-1* gene is specific to the pituiti ling synthesis of prolactin and mones). *Hox* gene complex animals other than *Drosophil* into a single continuous ch appears to be the primitive conu amphioxus has one cluster, ver four, suggesting that dupl occurred. This may have bee with the evolution of the Homeotic mutations probabl vide raw material for evolution indicate the genetic controls insects in the evolution of the terns characterizing their vario by vertebrates in controlling of neural crest derivatives (tr vertebrae and somites). So, altl ogenes affect axial informat groups, the manner by which very different. See CHROMOSOM GAP GENES.

homeosis Term coined by Wi in 1894 to indicate a form of v

Rational design of substituted tripyrrole peptides that complex with DNA by both selective minor-groove binding and electrostatic interaction with the phosphate backbone

(phosphodiester/hydrolysis/distamycin/polyamine/unwinding)

THOMAS C. BRUCE, HOUNG-YAU MEI, GONG-XIN HE, AND VAN LOPEZ

Department of Chemistry, University of California, Santa Barbara, CA 93106

Contributed by Thomas C. Bruce, October 8, 1991

ABSTRACT The structures of the compounds we call 3a, 3b, and 3c—compounds that incorporate (i) the tripyrrole peptide of the minor-groove-binding distamycin class of compounds and (ii) polyamine ligands that extend from the minor groove and can interact with phosphodiester bonds—were arrived at by computer-graphics designing by using the x-ray structure of distamycin A complexed in the minor groove of d(CGCAAATTTGCG)₂. Compounds 3a, 3b, and 3c are elaborations of distamycin analog 2, designed for improved stability in solution and easier synthesis and purification, which itself binds weakly to DNA. Compounds 3a, 3b, and 3c have been synthesized, and the interaction of distamycin A, 2, 3a, 3b, and 3c with calf thymus DNA, poly(dA-dT), poly(dG-dC), poly(dI-dC), pBR322 superhelical plasmid DNA, and, in the case of 3b, T4 coliphage DNA have been studied. The following pertinent conclusions can be drawn. Binding of 3a, 3b, and 3c occurs in the minor groove of DNA and, because of favorable electrostatic interaction of diprotonated polyamine side chains and DNA phosphodiester linkages, the tenacity of DNA binding and site specificity of 3a, 3b, and 3c are comparable to that of native distamycin A. 3b has been found to induce changes in the superhelical density of pBR322 plasmid DNA. The study establishes that the central pyrrole N—CH₃ substituent of 2 can be replaced by bulky polyamine metal ligands to create any number of compounds that bind into the minor groove at A+T-rich sites and are putative catalysts for the hydrolysis of DNA.

It has been estimated that the half-life for the hydrolysis of a simple dialkyl phosphate ester at pH 7.0 is about 200 million years (1). It is apparent then why phosphodiester bonds link the letters of the genetic code. Chemists have yet to design and prepare worthwhile catalysts for the hydrolysis of dialkyl phosphate esters. This remains a desirable goal. Having small molecules that catalyze the hydrolysis of DNA at given sequences could be of great advantage in the study of DNA structure and function.

The desired characteristics of a small molecule capable of hydrolyzing DNA would include: (i) its binding to a specific base sequence of DNA, and (ii) a catalytic site holding metal ions or protons and a nucleophile juxtaposed to the phosphodiester bond. The hydrolysis of DNA phosphodiester linkages is catalyzed by nuclease enzymes, which require metal ions for their activity. Both Mg²⁺ and Zn²⁺ are directly involved in the 3'-to-5' exonuclease activity of the Klenow fragment of DNA polymerase I from *Escherichia coli*. Evidence for the catalytic role of the metal ions comes from the x-ray crystallographic data of a cocrystal of DNA and the Klenow fragment (2, 3). It has been proposed that the established (4) in-line displacement of the 5' oxygen is by

HO⁻ ligated to the Zn²⁺ and that the incipient 5' oxyanion leaving group is coordinated by Mg²⁺. A combination of two metals has also been reported as essential to phosphodiester hydrolysis by *E. coli* alkaline phosphatase (5) and phospholipase C from *Bacillus cereus* (6). There are several model studies that support roles for metal ions in phosphodiester bond hydrolysis (7, 8). Positively charged arginines in the active site of hydrolytic nucleases (9) have also been suggested to play an important role in catalysis by interacting with the negatively charged dialkyl phosphate ester substrate (10). It is not inconceivable that a single low molecular weight molecule could play both types of catalytic roles. Thus, a catalytic protonated polyamine might also exhibit catalysis by ligation of the proper metal ion (11).

We report at this time the design, synthesis, and DNA binding of representatives of a class of compounds (3a, 3b, and 3c in Fig. 1) that incorporate the tripyrrole peptide of the minor-groove-binding distamycin (compound 1 in Fig. 1) class of compounds and, in addition, polyamine ligands that can interact with phosphodiester bonds and extend outwards from the minor groove. The complexity of the compounds we report here is sufficient to provide an answer to our initial concern as to whether steric hindrance by the bulky ligands and their tether prevents minor-groove binding or if electrostatic interaction of the putative catalytic groups with the phosphodiester linkage enhances minor-groove binding. We have found the latter situation to prevail.

MATERIALS AND METHODS

Materials. Distamycin A and ethidium bromide (EtdBr) were purchased from Sigma. T4 coliphage DNA was from Sigma and was extracted with phenol before use. Sonicated calf thymus DNA with an average length of 500 base pairs, pBR322 plasmid DNA, and all synthetic polynucleotides were from Pharmacia. Topoisomerase I from calf thymus was purchased from GIBCO/BRL.

Synthesis of Distamycin Analogs. Synthetic sequences for preparation of distamycin analogs 3a, 3b, and 3c are shown in Fig. 2 along with the conditions and reagents used. Compounds 2, 4a, and 4b were synthesized following similar procedures. With the exception of the use of diethyl cyanophosphonate (DECP) as the coupling reagent for peptide synthesis, the procedures used to create the tripeptide from its monomers are basically similar to the published methods (12-15). Detailed procedures will be published elsewhere. The structural identification of 3a, 3b, and 3c was established by Fourier transform IR (Perkin-Elmer 1600), ¹H NMR (General Electric GN-500), low-resolution MS (VGII-250), and elemental analysis.

The publication costs of this article were defrayed in part by page charge payment. This article must therefore be hereby marked "advertisement" in accordance with 18 U.S.C. §1734 solely to indicate this fact.

Abbreviations: DECP, diethyl cyanophosphonate; EtdBr, ethidium bromide.

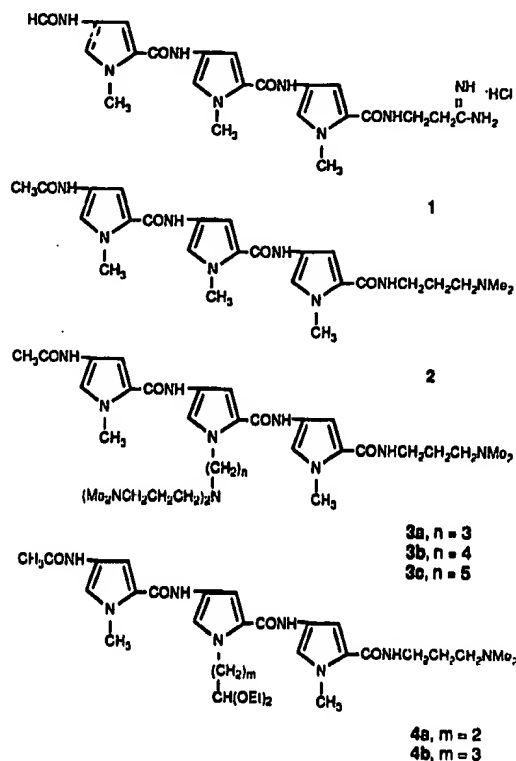


FIG. 1. Structures of compounds 1–4b.

Compound 3a. Analysis calculated for $C_{37}H_{61}N_{11}O_4 + 1.5H_2O$: C, 59.18; H, 8.59; N, 20.52. Found: C, 58.94; H, 8.29; N, 20.16.

Compound 3b. Analysis calculated for $C_{38}H_{63}N_{11}O_4 + 4H_2O$: C, 56.34; H, 8.83; N, 19.02. Found: C, 56.54; H, 8.63; N, 18.72.

Compound 3c. Analysis calculated for $C_{39}H_{65}N_{11}O_4 + 2.5H_2O$: C, 58.77; H, 8.85; N, 19.33. Found: C, 58.79; H, 8.86; N, 18.76.

Molecular Modeling and Computational Analysis. These procedures were carried out on a Silicon Graphics (Mountain View, CA) Iris 4D/220GTX workstation using CHARM_m (16) (version 21.2) and QUANTA (version 3.0) programs (Polygen, Waltham, MA). Coordinates for the distamycin A–d(CGCAAATTTGCG)₂ complex were from the Brookhaven Protein Databank (17). Coordinates for the amine ligand $-N(CH_2CH_2CH_2NMe_2)_2$ and for aliphatic chains $(CH_2)_n$ ($n = 3, 4$, and 5) tethered on pyrrole nitrogen were generated by using the chemnote program in QUANTA. Atomic partial charges of the atoms of 2, 3a, 3b, and 3c were calculated by using the MNDO program (18) incorporated in QUANTA.

DNA Binding Affinities. The EtdBr displacement method (19) was used to determine DNA binding affinities. Fluorescence measurements were performed on a LS-50 Perkin-Elmer spectrofluorometer with 546 nm as excitation wavelength and 591 nm as the emission wavelength. Standard solutions for fluorescence measurements contained 40 mM NaCl, 25 mM Tris (pH 7.5), 2 mM DNA, and 2.6 mM EtdBr. UV-visible absorption spectra were obtained, and spectral analysis and data fitting were performed with an OLIS (Athens, GA) Cary-14 spectrophotometer and OLIS software. Gel electrophoresis was performed on an H5 horizontal electrophoresis apparatus from GIBCO/BRL.

RESULTS AND DISCUSSION

Peter Dervan and associates (20) have developed molecules that bind in the minor groove of DNA with high selectivity for

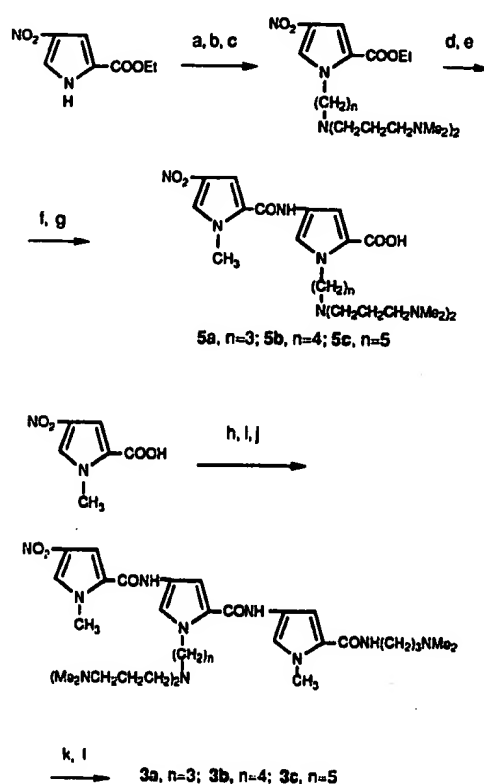


FIG. 2. Synthesis of 3a, 3b, and 3c. Reagents and conditions for synthetic steps a–i: a, K, KI, $CH(CH_2)_mCH(OEt)_2$, $m = 2, 3$, and 4 , dimethyl formamide (DMF), 80°C, 5 hr; b, 90% acetone/10% H_2O , pyridinium *p*-toluenesulfonate, reflux, 10 hr; c, $HN(CH_2CH_2CH_2NMe_2)_2$, $NaBH_3CN$, MeOH, AcOH, room temperature (RT), 72 hr; d, H_2 , 10% palladium on activated carbon (Pd/C), MeOH, RT, 1 atm; e, *N*-methyl-4-nitropyrrole-2-carboxylic acid, DECP, Et_3N , DMF, RT, 10 hr; f, NaOH, 80% EtOH/20% H_2O , reflux, 24 hr; g, 10% HCl, 0°C, to pH = 7; h, $H_2N(CH_2)_3Me_2$, DECP, tetrahydrofuran, RT, 10 hr; i, H_2 , 10% Pd/C, MeOH, RT, 1 atm; j, 5, DECP, Et_3N , DMF, RT, 10 hr; k, H_2 , 10% Pd/C, MeOH, RT, 1 atm; l, CH_3COCl , Et_3N , DMF, RT, 10 hr. (1 atm = 101.3 kPa.)

A+T-rich sequences and catalyze DNA oxidative cleavage by use of Fenton chemistry. An entire subfield now deals with the cleavage of DNA by sequence-selective degradation of deoxyribose or base entities with redox chemistry (21–23). Our ultimate goal is the design of molecules that selectively catalyze the hydrolysis of DNA. In the design of the molecules reported here, we have used Dervan's approach of modification of known A+T sequence-selective minor-groove-binding molecules.

Molecular Designing. Molecular designing was based upon the x-ray crystallographic structure of distamycin A (compound 1) complexed in the minor groove of d(CGCAAATTTGCG)₂ (17). As shown by this x-ray structure and numerous binding studies (24), the crescent-shaped distamycin tripeptide binds at A+T-rich regions of DNA with a binding constant of about $10^6 M^{-1}$. When one examines the atoms that neighbor the DNA phosphate groups in the 1–d(CGCAAATTTGCG)₂ complex, it becomes immediately evident that the DNA phosphate groups have about the same periodicity as do the distamycin pyrrole rings. Further, the carbon of the *N*-methyl groups substituted on the pyrrole rings of 1 are located about 5 Å away from the DNA phosphate phosphorous atoms (Fig. 3 Top). If 1 or a distamycin-like molecule were to be used to provide selective binding of a catalytic device for phosphate ester bond hy-

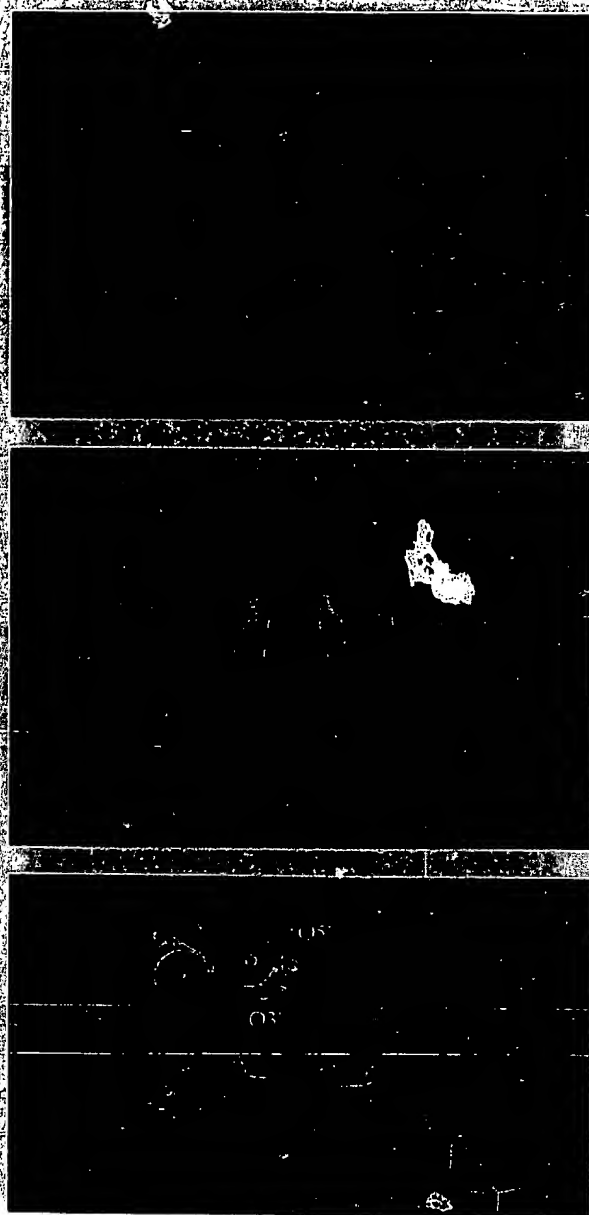


FIG. 3. (Top) From the crystal structure of the complex of distamycin A with d(CGCAAATTTGCG)₂ (ref. 17), it can be seen that the distances between the carbons (green, with Corey-Pauling-Koltun solid model) of the pyrrole *N*-methyl substituents of distamycin and the neighboring phosphate phosphorous atoms (yellow, with Van der Waals dot surface) is about 5 Å. (Middle) A proposed binding model for 3a interacting with A-T-rich region of DNA. Coordinates for the DNA and distamycin were from the x-ray crystal structure of the distamycin A complex with d(CGCAAATTTGCG)₂ (ref. 17), while the coordinates for the -(CH₂)₃N(CH₂CH₂CH₂NMe₂)₂ side chain was generated in chemnote of QUANTA. Energy minimization using the steepest descent and adopted-basis Newton Raphson method were performed before submitting these coordinates for molecular dynamics (Verlet) calculation. Coordinates displayed were obtained from the energy-minimized average coordinates of the last picosecond out of a 35-psec dynamics calculation. The structure shows that the triamine complexes the phosphate by hydrogen bonding to two of the phosphate oxygens. (Bottom) Plausible structure of metal-complexed 3a bound in the minor groove of d(CGCAAATTTGCG)₂. Placement is such that a ligated hydroxyl oxygen is in line with the departing OS'.

drolisis, then the catalytic device should be covalently attached in place of an *N*-methyl group. It has been established that the replacement of the *N*-methyl substituent of 1 by *N*-propyl (25) or even *N*-isoamyl (26) does not prevent binding to DNA.

Though the molecular designing was carried out by using the x-ray structure of 1-d(CGCAAATTTGCG)₂ complex, our synthetic compounds 3a, 3b, and 3c are, after Wade and Dervan (27), elaborations of compound 2 (Fig. 2). The rationale for our doing so follows. In the first place, compound 1 is unstable in solution, and this instability can be removed by replacing the formamido and 3-amidinopropyl groups by the acetamido and 3-dimethylaminopropyl groups to provide compound 2. Also, changing the positive amidine group of 1 to the neutral tertiary amino group of 2 makes both synthesis and purification much easier. In particular, one is not bothered by the unwanted side reaction to peptide synthesis of the reaction of the coupling reagent DECP with the amidine group to form a phosphamide. The x-ray structure of 1-d(CGCAAATTTGCG)₂ complex shows that the terminal amidine cationic group in distamycin lies deep in the minor groove. The pK_a value for the terminal tertiary amino group in 2, 3a, 3b, and 3c is about 9.5, so that it should be protonated at neutral pH. Modeling establishes that the conversion of 1 to 2 is not accompanied by unwanted steric effects. The key rationale for the synthetic scheme designed here is that numerous metal-chelating groups such as polyamines can replace the *N*-methyl substituent of the central pyrrole of 2 with little synthetic difficulty.

In compounds 3a, 3b, and 3c, the -(CH₂)_n-N[CH₂CH₂-CH₂N(CH₃)₂]₂ functional group in which *n* = 3, 4, and 5, respectively (Fig. 1), replaces the *N*-methyl substituent of the central pyrrole of 2. The pK_a values of CH₃N(H)[CH₂-CH₂CH₂N(H)(CH₃)₂]₂³⁺ were determined to be 6.8, 9.6, and 12.2. Therefore, at neutrality the -(CH₂)_n-N[CH₂CH₂CH₂N(CH₃)₂]₂ substituent exists to a considerable extent in the diprotonated form. Electrostatic interaction of the diprotonated side chain may occur with adjacent phosphodiester linkages on both DNA strands or with one or more phosphodiester linkages of a single strand (Fig. 3 Middle). In the instance of DNA complexes, with two molecules of 3 sitting staggered side by side in antiparallel orientation in the minor groove (as proposed in ref. 28), electrostatic interactions of the two diprotonated polyamine side chains can occur via interaction with adjacent phosphodiester linkages on both strands. Such structures can be created by computer graphics by using as base the two-dimensional NMR structure of the 2:1 complex of distamycin A-d(CGCAAATTTGCG)₂. It has been reported that CH₃N(CH₂CH₂CH₂NH₂)₂ is a moderately strong ligand for transition metal ions, such as Ni²⁺, Co²⁺, and Cu²⁺ (29). Thus, the -N[CH₂CH₂CH₂N(CH₃)₂]₂ end group should serve to hold a metal ion adjacent to a single phosphodiester linkage. The metal ions ligated by the -N[CH₂CH₂CH₂N(CH₃)₂]₂ moiety also may be bound to the PO⁻ of the phosphate ester or may act as a carrier of a nucleophilic hydroxyl group (Fig. 3 Middle).

Comparison of Binding Affinities. The binding affinities of compounds 1, 2, 3a, 3b, 3c, 4a, and 4b to sonicated calf thymus DNA and synthetic polymers poly(dA-dT), poly(dG-dC), and poly(dI-dC) have been compared by using the EtdBr displacement method (19). The ethidium moiety of the DNA-EtdBr complex is quite fluorescent, and binding of agents into the minor groove can be monitored because of the release of EtdBr, which, when free, is less fluorescent by a factor of 50. On a fluorescence scale of 0 to 1, the fractional decrease in fluorescence is determined at saturation of DNA by the complexing agent (Fig. 4). This value should be indicative of the number of DNA binding sites to which the agent can complex. The C₅₀ or concentration of the binding agent that displaces half of the bound EtdBr, which is dis-

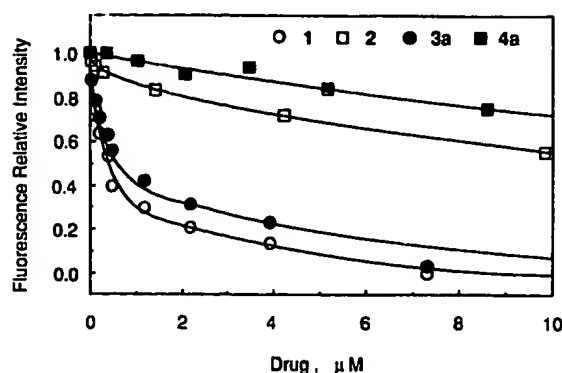


FIG. 4. Fluorescence intensity of EtdBr in the presence of calf thymus DNA and 1, 2, 3a, and 4a, respectively. The ethidium displacement curves for 3b and 3c are similar to that of 3a, and the plot for 4b is similar to that for 4a. Conditions are described in the legend of Table 1.

placed at saturation by the agent, has been used as an estimate of the binding constant for the agent. The index ($C_{50}/\%$ decrease in fluorescence at saturation) values for binding of 1, 2, 3a, 3b, 3c, 4a, and 4b are provided in Table 1.

Distamycin binds DNA with strong preference for A+T sequences (24). The index value obtained here for binding of 1 to poly(dA-dT) polymer is almost 220 times smaller than the index value for binding of 1 to poly(dG-dC). Index value for binding to calf thymus DNA, a natural DNA with 58% A+T content, is about 70 times smaller than that of poly(dG-dC). In short, to replace a similar amount of ethidium, a much larger quantity of 1 is needed for sequences of G+C than for A+T. The following conclusions may be drawn from the data of Table 1.

(i) The binding of 1 to DNA is much more favorable than is the binding of 2. The x-ray structure of the 1-d(CG-CAAATTTGCG)₂ complex shows that the protonated amidine substituent of 1 is within hydrogen-bonding distance of adenosine-4 of the DNA substrate. The protonated amine substituent of 2, which replaces the amidine substituent in 1, is not capable of such hydrogen-bond formation. The more dispersed positive charge and hydrogen-bonding capability of the amidine structure allows greater interaction than does the tertiary amine.

(ii) The index of binding of 2 to DNA serves as a standard to compare binding indexes of 3a, 3b, and 3c. We anticipated either a decrease in binding of 3a, 3b, and 3c as compared with 2 because of steric hindrance brought about by exchange of $N-(CH_2)_nN[CH_2CH_2CH_2N(CH_3)_2]_2$ for the *N*-methyl or an increase in binding because of the electrostatic interaction of the protonated tertiary amine of 3a, 3b, and 3c and the DNA phosphate groups. The latter situation prevails, so that the electrostatic interaction of DNA phosphate groups and the protonated polyamine side chain of 3a, 3b, and 3c overcome

the loss in binding capacity caused by loss of hydrogen bonding when the amidine group of distamycin is exchanged with a dimethylamine group to provide 2. Bifurcated hydrogen bonds found between 1 and DNA in the x-ray and NMR studies (17, 30) are probably missing for 3 should electrostatic interactions with phosphates prevail.

(iii) Indices for 3a, 3b, and 3c are comparable to one another and much the same as the indices for 1 in the complexing of calf thymus DNA, poly(dA-dT), poly(dG-dC), and poly(dI-dC). Poly(dI-dC) is the same as poly(dG-dC) except there is no amino group on position 2 of each guanine base protruding in the minor groove. The fact that there is strong binding to poly(dI-dC) indicates that 3a, 3b, and 3c share with 1 a minor-groove-binding mode. This conclusion is supported by a study of the interaction of 3a with T4 coliphage DNA monitored by the change in extinction coefficient and bathochromic shift of the longer wavelength absorption band of 3a on complexation by DNA. The λ_{max} of 3a has a similar red shift in binding to T4 DNA and to calf thymus DNA. T4 coliphage DNA is glycosylated throughout the major groove (31). Thus, complexing of 3a by T4 DNA should only occur in the minor groove. In accordance with the ethidium displacement results, 3a, 3b, and 3c have the same base specificity and groove-binding characteristics to DNA as does 1. The same conclusion is reached from spectral analysis. The extent of the red shift follows the order poly(dA-dT) (19 nm) \approx calf thymus DNA (18 nm) $>$ poly(dG-dC) (6 nm). Thus, the bulky pyrrole *N*-substituents of 3a, 3b, and 3c with associated positive charges do not alter the specificity for DNA binding, which is due to the poly(pyrrole amide) structure found in netropsin and distamycin. Binding a molecule of 3a, 3b, and 3c may, like distamycin, occupy a site of 4 or 5 base pairs and, therefore, may displace the same amount of bound ethidium as does 1. If this is so, and since the indices of 1, 3a, 3b, and 3c are comparable, it could be concluded that the equilibrium binding constants for 3a, 3b, and 3c are comparable to that of 1 (20) with poly(dA-dT) ($10^6 M^{-1}$) and poly(dG-dC) ($10^4 M^{-1}$).

(iv) Compounds 4a and 4b are derived from 2 by exchange of an $N-CH_3$ for the bulky and nonfunctional $-(CH_2)_n-CH(OCH_2CH_3)_2$ substituents ($n = 2$ and 3 , respectively). Thus, the binding of 4a and 4b should resemble the binding of 3a and 3b if the latter did not involve an electrostatic component. Binding of 4a and 4b to DNA is a bit weaker than is the DNA binding of 2. The index values for 4a and 4b are equal. At saturating concentrations of 4a and 4b, little ethidium is displaced, but some preference for A+T binding can still be found. The UV spectra of 4a or 4b show little or no change upon addition of DNAs. These data suggest that, due to steric constraints, the binding of 4a and 4b is restricted to a few A+T-rich sites and may also involve an outside electrostatic binding mode.

Interaction of 3a and 3b with Superhelical Plasmid pBR322 DNA. This interaction results in the relaxation of the pBR322 DNA in the absence of any reducing agents or metal ions

Table 1. Index values for binding of distamycin A (compound 1) and its analogs to DNA

Compound	ctDNA	Poly(dA-dT)	Poly(dG-dC)	Poly(dI-dC)
1	0.28/87 = 0.003	0.12/96 = 0.001	6.5/30 = 0.217	0.18/96 = 0.002
2	5.4/65 = 0.083	4.5/85 = 0.053	5.5/20 = 0.275	6.0/90 = 0.067
3a	0.50/82 = 0.006	0.21/93 = 0.002	10/37 = 0.270	0.38/90 = 0.004
3b	0.35/90 = 0.004	0.21/93 = 0.002	8.0/40 = 0.200	0.38/90 = 0.004
3c	0.35/95 = 0.004	0.21/93 = 0.002	8.0/40 = 0.200	0.38/90 = 0.004
4a	5.5/40 = 0.138	7.5/70 = 0.107	5.5/20 = 0.275	8.4/48 = 0.175
4b	5.5/40 = 0.138	7.5/70 = 0.107	5.5/20 = 0.275	8.1/52 = 0.156

Index values = $C_{50}/\%$ decrease of fluorescence at saturation; for details, see text. Typically, a 3-ml solution containing 40 mM NaCl, 25 mM Tris (pH 7.5), 2 μ M calf thymus DNA (ctDNA) DNA, and 2.6 μ M EtdBr was titrated with a concentrated solution of distamycin or an analog (100 μ M to 1 mM), and fluorescence was excited at 546 nm and measured at 591 nm at 37°C.



FIG. 5. The topoisomer patterns of pBR322 DNA obtained after relaxation with excess calf thymus topoisomerase I in the presence of 0, 10, 20, 70, 80 μ M, respectively (lanes 1–5), of 3b. In each sample, 5 μ g of negatively supercoiled pBR322 was incubated at 37°C for 17.5 hr with 20 units of topoisomerase I in a 50- μ l solution containing 1 mM EDTA, 50 mM KCl, 10 mM MgCl₂, 50 mM Tris (pH 7.5), and 3b. After relaxation, the DNA was extracted twice with phenol equilibrated with 20 mM Tris (pH 8.0). This was followed by a chloroform/octanol, 24:1 (vol/vol), extraction. The resulting solution was passed through a NACS PREPAC cartridge (GIBCO/BRL) and lyophilized. After lyophilization, aliquots of DNA were loaded on a 1% agarose gel at 1.5 V/cm for 17 hr in E buffer (40 mM Tris/20 mM sodium acetate/2 mM EDTA, pH adjusted to 7.7 with glacial acetic acid). The gels were stained with diluted EtBr solution and photographed on a UV transilluminator with Polaroid type 665 films.

(data not shown). It was found, in the presence of 3a or 3b, that the amount of conversion of supercoiled DNA form I to the relaxed form II did not continuously increase with time, nor was the observed conversion proportional to the concentration of 3a or 3b used. Therefore, rather than DNA strand breakage, mechanisms such as unwinding of supercoiled DNA must be responsible for the relaxation effect of 3a or 3b on pBR322.

To explore these possibilities, topoisomer families of pBR322 were prepared by relaxing negatively supercoiled DNA with calf thymus topoisomerase I (32, 33) in the presence of 3b. Supercoiled plasmid pBR322 was completely relaxed with an excess amount of topoisomerase I in the absence of 3b (Fig. 5, lane 1). With increasing concentrations of 3b, the gel shows (lanes 2 to 5) a family of bands reflecting the presence of DNA species with varying extents of superhelicities. Increasing concentrations of 3b first relocates the center of the Boltzmann distribution and shifts it toward DNA bands with higher superhelicities that will migrate faster than relaxed DNA on the agarose gel. Further increase in 3b concentration decreases the bands of higher superhelicities back to a relaxed form. These results provide direct evidence for the unwinding ability of 3b. At comparable concentrations, the change in superhelicity followed the order netropsin (34) \approx 3b \gg 1.

In summary, we have designed molecules (3a, 3b, and 3c) in which the central pyrrole *N*-methyl group of compound 2, which displays weak A+T minor-groove binding, is replaced by the positively charged metal-chelating polyamine group $-(CH_2)_nN(CH_2CH_2CH_2N(CH_3)_2)_2$. We have shown that 3a, 3b, and 3c are strong minor-groove binders, and this feature

must be associated with the electrostatic interaction of the positively charged polyamine side chain with phosphodiester linkages. This binding mode results in the unwinding of supercoiled DNA. Compounds such as 3a, 3b, and 3c may be useful in exploring DNA conformations. These results establish that the synthesis of putative catalysts for DNA hydrolysis, based upon the general concepts embodied in compounds 3a, 3b, and 3c is worthy of pursuit.

We express appreciation to the Office of Naval Research for a grant (N000 14-90-J-4132) to support this work. H.-Y.M. expresses gratitude to the National Institutes of Health for a National Research Service Award (GM 13040-02).

- Chin, J., Banaszczuk, B., Jubian, V. & Zou, X. (1989) *J. Am. Chem. Soc.* **111**, 186–190.
- Freemont, P. S., Friedman, J. M., Beese, L. S., Sanderson, M. R. & Steltz, T. A. (1988) *Proc. Natl. Acad. Sci. USA* **85**, 8924–8928.
- Beese, L. S. & Steltz, T. A. (1991) *EMBO J.* **10**, 25–33.
- Gupta, A. P. & Benkovic, S. J. (1984) *Biochemistry* **23**, 5874–5881.
- Kim, E. E. & Wyckoff, H. W. (1991) *J. Mol. Biol.* **218**, 449–464.
- Hough, E., Hunsen, L. K., Birknes, B., Jynge, K., Hansen, S., Hordvik, A., Little, C., Dodson, E. & Derewenda, Z. (1989) *Nature (London)* **338**, 357–360.
- De Rosch, M. A. & Trogler, W. C. (1990) *Inorg. Chem.* **29**, 2409–2416.
- Chin, J. (1991) *Acc. Chem. Res.* **24**, 145–152.
- Cotton, F. A., Day, V. W., Hazen, E. E., Larsen, S. & Wong, S. T. K. (1974) *J. Am. Chem. Soc.* **96**, 4471–4478.
- Springs, B. & Haake, P. (1977) *Tetrahedron Lett.* **37**, 3223–3226.
- Basile, L. A., Raphael, A. L. & Barton, J. K. (1987) *J. Am. Chem. Soc.* **109**, 7550–7551.
- Taylor, J. S., Schultz, P. G. & Dervan, P. B. (1984) *Tetrahedron* **40**, 457–465.
- Krowicki, K. & Lown, J. W. (1987) *J. Org. Chem.* **52**, 3493–3501.
- Baker, B. F. & Dervan, P. B. (1989) *J. Am. Chem. Soc.* **111**, 2700–2712.
- Rao, K. E., Bathini, Y. & Lown, J. W. (1987) *J. Org. Chem.* **52**, 3493–3501.
- Brooks, B. R., Bruccoleri, R. E., Olafson, B. D., States, D. J., Swaminathan, S. & Karplus, M. (1983) *J. Comp. Chem.* **4**, 187–217.
- Coll, M., Frederick, C. A., Wang, A. H.-J. & Rich, A. (1987) *Proc. Natl. Acad. Sci. USA* **84**, 8385–8389.
- Dewar, M. J. S. & Thiel, W. (1977) *J. Am. Chem. Soc.* **99**, 4899–4917.
- LePecq, J.-B. & Paoletti, C. (1967) *J. Mol. Biol.* **27**, 87–106.
- Schultz, P. G., Taylor, J. S. & Dervan, P. B. (1982) *J. Am. Chem. Soc.* **104**, 6861–6863.
- Dervan, P. B. (1986) *Science* **232**, 464–471.
- Sigman, D. S. (1986) *Acc. Chem. Res.* **19**, 180–186.
- Barton, J. K. (1986) *Science* **233**, 727–734.
- Zimmer, Ch. & Wahnert, U. (1986) *Prog. Biophys. Mol. Biol.* **47**, 31–112.
- Gursky, G. V., Zasedatelev, A. S., Zhuze, A. L., Khorlin, A. A., Grokhovskiy, S. L., Streltsov, S. A., Surovaya, A. N., Nikitin, S. M., Krylov, A. S., Retchinsky, V. O., Mikhailov, M. V., Bealashvili, R. S. & Gottikh, B. P. (1983) *Cold Spring Harbor Symp. Quant. Biol.* **47**, 367–378.
- Grokhovskii, S. L., Zhuze, A. L. & Gottikh, B. P. (1982) *Bioorg. Khim.* **8**, 1070–1076.
- Wade, W. S. & Dervan, P. B. (1987) *J. Am. Chem. Soc.* **109**, 1574–1775.
- Pelton, J. F. & Wemmer, D. E. (1989) *Proc. Natl. Acad. Sci. USA* **86**, 5723–5727.
- Goldberg, D. E. & Fernelius, W. C. (1959) *J. Phys. Chem.* **63**, 1328–1330.
- Pelton, J. G. & Wemmer, D. E. (1988) *Biochemistry* **27**, 8088–8096.
- Mokul'skii, M. A., Kaiptarova, K. A. & Mokul'skaya, T. D. (1972) *Mol. Biol. (Moscow)* **6**, 714–731.
- Keller, W. (1975) *Proc. Natl. Acad. Sci. USA* **72**, 4876–4880.
- Wang, J. C. (1980) *Trends Biochem. Sci.* **5**, 219–221.
- Snounou, G. & Malcolm, A. D. B. (1983) *J. Mol. Biol.* **167**, 211–216.